2007

Biodegradation and Characterization of a Bio-based Polyester

Benjamin Edward Stevens
Louisiana State University and Agricultural and Mechanical College, bsteve2@lsu.edu

BIODEGRADATION AND CHARACTERIZATION OF A BIO-BASED POLYESTER

A Thesis
Submitted to the Graduate Faculty of the
Louisiana State University and
Agricultural and Mechanical College
in partial fulfillment of the
requirements for the degree of

Master of Science in Biological and Agricultural Engineering

In

The Department of Biological and Agricultural Engineering

by
Benjamin Edward Stevens
B.S., Louisiana State University, 2005
December, 2007

Acknowledgements

Research provided in this thesis was made possible by Metabolix, Inc. and The Consortium for Plant Biotechnology Research, Inc. I would like to extend my gratitude to anyone who ever helped me in my endeavors to complete this work, most notably my two co-major advisors Dr. Kelly Rusch and Dr. Chandra Theegala and my committee members Dr. Ioan Negulescu and Dr. Todd Monroe, who have all pushed me to succeed. Others who have assisted me in completion of my research in some form or fashion (even the smallest ways count) or have just been good friends include Teresa Gutierrez-Wing, Cindy Henk, Dr. Rafael Cueto, Sarah Jones, Mariham Abraham, Carolina Rivera, Raleigh Jinks, Mallorie Albrecht, Rongman Cai, Lorna Putnam, Adam Janot, Fei Yao, Dr. Simioan Petrovan, Dr. Qinglin Wu, Dr. Yong Lei, Ioanella Chiparus Glover, Cristina Martinas, Brent Sellers, Dr. George Stanley, Jose Deras, Carlos Astete, Jason Midgett, Chris Akudo, Nick Gerbo, Jason Jordan, Mike Quintana, Tyler Ortego, Danielle Small, Dr. Steven Hall, Milton Saidu, Dr. Michael Mailander, Dr. Cristina Sabliov, Dr. Dorin Bolder, and Dr. Marybeth Lima. To all former and current officemates in addition to Teresa (already named; oh, and Rongman who's not here any more) – Hemant Chowdhary (who helped keep me awake but also dozed off himself sometimes), Amar Hegde (he also liked to sleep sometimes), Shannon Chambers, Haibo Cao, and Hongquiang Hu – thanks for all your companionship and all the laughs. To three people I hardly know – Benjamin Addo, Derek Evans, and Jennifer Ruley – I owe you thanks because I constantly referred to your theses when I was figuring out how to format mine. And last but certainly not least, I would like to thank all of my family and friends for always supporting me and being there for me and understanding that there is a huge difference between school and grad school (even though most of you still don't quite understand why) and it requires a lot of time and that's why it's hard to

pin me down. Don't worry, I'm not going to name all of my friends and family because if I forget one of them, they may take it personal. But, I would like to say thank you and that I love you to my two parents Prentiss Stevens Jr. and Paula Stevens and my girlfriend Sarah Blakey. They have always been there for me when I needed them the most. To anyone that I may have forgotten to mention or have misspelled their name or would rather not be included or is just mad that I did not mention their name, please forgive me.

Table of Contents

List of Tables

List of Figures

Abstract

Anaerobic biodegradation in sewage sludge and aerobic biodegradation in compost of polyhydroxybutyrate (PHB) were investigated to determine degradation kinetics and identify changes in polymer properties. To determine the impact of a natural plasticizer on biodegradation, tributyl citrate (TBC) was blended with some test specimens. For comparison to another bioplastic, polylactic acid (PLA) was biodegraded in the anaerobic study. Evolved gaseous carbon was measured to assess biodegradability according to ASTM standards D5210 and D5338. Mass loss experiments were performed to facilitate determination of degradation kinetics. Melt-pressed plates of the bioplastic with five different initial mass-to-surface-area ratios (plate thicknesses of 0.24, 0.5, 1.2, 3.5 and 5.0 mm) were biodegraded to investigate the relationship between this parameter and decay rate coefficients for first order decay kinetics.

Results showed that degradation rate coefficients were influenced by initial mass-to-surface-area ratio of the bioplastic seemingly according to saturation kinetics. In the first anaerobic mass loss experiment, degradation rate coefficients with respect to initial surface area of the 0.5-mm, 1.2-mm, and 3.5-mm PHB plates were 0.58, 1.29, and 2.07 mg cm^{-2} d^{-1}, respectively. In the second anaerobic mass loss experiment, coefficients for the 0.24-mm, 1.2-mm, and 5-mm PHB plates were 0.32, 0.73, and 0.95 mg cm^{-2} d^{-1}, respectively. Coefficients for the 1.2-mm PHB/15% TBC blend and PLA were 0.38 and 0.00 mg cm^{-2} d^{-1}, respectively. In the first aerobic mass loss experiment, coefficients for the 0.5-mm, 1.2-mm, and 3.5-mm PHB plates were 0.33, 0.62, and 1.57 mg cm^{-2} d^{-1}, respectively. In the second aerobic mass loss experiment, coefficients for the 0.24-mm, 1.2-mm, and 5-mm PHB plates were 0.16, 1.05, and 1.11 mg cm^{-2} d^{-1}, respectively, and 0.04 mg cm^{-2} d^{-1} for the PHB/15% TBC blend. In both degrading environments, the TBC additive hindered the degradation rate of the PHB. Thermal properties,

molecular bonding, and molecular weight as measured by DSC, FT-IR, and Size Exclusion Chromatography, respectively, seemed only slightly affected by biodegradation. Decreasing Izod pendulum impact strength of the PHB was the obvious result of polymer loss. Furthermore, scanning electron micrographs of degraded specimens were recorded for visual illustration of the degradation process.

Chapter 1: Global Introduction and Literature Review

1.1 Introduction

Historically, natural polymers have been used as materials. However, synthetic plastics have dominated the efforts of polymer science for over a century now due to their advantages over their natural predecessors. Three main reasons can be attributed to the continued success of synthetic plastics (Holmes, 1985). First, plant fibers and animal proteins are subject to dramatic fluctuations in quality and availability. One batch of polyethylene is very much like another but the same does not always hold true for most natural materials. Secondly, the petrochemical industry has developed in such a way that oil-derived polymers are cheaper than their natural counterparts, at least in developed countries. Current prices of some traditional plastics are $1.40/kg for polyethylene (PE) and $1.65/kg for polypropylene (PP) (ICIS, 2006). The most important factor is the ease of processing synthetic plastics due to their thermoplastic properties, while only a limited amount of natural materials have thermoplastic processability (Mecking, 2004).

Some major disadvantages of synthetic plastics are the issues involved with their disposal and the reliance on foreign oil for their manufacture. According to the most recent estimates by the USEPA, plastics accounted for 15.4% of approximately 149 billion kg of materials discarded in 2003 (USEPA, 2005). Discarded plastic was exceeded only by paper and paperboard products and food scraps, which accounted for 26.3% and 16.4% of disposed weight, respectively. These numbers should press the issue that non-renewable resources such as the oil used to make most of these petroleum-based plastics are being uselessly wasted rather than recycled. This issue is especially urgent since the proven oil reserves accessible throughout the world are currently estimated to last only 40.6 years at the current rate of production (BP, 2006) and fossil

feedstocks in the form of oil and gas account for more than 90% of the raw materials for the chemical industry (Mecking, 2004). Incineration of plastics has been one method for disposal of petroleum-based products, but other than being expensive, it is also dangerous since harmful chemicals like hydrogen chloride and hydrogen cyanide are released during this process (Reddy et al., 2003).

The biodegradation of bio-based plastics has become a growing topic of interest due to the environmental issues associated with the production and disposal of petroleum-based plastics and the finite supply of and reliance on foreign oil to produce these commodity plastics. A transition to these "bioplastics" would reduce reliance on fossil fuels that are used to make petroleum-based products. The end products of bioplastic degradation are non-toxic and already occur naturally in the environment: carbon dioxide gas (CO_2) and water (H_2O) in aerobic environments and CO_2 and methane (CH_4) gas in anaerobic environments. The degradation of bioplastic additives such as plasticizers could potentially release toxic by-products. However, this could be avoided by using natural additives such as tributyl aconitate (TBA) or tributyl citrate (TBC). Using biodegradable materials to manufacture plastic products that enter the waste stream would significantly reduce the negative environmental impact caused by the previously mentioned methods of disposal used for petroleum-based plastics.

Some of the most extensively studied and most promising bioplastics are Polyhydroxyalkanoates (PHAs). PHAs are a family of biodegradable thermoplastic polyesters that are currently produced as a carbon and energy storage material by many natural and/or recombinant bacteria such as *Escherichia coli*, *Pseudomonas oleovorans*, *Rhodospirillium rubrum*, and *Bacillus megaterium* (Kim and Rhee, 2003; Snell et al., 2002; Steinbüchel and Hein, 2001; Lee, 1996) under unfavorable growth conditions such as limited nitrogen, sulfur,

phosphate, iron, magnesium, potassium, or oxygen and in the presence of excess carbon source (Chen et al., 2001; Kessler and Witholt, 2001; Lee et al., 1999; Lee, 1996; Anderson and Dawes, 1990; Doi et al., 1990). The most prevalently studied PHA is Polyhydroxybutyrate (PHB). PHB exhibits material properties that are similar to those of some common plastics such as polypropylene (Kadouri et al., 2005; Madison and Huisman, 1999; Anderson and Dawes, 1990). Despite similar physical properties such as melting point, degree of crystallinity, and glass transition temperature, PHB is generally stiffer and more brittle and has inferior solvent resistance but better natural resistance to ultraviolet weathering (Holmes, 1985). The ability to modify the material properties of PHAs by controlling their monomeric composition, molecular weight, and final physical form as either a plastic resin or an amorphous latex suspension has attracted much commercial interest (Snell and Peoples, 2002). Raw PHAs are completely biodegradable and can be produced from renewable resources (Chen et al., 2001). Furthermore, the gases that are released by the biodegradation of PHAs will not contain the toxic substances released by the burning of petroleum-based plastics. Some commercially available items have already been produced from PHAs in Europe such as shampoo bottles, which have been demonstrated to be biodegradable in natural aquatic environments (Brandl et al., 1995; Brandl and Püchner, 1992). Another biologically-derived polyester that has attracted great interest as a biodegradable polymer is Polylactic acid (PLA), which is also known to be biodegradable.

One major hurdle in the development and application of PHAs is that their production costs are still higher than those of petroleum-based plastics (Choi and Lee, 1999; Lee and Choi, 1999; Lee et al., 1999). According to Metabolix Inc., the commercial producer of the bioplastic that will be investigated in this proposed research, "commercial scale productions [by fermentative bacteria] have validated production costs at well under $2.20 per kilogram

($1.00/lb)" (Metabolix, 2002). PHAs could potentially be produced at a cost of $0.20 – 0.50/kg if they could be synthesized in plants to a level of 20 – 40% dry weight and thus be competitive with the petroleum-based products (Reddy et al., 2003; Lee, 1996). British Petroleum (BP) and Metabolix are currently exploring routes to the production of PHAs by switchgrass (*Panicum virgatum*) (Tullo, 2005). Production costs should continue to decrease, though, since Metabolix and Archer Daniels Midland Company (ADM) recently announced that they would build the first commercial plant for production of eco-friendly bioplastics by bacterial fermentation that will have an initial annual capacity of 50,000 metric tons per year (Metabolix, 2006). The overall goals of this research thrust are to assess the biodegradation of the MBX3400 bioplastic (PHB) obtained from Metabolix Inc. and to determine how it affects the characteristics of the material.

1.2 Research Objectives

The overall goal of this research thrust will be to determine the biodegradation behavior of the MBX3400 bioplastic supplied by Metabolix, which will be accomplished by meeting the following objectives:

1. Assess and compare the biodegradability of the MBX3400 bioplastic in two waste-degrading environments, namely anaerobic sewage sludge and aerobic compost.
2. Characterize the MBX3400 plastic by several methods to determine physical, chemical, thermal, and mechanical properties before and after degradation in the waste-degrading environments to investigate how biodegradation affects the material's characteristics.

1.3 Literature Review

1.3.1 Background and History of Polyhydroxyalkanoates

PHAs are structurally simple macromolecules that are synthesized by numerous gram-positive and gram-negative bacteria (Madison and Huisman, 1999) as carbon and energy storage

materials when the presence of certain nutrients such as nitrogen, sulfur, phosphate, iron, magnesium, potassium, or oxygen becomes limited in the presence of excess carbon source (Chen et al., 2001; Kessler and Witholt, 2001; Lee, 1996; Anderson and Dawes, 1990; Doi et al., 1990). They are accumulated intracellularly as distinct granules (Madison and Huisman, 1999) and, in the case of Polyhydroxybutyrate (PHB), can constitute as much as 90% of the dry cell weight and reach sizes of up to 1.0 μm (Gerngross and Martin, 1995). PHB is the most common and extensively studied PHA, and the ability of bacteria to accumulate PHA is often used as a taxonomic characteristic for classifying microorganisms (Madison and Huisman, 1999). Since the discovery of the original homopolymer poly[(*R*)-(—)-3-hydroxybutrate] (PHB) by Lemoigne in 1925 (as cited in van der Walle et al., 2001; Lemoigne, 1926), the family of PHAs has been expanded dramatically (Gerngross and Martin, 1995). Patents for PHB were first filed in the United States by Baptist and Werber at W.R. Grace & Co. in 1962 (Phillip et al., 2007; Anderson and Dawes, 1990; Baptist, 1962a; Baptist, 1962b) to produce and isolate PHB for fabrication of articles such as sutures and prosthetic devices. However, they discontinued their efforts since fermentation yields were low and tainted with bacterial residues, and the solvent extraction was very expensive. PHB was long thought to be the only polyester produced by microorganisms until 1974 when polyesters containing 3-hydroxyalkanoate units longer than 3-hydroxybutyrate were discovered in microorganisms in sewage sludge (Kim and Lenz, 2001; Wallen and Rohwedder, 1974). Today, more than 100 different monomer units have been identified as constituents of PHAs creating the possibility of producing almost a limitless number of unique PHAs (Reddy et al., 2003). A review of many different hydroxyalkanoic acids (HAs) which have been found to be constituents of biosynthetic PHAs can be found in the work of Steinbüchel and Valentin (1995).

Further development of PHB was begun by Imperial Chemical Industries (ICI) in 1975–1976 largely in response to a renewed interest in biodegradable plastics as a result of the oil crisis of 1973 (Phillip et al., 2007; Reddy et al., 2003; Holmes, 1985). However, drawbacks included polymer brittleness, poor mechanical properties, and high production costs bringing the development of PHB to a halt after the oil crisis subsided. In the meantime, ICI began the first industrial production of PHAs in 1982 by fermenting the novel polymer polyhydroxybutyrate-*co*-hydroxyvalerate (PHBV) – a copolymer of 3-hydroxybutyrate and 3-hydroxyvalerate – from *Ralstonia eutropha* (formerly *Alcaligenes eutrophus*) and marketing it with the trade name BIOPOL® (Phillip et al., 2007; Reddy et al., 2003; Anderson and Dawes, 1990), which had improved properties over PHB homopolymer including lower crystallinity and more elasticity. ICI split in June 1993 and the Zeneca BioProducts branch of ICI took control of BIOPOL®, but then sold the technology to Monsanto in April 1996, which sold the license to Metabolix Inc. in 1998 (Phillip et al., 2007). A spin-off company which leads the technology in developing medical devices from biologically derived biodegradable polymers, Tepha Inc., was also formed in 1998 after collaboration between Metabolix Inc. and Children's Hospital, Boston (Phillip et al., 2007).

Over 75 different genera of bacteria are capable of producing PHAs (Reddy et al., 2003), while some of the most extensively studied species include *Alcaligenes latus*, *Azotobacter vinelandii*, recombinant *Escherichia coli*, *Pseudomonas oleovorans*, *Rhodospirillium rubrum*, and *Bacillus megaterium* (Kim and Rhee, 2003; Snell et al., 2002; Steinbüchel and Hein, 2001; Lee, 1996). Metabolic engineering is being intensely explored to introduce new metabolic pathways to broaden the utilizable substrate range and to enhance PHA synthesis (Reddy et al., 2003). Commercialization of plant-derived PHAs will require the creation of transgenic crop

plants that, in addition to high product yields, have normal plant phenotypes and transgenes that are stable over several generations (Reddy et al., 2003). The ultimate goal of the transgenic approach is to produce PHAs in plant crops to make them price competitive with traditional oil-derived plastics (Williams et al., 1999). Production of PHAs on an agronomic scale could allow synthesis of biodegradable plastics in the million-ton scale compared to bacterial fermentation, which produces in the thousand-ton scale (Reddy et al., 2003). Researchers have already successfully produced PHB in transgenic crops. Nawrath et al. (1994) incorporated modified bacterial genes coding for enzymes necessary to synthesize PHB from acetyl-CoA into *Arabidopsis thaliana* (Thale cress). The plants accumulated PHB up to 14% of the dry weight. Valentin et al. (1999) produced PHB in the same species at levels of 12 – 13% of plant dry mass. Other crops which have been successfully modified to produce PHB include rapeseed (*Brassica napus*) (Houmiel et al., 1999), corn (*Zea mays*) (Poirier and Gruys, 2002), tobacco (*Nicotiana tabacum*) (Lössl et al., 2003), flax (*Linum usitatissimum* L.) (Kourtz et al., 2005; Wróbel et al., 2004), and sugarcane (*Saccharum* spp. hybrids) (Petrasovits et al., 2007). However, increasing polymer yield in these plants has proven to be a major hurdle in this approach. Further efforts to increase polymer yield and in healthy plants without altered phenotypes often observed in high PHB producers (Poirier and Gruys, 2002; Bohmert et al., 2000) will probably require the expression of additional enzyme activities (Kourtz et al., 2005).

1.3.2 Properties of Polyhydroxybutyrate and Other Copolymers

Most of the known PHAs are polymers of 3-hydroxyacids (Anderson and Dawes, 1990) and have the general molecular structure shown in Figure 1.1. For PHB, the substituent group (R) is a methyl group

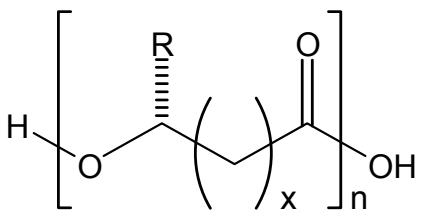

Figure 1.1. General structure of a PHA.

(CH_3). PHAs can be classified as either short-chain-length PHA (PHA_{SCL}) consisting of 3 – 5 carbon atoms or medium-chain length PHA (PHA_{MCL}) (Lee and Choi, 1999; Lee and Chang, 1995). PHB is classified as a PHA_{SCL}. PHA_{SCL} generally have thermoplastic properties while PHA_{MCL} are more elastomeric (Kim and Lenz, 2001). PHB is in a fluid amorphous state inside the bacterial cell but becomes highly crystalline and, therefore, a more stiff and brittle material following extraction using organic solvents (Madison and Huisman, 1999). Kawaguchi and Doi (1990) characterized the structure of native PHB granules from *Alcaligenes eutrophus* by X-ray diffraction both before and after isolation from the cells by treatment with enzymes and sonic oscillation. The PHB granules in intact cells were completely amorphous, but became crystalline after treatment with alkali or sodium hypochlorite. Isolated PHB granules remained amorphous in suspension but were crystallized by various treatments with aqueous acetone, alkaline solution (either NaOH or sodium hypochlorite), and lipase in an aqueous environment indicating that crystallization of PHB molecules is started by the removal of a lipid component from native granules by various treatments.

PHB is a rather brittle material and is somewhat difficult to process since it decomposes at a temperature roughly 10ºC above its melting point (Luzier, 1992). Adding hydroxyvalerate (HV) to PHB causes several improvements, including a drop in melting point, reduction in average crystallinity, and increased flexibility and toughness, but a decrease in tensile strength (Kim and Lenz, 2001; Barham and Organ, 1994; Luzier, 1992). This assertion is supported by the work of Mitomo et al. (1987) who analyzed single crystal mats of PHB and its copolymers of Polyhydroxybutyrate-*co*-hydroxyvalerate (PHBV) by differential scanning calorimetry (DSC). They demonstrated that the melting peaks shift to lower temperatures and decrease in their peak areas (proportional to both melting enthalpy and crystallinity) as the HV content increases. The

researchers also showed that the temperature at which the polymers are allowed to crystallize from the melt will affect the melting temperature. Many works such as that of An et al. (1998) have shown that the final properties of PHB will depend largely on the degree of crystallinity, which, in turn, is affected by crystallization conditions. Results show that the crystallization rate increases with increasing heating/cooling rates, while the half-time of crystallization decreases. El-Taweel et al. (2004) demonstrated the influence of molar mass and glass-transition temperature (T_g) of the amorphous component, and the influence of composition and crystallinity on tensile properties of PHB blends. It was shown that the addition of low molecular mass additives to PHB decreases T_g, stress at rupture (σ_r), and the extension ratio (λ_r). Also, a decrease of Young's modulus (E) and σ_r can be correlated to a decrease in crystallinity. Like PHB, its copolymer, PHBV has been studied to a great extent, but mostly for copolymers containing less than 25% HV with only a few reports containing data for PHBV with greater than 50% HV (Kim and Lenz, 2001). In one rare study, Choi and researchers (2004) studied the relationship between HV content and average crystallinity for PHBV with up to 60% HV content. Table 1.1 lists some of the typical properties of PHB and PHBV (with 10% and 20% HV content).

Table 1.1. Typical properties of PHB and of PHBV with 10% and 20% HV content (adapted from Luzier, 1992).

	HV content, mol%		
Property	0	10	20
Melting Point, °C	177	140	130
Crystallinity, %	80	60	35
Tensile Strength, MPa	40	25	20
Flexural Modulus, GPa	3.5	1.2	0.8
Extension at break, %	8	20	50
Notched Izod impact strength, J/m	60	110	350

The molecular weight (M_w) of PHAs is generally around 50,000 to 1,000,000 Da (Madison and Huisman, 1999) and is dependent upon both biotechnological and downstream processing conditions involved in the production process. Although the exact mechanisms that affect the molecular weights of PHAs in bacterial cells are not completely understood, it is known that the parameter varies greatly depending on the microorganism and feedstock used, as well as the method of extraction (van der Walle et al., 2001).

Processing conditions tend to have major effects on the properties of PHAs in addition to post-processing conditions. The melting temperature decreases with increasing processing temperature, which is caused by decreasing molecular weight as demonstrated by Renstad et al. (1997). The researchers found that the recrystallization processes during DSC analysis give variations in the melting endotherms and/or perfection governed by the processing conditions. Additionally, it was concluded that double melting endotherms, which are often found in PHB and PHBV, are caused by melting and recrystallization of thin, unstable crystals during the DSC scan. However, X-ray scattering results indicated that the degree of crystallinity is largely unaffected by the processing conditions. Even after processing and under normal ambient conditions, PHB undergoes changes due to physical aging such as an asymptotic increase of the tensile modulus from approximately 1.5 GPa to 3.5 GPa caused by progressive crystallization (de Koning and Lemstra, 1993; Scandola et al., 1989; Barham et al., 1984).

Since PHAs are partially crystalline polymers, their thermal and mechanical properties are often represented in terms of the glass-transition temperature (T_g) of the amorphous phase and the melting temperature (T_m) of the crystalline phase (Anderson and Dawes, 1990). Barham et al. (1984) estimated the glass-transition temperature of PHB using two methods, one mechanical and the other dilatometric. The mechanical data suggested that at 0.1 Hz, T_g lies

between –5 and 5°C, and dilatometric results suggested T_g lies between –4 and 1°C. The same researchers also determined that the degree of crystallinity of PHB can be calculated from the ratio $\Delta H_f/\Delta H_f^0$, where ΔH_f and ΔH_f^0 are the observed enthalpy of fusion and the enthalpy of fusion of perfect PHB crystal (= 146 J g^{-1}), a technique which has also been widely used by many other researchers (Chiu and Shu, 2005; El-Hadi et al., 2002; Yoshie et al., 2000; Ikejima et al., 1999; Barham and Keller, 1986). The melting temperature (T_m) of PHB reported in literature varies widely, but seems to be in the range of 174 – 180°C (Luzier, 1992; Anderson and Dawes, 1990; Barham et al., 1984). Carrasco et al. (2006) reported the temperatures at which 5% and 95% of mass was lost during thermogravimetric analysis (TGA) of PHB and PHBV and denoted the values T_5 and T_{95}, respectively. For PHB, they reported T_5 and T_{95} values of 246.3°C and 275.0°C, and for PHBV, values of 260.4°C and 287.7°C, respectively. Cyras et al. (2000) tested the thermal stability of PHBV (8% HV) by TGA and the effects of thermal degradation on other characteristics as measured by Fourier Transform infrared spectroscopy (FT-IR), ^{1}H-NMR spectroscopy, viscosity-average molecular weight analysis, DSC, and tensile testing. Samples degraded for 30 min at 175 and 240°C were analyzed by FT-IR. Carbonyl and double-bond peaks appeared for the samples degraded at 240°C when compared to those that were not thermally degraded. The double-bond peaks did not appear for the sample treated for 30 min at 175°C, but did appear after 120 min. The carbonyl peak shifted to a lower wavenumber (cm^{-1}) because the ester C=O is conjugated with C=C groups. The ^{1}H-NMR spectrum of the sample degraded at 175°C showed a signal at 2.9 ppm that was attributed to methylic protons in the ending vinyl group. The results confirmed that the mechanism of thermal degradation can be explained in terms of chain scission of the ester linkages, which leads to the formation of crotonic acid. Results of the viscosity-average molecular weight, M_v, showed that a high

decrease of the molecular weight occurred during the first 15 min during thermal degradation at 175°C. DSC analysis showed that the melting enthalpy of the samples crystallized after isothermal degradation decreased with degradation time and elongation-to-break values obtained by tensile testing decreased during the first stage of thermal degradation, maybe due to a higher degree of crystallinity.

Kemnitzer et al. (1995) observed crystallization behavior of predominantly syndiotactic PHB. The researchers compared thermal properties obtained by DSC of natural origin PHB to predominantly syndiotactic PHB (Syn-PHB) of variable syndioregularity (syndad fractions of 0.59, 0.62, 0.64, and 0.71). After crystallization of syn-PHB at elevated temperatures, ambient temperature annealing resulted in an initial melting transition at ~50°C, which showed little to no dependence on syndioregularity or the elevated T_c used. Both 0.62- and 0.71-syn-PHB showed low levels of crystallinity (17% and 25%, respectively) and poorly formed crystals by wide-angle X-ray scattering (WAXS). Isothermal crystallization monitored by DSC showed that the fastest crystallization rates for predominantly syn- and natural PHB occur between ~50 to 70°C and ~60 to 90°C, respectively. From study of the dependence of a second melting transition on T_c, it was determined that the equilibrium T_m for 0.62- (M_n = 83,700 g/mol) and a 0.64-syn-PHB (M_n = 11,900 g/mol) were ~157 and 154°C, respectively. Chun and Kim (2000) observed thermal properties of blends of PHBV with Poly(styrene-*co*-acrylonitrile) (SAN). PHBV (7% HV)-SAN (28% AN) blends of 10:0, 7:3, 5:5, 3:7, and 0:10 PHBV/SAN were subjected to analyses by DSC and TGA. PHBV and SAN are immiscible as indicated by the almost unchanged T_g and T_m of PHBV-SAN blends compared to pure PHBV. Nucleation of PHBV in the blends was suppressed by the addition of SAN as indicated by decreased crystallization rate during isothermal crystallization as compared to pure PHBV. Other literature which provides ample research

Table 1.2. Outline of additional literature concerning thermal properties of PHAs.

Researchers	Materials Tested	Significant Findings
Bauer and Owen (1988)	PHB PHBV (17%, 25-30% HV)	Copolymerization of PHB with PHV forms a more ductile material with more amendable orientation properties. The behavior of cracks in the copolymer spherulites suggests that the morphology is less continuous than that of the homopolymer. Copolymerization lowers the softening point of the films, but can be influenced to some extent by heat conditioning and appears to be correlated with the onset of melting observed by DSC. WAXS measurements suggest that HV units act as distortions in the PHB lattice.
He et al. (2001)	PHB PHBV (30% HV) P(HB–HHx) (15% HHx) (PHB-*co*-hydroxyhexanoate)	Weight loss of PHB, PHBV, and P(HB–HHx) by thermal degradation was a one-step process with degradation temperatures increasing with heating rate. Peak widths of DTG curves increased with heating rate and were also wider for PHBV and even higher for P(HB–HHx), indicating that the copolymers degraded slower than the homopolymer and all did so with increase in heating rate. Incorporation of HV or HHX into the homopolymer rendered the polymer chain more flexible, as indicated by decreases in T_g and T_m, so PHBV and P(HB–HHx) were more thermally stable.
Li et al. (2001)	PHB PHBV (10% HV) PHBV (30% HV)	The weight loss of PHB due to thermal degradation is a one-step process, while that of PHBV is a two-step process, most likely due to different evaporation rates of the HB and HV monomers. Thermal degradation temperatures of the polymers increase with increasing heating rate as a result of heat hysteresis. Thermal degradation temperatures increased with increasing HV content, indicating that the incorporation of HV improves thermal stability.
Chan et al. (2004)	PHB (R-configuration) D-PHB PHBV (12% HV) Blends of PHB and one of the other polymers in varying composition	Longer annealing times after melting for PHB and PHBV result in relatively fast thermal degradation. Weight average molecular mass of PHB and PHBV decrease linearly with annealing temp. at constant annealing time. The equilibrium melting point of D-PHB is significantly lower than that of PHB. Melting enthalpy and, therefore, crystallinity, of PHB/D-PHB blends does not change with blend composition. Melting enthalpy and crystallinity of PHB/PHBV blend decrease slightly with increasing PHBV content.
Chen et al. (2005)	P(HB–HHx) (15% HHx)	Multiple DSC melting peaks were observed for samples which had undergone isothermal and non-isothermal crystallization. The melting peak at the lower temperature was attributed to the melting of crystals formed during isothermal and non-isothermal crystallization, while the melting peak at the higher temperature was a result of recrystallization that took place during the heating process.

concerning thermal stability and thermal analysis of PHAs and the effects of thermal degradation on properties analyzed by these methods and others can be found in the works of Bauer and Owen (1988), He et al. (2001), Li et al. (2001), Chan et al. (2004), and Chen et al. (2005). Significant findings of these works are outlined in Table 1.2.

Verhoogt et al. (1996) studied the viscosity of PHBV by Dynamic Shear Rheometry (DSR). They reported viscous stability only at 160ºC for PHBV (12% HV). At 170ºC, they observed a 10% reduction in the complex viscosity was already obtained after 200 s, while a residence time of only 2 min resulted in a decrease in viscosity of almost 10% at 180ºC and of more than 20% at 200ºC.

1.3.3 Previous Biodegradation Research

In past years, it has been more prevalent for PHAs to be studied *in vivo* while in the form of microscopic granules or inclusions within the bacterial cells in which they were synthesized. The mechanisms of their intracellular formation (Snell et al., 2002; Steinbüchel and Hein, 2001; Madison and Huisman, 1999; Wong and Lee, 1998; Gerngross and Martin, 1995; Lee and Chang, 1995; Byrom, 1987) and the formed inclusions (Song et al., 1998; Amor et al., 1991; Kawaguchi and Doi, 1990) have been observed and characterization of the involved enzymes performed. Characterization of the intracellular degradation and involved enzymes has also been common (Handrick et al., 2004; Jendrossek and Handrick, 2002; Jendrossek et al., 1996). However, the properties of PHAs are usually somewhat different *in vivo* than they are once extracted from the bacterial cells. For example, isolation of PHB granules by all but the mildest techniques causes seemingly irreversible crystallization of the polymer (Horowitz and Sanders, 1994). Only in more recent years has research of their extracellular degradation and characterization become more prevalent.

1.3.3.1 Mechanisms of Extracellular PHA Biodegradation

The presence of ester bonds in PHAs (Brandl et al., 1995) and the material's susceptibility to microbial attack of its carbon backbone as a carbon source (Jayasekara et al., 2005; Gage, 1990) facilitate biodegradation of the polymer. Outside of PHA-accumulating cells, PHA degradation is carried out by extracellular PHA depolymerases possessed by many PHA-degrading bacteria and fungi. Examples of the many genera of PHA-degrading bacteria include *Bacillus*, *Pseudomonas*, *Streptomyces*, and *Alcaligenes* (Jendrossek et al., 1996) while examples of fungi include the genera *Aspergillus*, *Penicillium*, *Paecilomyces*, *Ascomycetes*, *Basidiomycetes*, *Deuteromycetes*, *Mastigiomycetes*, *Myxomecetes*, and *Zygomycetes* (Lee et al., 2005; Kim and Rhee, 2003; Sang et al., 2002; Jendrossek et al., 1996). The PHA depolymerases of these microorganisms are secreted for utilization of PHA left in the environment after the bacteria that synthesized the PHAs have died and their cells have lysed (Jendrossek et al., 1996). It is necessary to differentiate between intracellular and extracellular PHAs since they are present in two different biophysical states and must be degraded by two different types of depolymerases (Jendrossek and Handrick, 2002; Jendrossek, 2001; Jendrossek et al., 1996). The differences in intracellular and extracellular PHAs were discussed in section 1.3.2.

Extracellular biodegradation of PHAs occurs in two steps (Hakkarainen, 2001; Lee and Choi, 1999; Scherer et al., 1999; Iwata et al., 1997; Hocking et al., 1996). First, enzymatic hydrolysis at the surface degrades polymer chains by *endo*-scissions randomly throughout the chain. Second, the resulting oligomers are cleaved by *exo*-scissions from the chain ends. The resulting monomers are taken up and metabolized in the cell to yield carbon dioxide (CO_2) and water (H_2O) in aerobic conditions and methane (CH_4), H_2O, and CO_2 in anaerobic conditions. This enzymatic degradation occurs at the exposed surface of the polymer as has been

demonstrated by Iwata et al. (2002). All PHA depolymerases examined to date are specific for polymers consisting of monomers in the (R)-configuration.

There are three key elements indispensable for biodegradation. If any one of these elements is lacking, biodegradation will not occur (Grima et al., 2000). Additionally, all of these parameters will affect the rate of biodegradation of PHA:

1. Organisms: The basis for any biodegradation process is the existence of microorganisms with the appropriate metabolic pathways to synthesize enzymes specific for the depolymerization process and to mineralize the monomers and oligomers formed by these polymers.
2. Environment: Important environmental factors include temperature, moisture, salts, and oxygen. The presence or absence of each of these and the level, if present, will also affect the consortia of microorganisms that will degraded the PHA since environmental factors are so important to how well and where microorganisms will thrive. The most significant element is the moisture factor since without it, biodegradation cannot occur.
3. Substrate: The structure of the polymer influences the biodegradation process. These structural factors include chemical bonds, degree and type of branching, degree of polymerization, degree of hydrophobicity, stereochemistry, molecular weight distribution, crystallinity, and other aspects of morphology.

The following equations summarize the chemical degradation process (Grima et al., 2000):

Aerobic Conditions (C = carbon):

$$C_{polymer} + O_2 \rightarrow CO_2 + H_2O + C_{residue} + C_{biomass} + salts \quad (1)$$

Anaerobic Conditions:

$$C_{polymer} \rightarrow CO_2 + CH_4 + H_2O + C_{residue} + C_{biomass} + salts \quad (2)$$

Under anaerobic conditions, the mole fraction of CO_2 and CH_4 produced by a substance can be calculated based on the stoichiometry of the reaction using the Buswell-equation (Buswell and Mueller, 1952):

$$C_n H_a O_b + \left[n - \frac{a}{4} - \frac{b}{2} \right] H_2 O \rightarrow \left[\frac{n}{2} - \frac{a}{8} + \frac{b}{4} \right] CO_2 + \left[\frac{n}{2} + \frac{a}{8} - \frac{b}{4} \right] CH_4 \quad (3)$$

The Buswell-equation has been solved below for PHB ($C_4H_6O_2$):

$$C_4 H_6 O_2 + \left[4 - \frac{6}{4} - \frac{2}{2} \right] H_2 O \rightarrow \left[\frac{4}{2} - \frac{6}{8} + \frac{2}{4} \right] CO_2 + \left[\frac{4}{2} + \frac{6}{8} - \frac{2}{4} \right] CH_4 \quad (4)$$

$$C_4 H_6 O_2 + 1.5 H_2 O \rightarrow 1.75 CO_2 + 2.25 CH_4 \quad (5)$$

Upon further calculation, the theoretical CH_4/CO_2 ratio of gas produced by anaerobic degradation of PHB is 56.25%/43.75%. Knowledge of the mole fraction of each gas is necessary if only CH_4 is measured or if total gas is measured and an aqueous medium is used because of the high water solubility of CO_2 (Shelton and Tiedje, 1984). Anaerobic methods are always subject to error from O_2 contamination. However, the high O_2-consuming capacity of most sludges, the use of new, thick butyl rubber stoppers (Fulghum and Worthington, 1977; Hungate et al., 1966), and the use of standard anaerobic methods should prevent any serious errors (Shelton and Tiedje, 1984). There are many different methods and standards available for assessing the biodegradation of polymers and plastics upon exposure to many different environments under both aerobic and anaerobic conditions. Many widely-used standards for assessing biodegradation are distributed by ASTM International. The standards used for this research thrust are ASTM D5210-92 (Standard Test Method for Determining the Anaerobic Biodegradation of Plastic Materials in the Presence of Municipal Sewage Sludge; Reapproved 2000) for anaerobic biodegradation in municipal sewage sludge and ASTM D5929-96 (Standard Test Method for Determining Biodegradability of Materials Exposed to Municipal Solid Waste

Composting Conditions by Compost Respirometry; Reapproved 2004) and ASTM D5338-98 (Standard Test Method for Determining Aerobic Biodegradation of Plastic Materials Under Controlled Composting Conditions; Reapproved 2003). These standards assess biodegradation based on monitored biogas consumption/production due to the degradation process. A survey of many common methods used for monitoring biodegradation for both anaerobic and aerobic conditions can be found in the works of Gu and Gu (2005) and Calmon-Decriaud et al. (1998).

1.3.3.2 Biodegradation Experiments in Anaerobic Sewage Sludge

Table 1.3 summarizes the studies outlined in this section for easy comparison.

Table 1.3. Comparison of results of the anaerobic degradation experiments outlined.

Researchers	Materials Degraded	Significant Findings
Budwill et al. (1992)	PHB	87% ThGP in 16 days
	PHBV (10% HV)	96% ThGP in 16 days
	PHBV (20% HV)	83% ThGP in 16 days
Abou-Zeid et al. (2004)	PHB	In sewage sludge, 100% degradation by both mass loss and biogas within 6 weeks
	PHBV (11.6% HV)	In sewage sludge, 100% degradation by both mass loss and biogas within 14 weeks
	PCL	In 6 weeks, degraded only 17 and 30% by mass loss and biogas, respectively
		Slightly less degradation occurred for all materials in laboratory sludge than sewage sludge
Puechner et al. (1995)	PHB	80% ThGP after 20 days
	Mater-Bi ZF03U	22% ThGP after 60 days
	Bioceta	28% ThGP after 60 days
	PCL	0% ThGP after 60 days
Federle et al. (2002)	PHBO (10% HO)	88% ThGP after 61 days
	PCL	0% ThGP after 122 days
Shin et al. (1997)	PHBV (8% HV)	89% ThGP in 40 days
	Cellophane	80% ThGP in 30 days
	Poly-L-Lactic Acid (PLA)	No degradation in 100 days
	Eslon Green grade AI1010	No degradation in 100 days
	Sky Green grade I111	No Degradation in 100 days
Gartiser et al. (1998)	PHBV	60 – 75% ThGP in 30 days
Reischwitz et al (1998)	PHBV (8.4% HV)	95% ThGP on basis of CH_4 production in 30 days
Imam et al. (1995)	PHBV (12% HV)	78% mass loss in 35 days
	PHBV/30% cornstarch	68% mass loss in 35 days
	PHBV/50% cornstarch	70% mass loss in 35 days
	PHBV/30% PEO-coated starch	48% mass loss in 35 days
	PHBV/50% PEO-coated starch	59% mass loss in 35 days

PHAs are known to degrade well in anaerobic environments such as anaerobically digested sewage sludge. In a biodegradation experiment performed by Budwill et al. (1992), poly(3-hydroxybutyrate) (PHB), and two copolymers of 3-hydroxybutyrate and 3-hydroxyvalerate [P(HB-co-HV)]: P(HB-co-13% HV) and P(HB-co-20% HV) were degraded in an anaerobic sewage sludge consortium. After 16 days of incubation, the total amount of gas produced was 87, 96, and 83% of the theoretical gas production (ThGP), respectively, showing the rapid rate of degradation of the materials.

PHAs commonly show superior biodegradability to other commonly studied biodegradable plastics. Abou-Zeid et al. (2004; Abou-Zeid et al., 2001) studied the degradation of PHB, PHBV, and poly(Є-caprolactone) (PCL) in anaerobic sewage sludge at 37°C by methods of mass loss determination and biogas formation. For PHB and PHBV, 100% degradation was observed by both mass loss determination and biogas formation within 6 and 14 weeks of degradation, respectively. PCL showed only 17% and 30% degradation by mass loss determination and biogas formation, respectively, after 6 weeks of degradation. Furthermore, the fact that PHB degraded more quickly than PHBV indicates that HV content may hinder the degradation process. Samples were also degraded anaerobically in a methane-producing laboratory sludge (LS) at 37°C, which caused less degradation than the sewage sludge for all the samples. A plethora of related work from the same researchers can also be found in the Ph.D. dissertation completed by Abou-Zeid (2004) in which the degradation of these polymers is compared among many different types of conditions including a pH-controlled bioreactor, which greatly enhanced the degradation of the polymers. PHA-degrading microorganisms were also isolated from degrading sludges and further analyzed and characterized using clear-zone plating techniques. Also, the effects of additional substrates were evaluated for their effects on the

biodegradation of the polymers of interest. In another experiment involving both PHB and PCL, Puechner et al. (1995) assessed biodegradation of the materials based on biogas production upon exposure to a diluted domestic sewage sludge medium incubated at 35°C. For PHB, 80% of ThGP was observed after 20 days while biogas production in reactors containing PCL films never exceeded that of the blanks after 60 days of incubation. Other materials tested were the commercial polymers Mater-Bi ZF03U (starch; natural additives, and PCL as main component, vinyl-alcohol copolymer as minor component) and Bioceta (cellulose diacetate with approximately 20% natural additives) which reached 22% and 28% of ThGP, respectively, after 60 days of incubation. Federle et al. (2002) also degraded PCL in addition to poly(3-hydroxybutyrate-*co*-hydroxyoctanoate) (PHBO) in an anaerobic sewage sludge medium. The researchers observed 88% ThGP for the PHBO after 61 days and 0% ThGP for the PCL after 122 days.

In some cases, PHAs may exhibit slower rates of degradation than other polymers, yet still show more biodegradability. Shin et al. (1997) degraded films of PHBV copolymer containing 8% hydroxyvalerate and films of cellophane in diluted digester sludge. Within 40 days, 89% degradation of the PHBV was observed on the basis of gas evolution after an apparent slow start compared to 80% for cellophane within 30 days without an apparent lag phase. Three synthetic aliphatic polyesters, poly-L-lactic acid (PLA) and two commercial polymers, Eslon Green grade AI1010 [poly(butylene succinate) supplied by Cheil Synthetics, Inc.] and Sky Green grade I111 film [poly(butylene succinate-*co*-ethylene succinate) supplied by SunKyung Ind. Inc.] did not show any significant biodegradation during 100 days of exposure in the same experiment.

Two additional experiments further illustrate the biodegradability of PHAs in anaerobic sewage sludge. Gartiser et al. (1998) studied the degradation of PHBV films in diluted digester sludge and observed 60–75% of theoretical biogas production from the PHBV copolymer within 30 days. Reischwitz et al. (1998) investigated the biodegradation of PHBV (8.4% HV) in a 10% (w/w) methanogenic sludge (0.25% VSS) dissolved in mineral salts solution and 1% (w/w) polymer powder at 35ºC and pH 7.2 in the dark. Within 30 days, the polymer was converted to carbon CO_2 and CH_4. On the basis of the amount of methane produced, a conversion of 95% to biogas was calculated. Assuming 4% polymer-carbon conversion to biomass (calculated from protein content), a total degradation of 99% was reached in 30 days. In the work of Imam et al. (1995), injection-molded composites were prepared by blending PHBV with native cornstarch (30% and 50%) and with cornstarch pre-coated with polyethyl-eneoxide (PEO) as a binding agent in addition to the pure PHBV (12% HV) and degraded in municipal activated sludge. In that work, all composites lost mass, ranging from 48 to 78% within 35 days.

1.3.3.3 Biodegradation Experiments in Aerobic Compost

Table 1.4 summarizes the studies outlined in this section for easy comparison. Another widely studied environment for biodegradation of bioplastics is aerobic compost since it has become such a widely used method of waste disposal. One problem with what can be found in the literature is the dissimilar results that are obtained among different experiments. Some literature will report long periods of time (on the order of months being required for extensive degradation of PHAs and other bioplastics), while others may report that it requires only weeks or even days. This may be due to the solid-state conditions of compost where critical factors such as moisture and microbial consortia can be hard to control, while it may also largely depend on the type of compost used, the degrading organisms involved, and incubation temperature.

Table 1.4. Comparison of results of the aerobic degradation experiments outlined.

Researchers	Materials Degraded	Significant Findings
Manna and Paul (2000)	PHB	After 100 days 8.5 ± 0.3% mass loss at 20°C 15.9 ± 0.5% mass loss at 30°C 14.3 ± 0.5% mass loss at 40°C After 200 days 14.8 ± 0.3% mass loss at 20°C 24.5 ± 1.0% mass loss at 30°C 23.4 ± 0.8% mass loss at 40°C
Gilmore et al. (1992)	PHBV (26.5% HV)	58.8% mass loss in 186 days
Ohtaki and Nakasaki (2000a)	PHBV PCL	57.9% mass loss in 8 days 81.4% mass loss in 8 days
Gilmore et al. (1992)	30% PCL/70% LLDPE	Duplicate pieces lost 3.4% and 4% mass after 126 days. No more than 13% of PCL was degraded
Mergaert et al.(1994)	PHB	6% mass loss (compost A) in 150 days
	PHBV (10% HV)	4% mass loss (compost A) in 150 days 5% mass loss (compost B) in 150 days 14% mass loss (compost C) in 150 days
	PHBV (20% HV)	70% mass loss (compost A) in 150 days
Imam et al. (1998)	PHBV (12% HV) PHBV/30% cornstarch PHBV/50% cornstarch PHBV/30% PEO-coated starch PHBV/50% PEO-coated starch	7% mass loss in 125 days 25% mass loss in 125 days 49% mass loss in 125 days 21% mass loss in 125 days 55% mass loss in 125 days

In an experiment performed by Manna and Paul (2000), sheets of PHB (0.25-mm thick) were aerobically degraded in an unspecified type of compost and mass loss over time was measured at three different temperatures. Average triplicate sets ± standard deviation were reported. After 100 days of degradation, 8.5 ± 0.3% mass loss was observed at 20°C, 15.9 ± 0.5% at 30°C, and 14.3 ± 0.5% at 40°C. After 200 days of degradation, 14.8 ± 0.3% mass loss was observed at 20°C, 24.5 ± 1.0% at 30°C, and 23.4 ± 0.8% at 40°C. It seems that the optimal incubation temperature to achieve degradation for the compost used would have been between 30 and 40°C. In contrast, Gilmore et al. (1992) observed 58.8% mass loss of dog bone-shaped films of PHBV (26.5% HV; from ICI, Billingham, UK) with 0.5-mm thickness after 186 days in a natural leaf compost pile in which the temperature ranged from 40 to 52°C. Ohtaki and

Nakasaki (2000a) observed 57.9% degradation of PHBV films with 0.05-mm thickness after just 8 days of exposure to a municipal solid waste consisting of commercial dog food with the trade name VITA-ONE™, sawdust as a bulking agent, and an inoculum with the trade name Ohless G™ while incubating the system at 50°C. In the two latter works, other biodegradable plastics were also degraded in the described environments including PCL, which was reported earlier in this review to be less degradable than PHB or PHBV in anaerobic sewage sludge. The researchers observed 81.4% degradation for PCL after just 8 days of exposure indicating that it was significantly more degradable than the PHBV. However, another modified PCL was also tested which showed 57.8% degradation after 14 days which was just slightly less than observed for PHBV. Other materials tested by Ohtaki and Nakasaki (2000a) are listed in Table 1.5 and the results obtained in Table 1.6, and a related work from the same researchers can be also be found (Ohtaki and Nakasaki, 2000b). The PCL tested by Gilmore et al. (1992) was blended with linear low density polyethylene (LLDPE) to make a 30% PCL mixture, although the two components were immiscible leaving a matrix of LLDPE with enclosed spheres of PCL. Duplicate test

Table 1.5. Eight types of biodegradable plastic that were tested for biodegradation in the aerobic experiment in compost performed by Ohtaki and Nakasaki (2000a).

Type	Trade name	Manufacturer/provider	Composition of polymer (molecular formula)
BP1	CELGREEN (PH7)	Daicel Chemical Industries, Osaka, Japan	Poly (ε-caprolactone) —[O—(CH_2—)$_5$—CO—] n—
BP2	CELGREEN (PHB02)	Daicel Chemical Industries, Osaka, Japan	Modified poly (ε-caprolactone)
BP3	Biopol	Monsanto Japan, Tokyo, Japan	Condensation polymer of β-hydroxybutyrate and β-hydroxyvalyrate —[O—$CHCH_3$—CH_2—CO—]x—[O—CHC_2H_5—CH_2—CO—] y—
BP4	Mater-Bi	Nippon Synthetic Chemical Industry, Osaka, Japan	Polymer alloy of starch, modified polyvinyl alcohol and aliphateic polyester —[CH_2CH_2—]x—[CH_2CH—OH—]y—, and starch
BP5	BIONOLLE (#1001)	Showa Denko K.K. / Showa Highpolymer, Tokyo, Japan	Condensation polymer of 1, 4-butanediol, succinic acid —[O—(CH_2—)$_4$—O—CO—(CH_2—)$_2$—CO—]n—
BP6	BIONOLLE (#3001)	Showa Denko K.K. / Showa Highpolymer, Tokyo, Japan	Condensation polymer of 1, 4-butanediol, succinic acid and adipic acid —[O—(CH_2—)$_4$—O—CO—(CH_2—)x—CO—]n— (x = 2, 4)
BP7	LACTY	Shimadzu, Kyoto, Japan	Polymerized lactic acids —[O—$CHCH_3$—CO—]n—
BP8	LACEA	Mitsui Chemicals, Tokyo, Japan	Polymerized lactic acids —[O—$CHCH_3$—CO—]n—

Table 1.6. The thickness of the film and the weight of the test piece before and after composting, and the weight-loss degradability calculated from the change in the weight of the test piece for each biodegradable plastic tested in the degradation experiment of Ohtaki and Nakasaki (2000a).

Type	Thickness of film (μm)	Weight of film (g)		Weight-loss degradability (%)	Average degradability (%)	Composting time (days)
		Before	After			
BP1	50	0.4766	0.0843	82.3	81.4	8
		0.4505	0.0879	80.5		
BP2	50	0.4534	0.1976	56.4	57.8	14
		0.4571	0.1866	59.2		
BP3	50	0.4816	0.1936	59.8	57.9	8
		0.4735	0.2088	55.9		
BP4	30	0.2817	0.0253	91.0	91.0	14
		0.2852	0.0255	91.1		
BP5	50	0.4939	0.4754	3.8	3.5	14
		0.4846	0.4686	3.3		
BP6	25	0.2008	0.0358	82.2	83.9	14
		0.2018	0.0292	85.5		
BP7	25	0.2438	0.1493	38.8	38.4	14
		0.2559	0.1402	37.9		
BP8	100	0.9632	0.9611	0.2	0.4	14
		0.9573	0.9525	0.5		

pieces lost 3.4% and 4% of their initial weights after 126 days, so assuming no loss of LLDPE, no more than 13% of the PCL was degraded.

Similar to the work of Gilmore et al. (1992), Mergaert et al. (1994) degraded test pieces in compost piles. Dog-bone-shaped pieces of PHB and PHBV (10% and 20% HV) obtained from ICI Biological Products (Billingham, U.K.) were buried in three small household compost heaps designated A, B, and C. After 150 days in compost A, the homopolymer exhibited mass loss of 6%, while the 10% HV-containing copolymer showed 4% mass loss, and the 20% HV-containing copolymer lost 70% of its mass with mass loss of the samples corresponding to a temperature increase of the heap to over 30°C up from about 7°C. In compost B, the 10% HV-containing copolymer showed only 5% mass loss with temperature remaining low (13–15°C) throughout the 150-day incubation period while the same material showed 14% mass loss in compost C with the temperature reaching 30°C (comparable to compost A).

Imam et al. (1998) degraded neat PHBV (12% HV) and blends of the polymer with either 30% or 50% cornstarch or poly-(ethylene oxide) (PEO)-coated cornstarch in a natural compost

consisting of organic mulch, grass clippings, leaves, and dirt for 125 days. PEO enhanced the adherence of starch granules to PHBV. The total percent weight loss of specimens and the individual weight loss of starch and PHBV (except for blends containing PEO-coated starch) in each specimen was calculated. Neat PHBV only showed 7% weight loss while the 30% and 50% starch blends showed 25% and 49% weight loss, respectively, and the 30% and 50% PEO-coated starch blends showed 21% and 55% weight loss, respectively. Upon analysis of individual weight losses of PHBV and starch in the PHBV/starch blends, it appeared that higher concentration of PHBV did not hinder starch degradation while, instead, the presence of starch enhanced degradation of the PHBV since 13% and 41% weight loss of PHBV was observed in the blends containing 30% and 50% starch, respectively. The weight loss of starch in the blends was 65% and 69% respectively.

1.3.3.4 Characterization Studies of Extracellular Polyhydroxyalkanoates Post-Degradation

Very few studies have investigated the changes in physical, chemical, rheological, or thermal characteristics of PHAs caused by biodegradation. Of the few that have, the investigators usually investigated just one of these types of properties. Tercjak et al. (2003) investigated the effects of biodegradation on the thermal properties of blends of four variations of PHBV with a commercial product named polyamide 11 (PA11). After degradation in compost, samples were subjected to DSC analysis. Results showed that the melting enthalpy of the PHBV phase decreased as a result of degradation. Melting temperatures did not change meaningfully with degradation, but widths of melting endotherms did increase with longer composting time maybe due to a decrease in crystallinity or a result of proteins from the degrading microorganisms becoming incorporated into the polymer.

In the degradation experiments of Mergaert et al. (1994) from the previous section, degradation of the PHB and PHBV test pieces was also estimated based on molecular weight decrease and loss of mechanical properties due to exposure to the compost. The weight-average molecular weights (M_w) of the polymers tested did not change significantly during the 150-day degradation period. However, elongation-to-break values of the samples did decrease significantly. In a previous study by the same researchers, Mergaert et al. (1993) degraded the same PHB homopolymer and 10% HV-containing copolymer test pieces in five different soils at temperatures of 15°C, 28°C, and 40°C. For all soils, M_w decreased slightly or not at all at 15 and 28°C but decreased significantly at 40°C while elongation-to-break values of PHB test pieces decreased dramatically indicating a significant reduction in mechanical strength. For both studies, the researchers concluded that there appeared to be no correlation between mass loss and decrease in molecular weight. Other enzymatic degradation experiments have also reported weight loss of PHB with no decrease in molecular weight (Doi et al., 1990). This has led the researchers to believe that the polymer is degraded enzymatically at the surface to lower molecular weight fragments that are rapidly metabolized by the degrading microorganisms causing mass loss but no affect on M_w of the remaining polymer. In the degradation experiments of Gilmore et al. (1992), also reviewed in the previous section, the PHBV samples degraded showed a steady decrease in M_w over the first 4 months of exposure to the leaf compost. However, the phenomenon was attributed to abiotic hydrolysis since sterile samples incubated aseptically in bags of wet leaves which had been autoclaved showed similar results. Tensile properties were also measured for undegraded and degraded samples after only one month of exposure. Extensibility decreased by nearly one half while, after four months, both extensibility and strength decreased to zero. However, not all of this loss of tensile properties can be

attributed to biodegradation since the sterile control samples became very brittle over the 6-month exposure period and had no measurable extensibility or strength. Furthermore, the decrease in M_w was correlated to a loss in tensile strength ($r = 0.98$). Eldsäter et al. (1997) degraded poly(3HB-*co*-6%-3HV) in a simulated compost environment (nutrient salt medium inoculated with *Aspergillus fumigatus*) at room temperature and observed no changes in the weight-average molecular weight after 17 days with no polymer remaining after 21 days. However, samples exposed to sterile water at 60°C exhibited a significant decrease in molecular weight rather quickly but with no mass loss, again supporting the theory that abiotic hydrolysis will decrease molecular weight especially at higher temperatures. Similar results were also observed by Kanesawa and Doi (1990) with a steady decrease in molecular weight occurring during 86 days of hydrolysis at 60°C with negligible mass loss. However, mass loss was observed after 60 days at 70°C while a critical M_n value of 13,000–17,000 was observed at the onset of mass loss.

Day et al. (1994) studied the effects of biodegradation on physical and chemical changes of PHBV as a result of exposure to an anaerobic sewage sludge medium for 40 days. The data suggested that degradation and chain scission had taken place within the PHBV polymer since a reduction in molecular weight was noted. However, the change was not large since only a 12.7% reduction in intrinsic viscosity was observed. Analyses of samples by FT-IR before and after degradation indicated no significant changes in the samples. Proton NMR spectra indicated a butyrate-to-valerate ratio of 7.3:1, but comparison of degraded and undegraded samples showed that no apparent change in this ratio had occurred.

Rossini et al. (2001) used both *ex-situ* and *in-situ* atomic force microscopy (AFM) to monitor the degradation of thin films (35-nm thick) of PHBV (14% HV) by the PHA

depolymerase of an untyped strain of *Streptomyces sp.* bacteria isolated from soil samples. *Ex-situ* results showed that biodegradation occurs uniformly at the surface, and can be observed within 30 min of exposure to the depolymerase. Within three hours, the films have degraded completely through the thickness of the polymer film. The films analyzed by *in-situ* procedures appeared to degrade more slowly most likely due to being performed at different times with a different strain and purity of depolymerase and other differences in experimental factors. Furthermore, *in-situ* AFM analysis yields a linear degradation rate as function of time, while the *ex-situ* procedure indicated more complex kinetics with a slower initial rate followed by a faster rate as the surface is opened up by the enzyme attack.

Spyros et al. (1997) characterized films of PHB and PHBV (23% HV) degraded enzymatically by depolymerases from *Pseudomonas lemoignei* using ^{1}H-NMR analysis in order to examine the deterioration of the amorphous regions of samples and compare with degradation rates of the crystalline regions of the polymer. Figure 1.2 shows ^{1}H-NMR images of a degraded PHB film with respect to time as compared to an undegraded control sample. For both polymers, it was found that in the initial stages of degradation, most of the mass loss was due to loss of amorphous region of the sample with the integral of the ^{1}H-NMR image decaying exponentially at first and then linearly once the crystalline region begins to degrade along with the amorphous region (Figure 1.3). For PHB, 50% mass loss was observed after 220 h while almost 70% of the amorphous PHB ^{1}H-NMR image integral had been lost. For PHBV, 32% mass loss was observed at 140 h while amorphous polymer loss was 46%. DSC analysis of the PHB film before and after 220 h of degradation gave crystallinity values of 65 ± 5% and 90 ± 5%, respectively. An increase in crystallinity was also confirmed by DSC for the PHBV sample after 140 h.

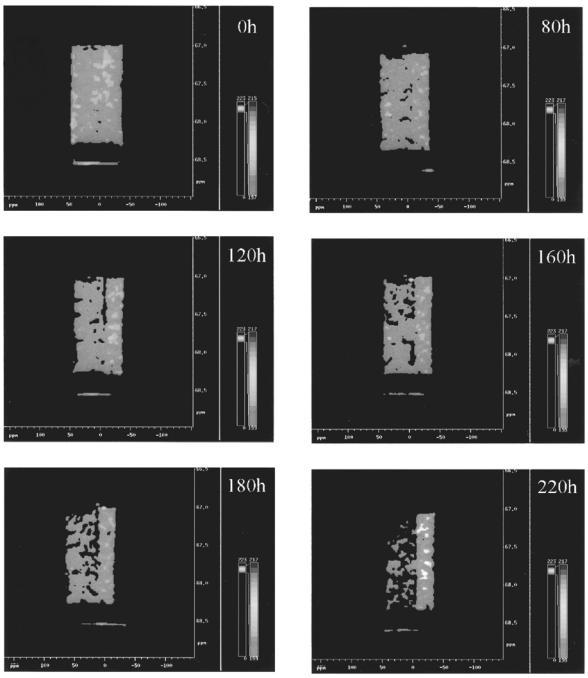

Figure 1.2. ^{1}H-NMR images of a PHB film (large piece of film on the left), as a function of degradation time indicated at the top right of each image (FOV 3 × 3 cm^2). A smaller but identical undegraded piece of PHB film, used as a control, can be seen at the right of the degraded one in all images. The small intensity appearing at the bottom of the images comes from the Teflon sample holder (from Kadouri et al., 2005; Spyros et al., 1997; Doi et al., 1990).

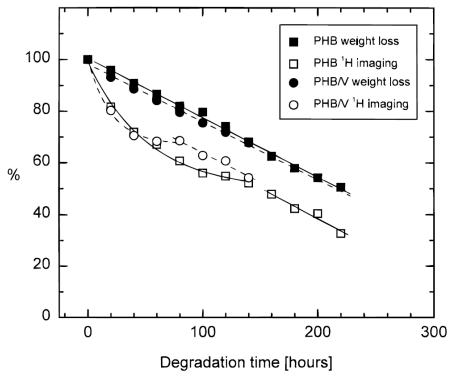

Figure 1.3. Total weight loss and ^{1}H- image integral loss (%) of degraded PHB and PHBV as a function of degradation time by PHB depolymerase B from *P. lemoignei*. The curves for the initial ^{1}H imaging data (PHB, 0-140 h; PHBV, 0-80 h) are single exponential fits, while all others are linear fits (from Spyros et al., 1997; Lee, 1996; Anderson and Dawes, 1990; Doi et al., 1990).

Molitoris et al. (1996) examined sheets of PHB, PHV, PHBV, and Poly(3-hydroxoctanoate) (PHO) by scanning electron microscopy after degradation by *Comamonas* sp., *Pseudomonas lemoignei*, and *Pseudomonas fluorescens* GK13 in an aerobic mineral medium. The researchers found that for all polymers, hydrolysis started at the surface of the sample and at lesions on the surface and proceeded inward. This was true even for PHO, which was not hydrolyzed by the *Comamonas* sp. or *P. lemoignei* due to their specificity for PHA_{SCL} while PHO is a PHA_{MCL}. Figure 1.4 shows various SEM images of the undegraded and degraded PHB samples.

The work of Ferreira and Duek (2005) tested the biomedical aspects of PHBV as a bioabsorbable polymer *in vivo*. Pins made from blends of Poly-L-Lactic acid (PLLA)/PHBV of varying compositions were degraded in a phosphate buffer and characterized by TGA, DSC, DMA, and SEM. The blends were found to be immiscible. PLLA began to degrade after approximately 12 weeks, while PHBV showed very little degradation after 53 weeks. Crystallinity of the blends increased with degradation while PHBV was found to improve the thermal properties of the PLLA and reduced the brittleness of the blends.

1.4 Chapter Summary

In summary, a transition to the use of bio-based plastics rather than their petroleum-based predecessors is becoming more widespread and even more economical with their decreasing production costs and advances in genetic engineering which are expected to make these so-called "bioplastics" more price-competitive with their counterparts. These bioplastics have the obvious advantages that they are much more eco-friendly and are produced from readily renewable resources. However, their production costs (especially for PHAs) are still higher than those of

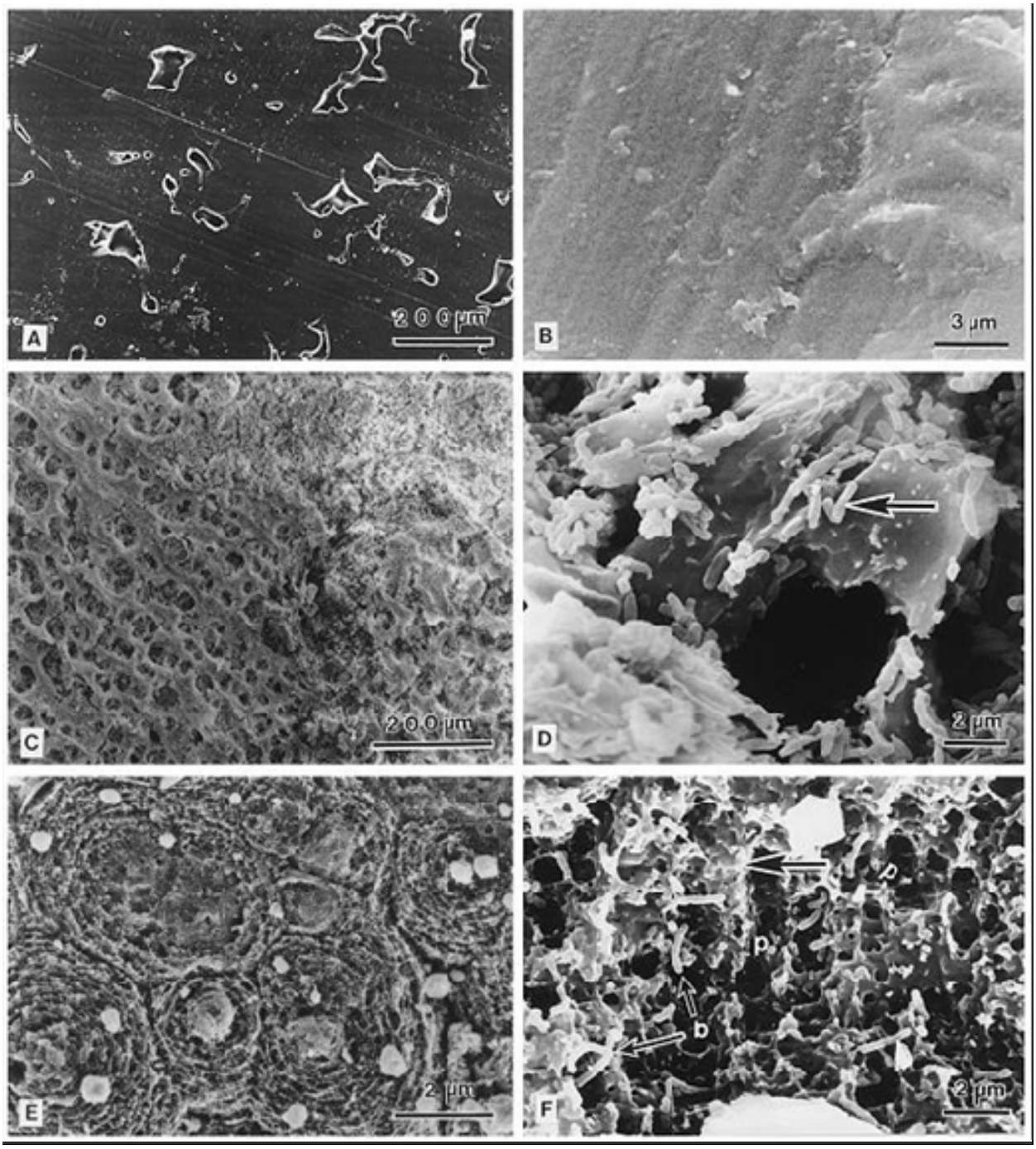

Figure 1.4. SEM images of various magnitude of PHB before degradation at low (A) and higher (B) magnifications, after exposure to Comamonas sp. for 7 days at low (C) and higher (D) magnifications showing eroded surface with numerous irregular pits between less eroded areas, and after exposure to P. lemoignei for 14 days at low (E) and higher (F) magnifications showing circular erosion patterns comprising many concentric pit zones to which bacteria (b, F) are attached. In D, note the bacteria (arrow) attached to the eroded surface adjacent to a pit and in F, the regions of less degraded polymer (arrows) separated by concentric pitted regions (from Chen et al., 2001; Lee, 1996; Molitoris et al., 1996; Anderson and Dawes, 1990).

petroleum-based plastics and steps are being taken to reduce these costs to make them more price-competitive such as genetically modifying crops to produce the materials more efficiently.

Properties of many PHAs such as PHB and PHBV have been well-documented in literature such as degree of crystallinity, melting point (T_m), glass-transition temperature (T_g), tensile strength, notched Izod impact strength, molecular weight (M_w), and viscosity. The mechanisms of extracellular PHA biodegradation by PHA-degrading organisms are also well-known and many studies of the metabolic process and involved enzymes have been performed. Other studies have focused on the biodegradability of PHAs and other bioplastics in specific environments such as municipal waste. PHAs have been shown to degrade extensively in both anaerobic sewage sludge and aerobic composts and many studies have shown how biodegradation affects material properties. As more studies continue to provide insight to the physical characteristics and biodegradation of PHAs, further progress will also be made toward their life-cycle design in the manufacture of consumer products.

Chapter 2: Anaerobic Biodegradation of Polyhydroxybutyrate (PHB) in Municipal Sewage Sludge

2.1 Introduction

The biodegradation of bio-based plastics has become a growing topic of interest due to the environmental issues associated with the production and disposal of petroleum-based plastics and the finite supply of and reliance on foreign oil to produce these commodity plastics. "Bioplastics" are thermoplastic materials that can be naturally made from renewable resources and will biodegrade in natural environments. To be classified as biodegradable, more than 60% of a material's organic carbon must be converted within a maximum of six months in laboratory experiments; in real-life conditions of composting, more than 90% of the plastic is required to be degraded to fragments not more than 2 mm in size (Mecking, 2004). The end products of bioplastic degradation are non-toxic and already occur naturally in the environment: carbon dioxide (CO_2) gas and water (H_2O) in aerobic environments and CO_2 and methane (CH_4) gas in anaerobic environments. The degradation of bioplastic additives, such as plasticizers, could potentially release toxic by-products, but this could be avoided by using natural additives such as tributyl citrate (TBC). The manufacture of plastic products that enter the waste stream from biodegradable materials would significantly reduce the negative environmental impact caused by the previously mentioned methods of disposal used for petroleum-based plastics.

Biodegradation of PHAs is often studied using isolated microorganisms *in vitro* that have been identified as PHA degraders (Lee et al., 2005; Elbanna et al., 2004; Handrick et al., 2004; Kim and Rhee, 2003; Jendrossek and Handrick, 2002; Sang et al., 2002; Jendrossek, 2001; Scherer et al., 1999; Iwata et al., 1997; Hocking et al., 1996; Jendrossek et al., 1996; Molitoris et al., 1996). The type of microorganism used and the environmental conditions will greatly affect the degradation rate and the rate at which a certain species will degrade under certain conditions

can be determined with very reproducible results. However, only very few studies have studied the biodegradation of PHAs in natural environments or municipal waste environments consisting of mixed cultures of species. It is very important that more research be performed in such environments so that more can be understood about how to increase confidence that PHAs will degrade at a certain rate under given conditions in a mixed-culture environment or to at least understand more about what other factors will affect those results. One municipal waste environment that has attracted great interest for the biodegradation of PHAs is sewage sludge under anaerobic conditions. Several research groups have published work involving the biodegradation of PHAs in anaerobic sewage sludge (Abou-Zeid et al., 2004; Abou-Zeid, 2004; Federle et al., 2002; Abou-Zeid et al., 2001; Gartiser et al., 1998; Reischwitz et al., 1998; Shin et al., 1997; Imam et al., 1995; Puechner et al., 1995; Budwill et al., 1992) and it has been demonstrated to be an environment in which these bioplastics will completely degrade and often show superior biodegradability to other biodegradable plastics or polymers. Anaerobic sewage sludge has widely been recognized as the waste environment in which biodegradable materials perish most rapidly. The typical time that can be expected for a 1-mm molding of polyhydroxybutyrate-*co*-hydroxyvalerate (PHBV) to completely biodegrade in anaerobic sewage is six weeks, compared to forty weeks in estuarine sediment, sixty weeks in aerobic sewage, seventy-five weeks in soil, and 350 weeks in sea water (Luzier, 1992). Additionally, the anaerobic sewage sludge environment has the added benefit of biogas recovery of CH_4 which can be used as a fuel source.

Some research studies in literature have examined the biodegradation behavior of PHAs through characterization of the degraded polymers but usually only focus on a limited number of aspects of the material characteristics. This work has combined the results from several different

characterization analyses of a PHA degraded in aerobic compost to provide further insight to PHA degradation with focus on the characteristics of the material that have more implications concerning the life-cycle design of the polymer. The overall goals of this research thrust were to assess the biodegradation of a bioplastic obtained from a commercial producer in anaerobic municipal sludge and determine how biodegradation affects the characteristics of the material. Additionally, a blend of the bioplastic with a natural additive was also tested for biodegradation to gain insight to the impact of such additives.

2.2 Materials and Methodology

The methodology consisted of three major sections: (1) material characterization and preparation, (2) characterization analyses, and (3) biodegradation studies. The characterization analyses consisted of chemical properties, thermal properties, mechanical properties, and physical properties. The biodegradation studies consisted of three experiments assessing biodegradation based on biogas production and two mass loss experiments. The materials tested for biodegradation in the both the biogas production experiments and mass loss experiments were PHB powder, PHB melt-pressed plates, PHB/15% TBC blend melt-pressed plates, and polylactic acid (PLA) melt-pressed plates. In one biogas production experiment, low-density polyethylene (LDPE) beads were tested as a negative control. The negative control was not deemed necessary in later experiments since the ASTM D 5210 standard did not require them.

2.2.1 Material Preparation

The bioplastic was obtained from Metabolix, Inc. which identified it as a blend of polyhydroxybutyrate (PHB), the most prevalent PHA. Wide-angle X-ray diffraction (WAXD) performed on the raw material confirmed that the bioplastic was PHB (Figure 2.1). The material in its raw form was a fine, white plastic powder produced and extracted from the aerobic

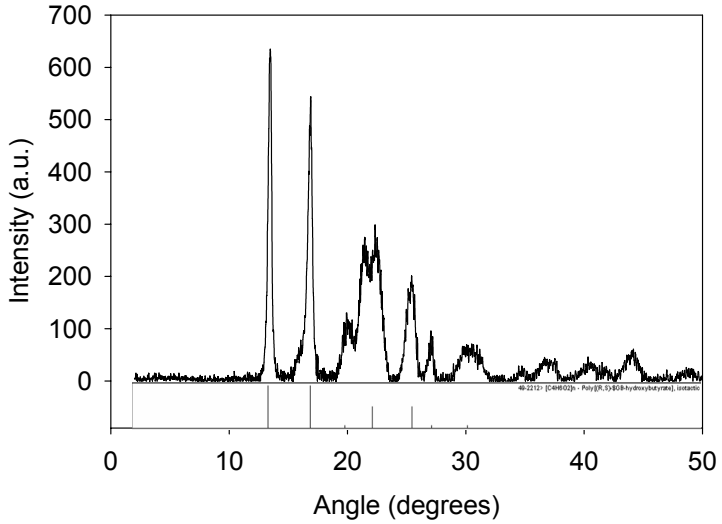

Figure 2.1. The WAXD spectrogram of the bioplastic obtained from Metabolix, Inc. The spectrogram was used to identify the material as PHB when compared to a database of many known spectrograms. The legend under the spectrogram shows where the peaks that are characteristic of isotactic polyhydroxybutyrate should appear and their relative intensity. Any additional peaks of the spectrogram were considered to be caused by impurities or other remnants from the extraction process after intracellular production in *E. coli*.

fermentation of recombinant *E. coli*. The PHB was also blended with 15% tributyl citrate (TBC) as an additive and degraded for comparison and to determine the impact of the additive on the biodegradation of the material. Additionally, an experiment assessing the biodegradation of a commercial blend of PLA was conducted for additional comparison to the results for the PHB bioplastic. Lastly, for the first biogas production experiment, LDPE was tested for biodegradation as a negative control.

The PHB powder was melted at 179°C (355°F) for 5 – 10 min (longer for thicker plates), and pressed with a hydraulic jack into plates of different thicknesses (0.24 mm, 0.5 mm, 1.2 mm, 3.5 mm, and 5 mm) using a Carver Laboratory Press. The plates were allowed to cool to room temperature while still enclosed in the steel plates and mold or spacers used. The prepared plates were then cured for at least 7 days to allow for complete chemical equilibrium and crystallization

prior to use in the degradation experiments and characterization analyses. Plates of the PHB/15% TBC blend and the PLA blend were prepared in the same way except that the melting temperature of the PLA was 149°C (300°F).

2.2.2 Material Characterization

2.2.2.1 Chemical Properties

WAXD was performed on the PHB raw powder to identify its chemical composition. Two-dimensional wide angle X-ray diffraction images of the samples were obtained using an X-ray diffractometer (Siemens/Bruker D5000 XRD) equipped with KEVEX solid state detector. The Siemens D5000 XRD has a large diameter goniometer (600 mm), low divergence collimator, and Soller slits. The X-ray source was Copper radiation generated at 40 kV and 30 mA. The collected data were analyzed using the Siemens Kristalloflex V3.1 software application and compared to a database of many known spectrograms to identify the chemical composition.

Molecular bonding characteristics were investigated by Fourier Transform Infrared Spectroscopy (FT-IR) for the raw powder form of the PHB bioplastic, undegraded and degraded melt-pressed plates (0.24-mm, 1.2-mm, 3.5-mm, and 5-mm thick) of the bioplastic, and of PHB/15% TBC blend melt-pressed plates (1.2-mm thick). IR determinations were performed using a Bruker Tensor 27 microspectrometer. Both the sample scan time and the background scan time were 16 scans at a resolution of 4 cm^{-1}. Spectrograms were processed using OPUS Version 4.2 software.

Molecular weight was measured by Size Exclusion Chromatography (SEC) for the raw powder form of the PHB bioplastic, undegraded and degraded melt-pressed plates (0.24-mm, 0.5-mm, 1.2-mm, 3.5-mm, and 5-mm thick) of the bioplastic, and of PHB/15% TBC blend melt-

pressed plates (1.2-mm thick). For all samples, the plastic was dissolved in solution at an approximate concentration of 5 mg mL^{-1} in chloroform ($CHCl_3$). For the separation, three Phenogel 300 x 7.8 mm columns (Phenomenex, Torrance, CA), connected in series were used: (1) 5 μ, 500 Å (1 K – 15 K); (2) 5 μ, 10-4Å (5K – 500 K); (3) 10μ, MXM (100 – 10,000 K) and a guard column (5 μ, 50 x 7.8 mm) was used. The SEC instrumentation consisted of an Agilent 1100 pump, and an Agilent 1100 autosampler. For detection, three detectors connected on series were used: A Wyatt Heleos Multi Angle Light Scattering (MALS) detector equipped with a QUELS DLS detector, a Wyatt ViscoStar viscosity detector, and a Wyatt rEX Differential Refractive Index detector. All separations were performed using an injection volume of 100 μL. Chloroform (1 mL min^{-1}) was used as the solvent.

2.2.2.2 Thermal Properties

Thermal analyses were performed by Differential Scanning Calorimetry (DSC) using a TA Instruments DSC 2920 for the raw powder form of the PHB bioplastic, undegraded and degraded melt-pressed plates (0.24-mm, 1.2-mm, 3.5-mm, and 5-mm thick) of the bioplastic, and PHB/15% TBC blend melt-pressed plates (1.2-mm thick) in accordance with ASTM D 3418 – 03 (Standard Test Method for Transition Temperatures and Enthalpies of Fusion and Crystallization of Polymers by Differential Scanning Calorimetry). A heating rate of 5°C min^{-1} in a liquid nitrogen atmosphere was utilized. Sample sizes of approximately 5-10 mg were used for all analyses. The samples were heated to 200°C and held for 0.5 min, then cooled to –20°C for 1 min and reheated to 200°C. Melting temperature (T_m), melting enthalpy (ΔH_m), crystallization temperature (T_c) and crystallization enthalpy (ΔH_c) were obtained from the thermograms. T_m and T_c were taken as the onset points of melting or crystallization, respectively, as determined using the TA Universal Analysis V3.9A software.

2.2.2.3 Mechanical Properties

The mechanical strength of the undegraded PHB melt-pressed plates was determined using an Instron 4301 tensile test machine and in accordance with ASTM D 638 – 03 (Standard Test Method for Tensile Properties of Plastics). Specimens with a thickness of 1.2 mm were tested at a crosshead speed of 3.0 mm min^{-1} and sample rate of 6.667 points s^{-1}. The specimens were cured at room temperature for at least 7 days after the plates were melt-pressed and then for three additional days at 23°C (73°F) and relative humidity of 50% prior to testing.

Impact resistance was measured by notched Izod pendulum impact testing using a Tinius Olsen Model 892 Pendulum Impact tester for undegraded and degraded specimens of the PHB melt-pressed plates (3.5-mm thick) and in accordance with ASTM D 256 – 06a (Standard Test Methods for Determining the Izod Pendulum Impact Resistance of Plastics). Plates with a thickness of 3.5 mm were used for this analysis.

Dynamic Shear Rheometry (DSR) was performed on the raw PHB powder to determine rheological properties of the material. This analysis was performed by Dr. Simioan Petrovan at the University of Tennessee.

2.2.2.4 Physical Properties

To examine surface morphology, Scanning Electron Microscopy (SEM) images were recorded of undegraded and degraded melt-pressed plates of the PHB and the PHB/15% TBC blend using a Stereoscan 260 scanning electron microscope. Samples were sputter-coated with gold. Some samples were prepared so that the degrading microorganisms attached were fixated and could be recorded by SEM. These samples were removed from the degrading medium to a 2% glutaraldehyde, 1% formaldehyde, 0.1M cacodylate buffer solution for 30 min to fixate the sample. Then, samples were rinsed with 0.1M cacodylate buffer and transferred to a 1:1 mixture

of distilled water and 95% ethanol, replacing half of the mixture with 95% ethanol every 5 min for 30 min to gradually dehydrate the sample. Then, the entire mixture was replaced with 95% ethanol every 5 min for 15 min before critical point drying with CO_2 and sputter-coating with gold.

2.2.3 Biodegradation Study

2.2.3.1 Biogas Production Experiments

Three anaerobic biodegradation experiments (EXP1, EXP2, and EXP3) were performed according to ASTM D 5210 – 92 (Standard Test Method for Determining the Anaerobic Biodegradation of Plastic Materials in the Presence of Municipal Sewage Sludge; Reapproved 2000) in a diluted sewage sludge medium (1/10 dilution) with added macro- and micro-nutrients. Table 2.1 lists the materials that were tested for biodegradation in each experiment in addition to the positive and negative controls. Sigmacell® cellulose powder (20 μm particle size) was used as a positive control to verify viability of the sludge inoculum. Melt-pressed plates of NatureWorks® PLA and the PHB/15% TBC blend were tested for biodegradation in addition to the PHB plates. The PLA was tested to compare the biodegradation of the PHB to that of another bioplastic while the PHB/15% TBC blend was tested for the purpose of evaluating the

Table 2.1. The materials tested for biodegradation in each of the three gas production experiments in addition to cellulose positive controls.

Experiment	Materials Tested
EXP1	PHB raw powder, PHB melt-pressed plates (1.2-mm thick plates; 1.1 cm x 4.5 cm; 4 per flask), Sigmacell® cellulose powder, Polyethylene beads (LDPE; Dow Chemical, Inc.)
EXP2	PHB raw powder, PHB melt-pressed plates (1.2-mm thick plates; 1.1 cm x 4.5 cm; 2 per flask), Sigmacell® cellulose powder
EXP3	PHB plates, NatureWorks® PLA plates, PHB/15% TBC blend plates (all 1.2-mm thick plates; 1.1 cm x 4.5 cm; 2 per flask), Sigmacell® cellulose powder

impact of additives on the biodegradation of the PHB. TBC, a citrate ester derived from naturally occurring citrate, is non-toxic and has been approved as an additive/plasticizer for polymers (Labrecque et al., 1997; Encyclopedia of Chemical Technology, 1986). The LDPE beads tested for biodegradation in EXP1 served as negative controls.

The volatile solids (VS) content of the raw sludge used for inoculation of the medium was measured as an indicator of organic content for each experiment; this analysis was completed according to APHA Standard Method 2540-E. For EXP1 and EXP2, sewage sludge was obtained (and filtered through a 2-mm sieve) from an anaerobic digester (solids retention time of approximately 15 – 30 days) located at the Central Wastewater Treatment Facility, Baton Rouge, Louisiana. For EXP3, sewage sludge was obtained (and filtered through a 2-mm sieve) from an anaerobic digester (solids retention time of approximately 15 – 30 days) located at the North Wastewater Treatment Facility, Baton Rouge, Louisiana. The concentrations of polymer carbon (C) in the sewage medium of vials in EXP1 and EXP2 were 500 mg/L and 1,000 mg/L, respectively, for both the PHB and cellulose powders; the carbon concentration for the cellulose powder in EXP3 was also 1,000 mg/L. The polymer carbon loading of the sludge for all melt-pressed plates degraded in the anaerobic sewage sludge medium was arbitrarily based on plate sizes but the concentration of the PHB plates in EXP1 was ~8,000 mg/L and the concentration ranged from ~4,000 – 4,500 mg/L for all other plates of all the materials tested in the remaining experiments.

The degradation of each specimen was performed in triplicate using serum bottles of approximately 240-mL volume containing 150 mL of the prepared diluted sludge medium. The diluted sludge medium was transferred to the serum bottles under anaerobic conditions. The headspace of the bioreactors used for these experiments were sparged with nitrogen (N_2) gas in

EXP1 and EXP2 and with a 70% N_2/30% CO_2 gas mixture in EXP3 to prevent re-entry of oxygen (O_2) that had been purged from the medium during preparation. The pH of the resulting medium ranged between 7.0 and 7.5 for the three experiments performed. The serum bottles containing the medium with test materials were incubated at 35ºC in the dark until gas production due to degradation ceased. The CH_4 and CO_2 biogases that evolved during biodegradation were collected by an apparatus consisting of inverted graduated cylinders connected to the serum bottles by Tygon® tubing; gas volumes were measured daily. A diagram of the experimental setup was prepared for EXP1 using AutoCAD® 2006 drawing software and can be found in Appendix A. The maximum theoretical gas production (ThGP) from the organic test materials was calculated based on the fact that 1 mmol of organic carbon is 12 mg and, when converted to gaseous carbon, will occupy 22.4 mL at NTP. When the experiments were concluded, actual amounts of gas produced could be compared to the theoretical amounts to assess biodegradation of the test materials. Maximum ThGP was calculated based on the original mass of test material as follows:

$$ThGP\ (mL) = mass\ (mg) \times (\%\ by\ weight\ carbon) \times \frac{1\ mmol\ gaseous\ Carbon}{12\ mg\ Carbon} \times \frac{22.4\ mL}{mmol\ gaseous\ Carbon} \quad (1)$$

Observed gas volumes were corrected for vapor pressure at 35ºC, the average temperature of the graduated cylinders throughout the experiments, using the following equation:

$$22.4 \times \frac{308}{273} \frac{760}{760 - 41} = 26.71\,mL \quad (2)$$

The composition of collected biogases was analyzed periodically by gas chromatography (GC) using an SRI 8610C gas chromatograph equipped with a thermal conductivity detector. This was performed at least once per week but only when sufficient amounts of biogas were produced to warrant a sampling event. The GC data would serve as an indication of the

microbial consortia that had degraded the test substances (i.e. the relative presence of methanogens rather than CO_2-producing microbes). Volumes of gas samples extracted for GC analysis were accounted for when making calculations throughout the experiment to ensure that volumes of gas extracted from serum vials were included in calculations to determine cumulative gas evolution.

In the data analysis, the cumulative-average (of triplicate results) gas volumes from anaerobic biodegradation of the test materials was calculated by subtracting the cumulative-average gas volume production of the blank controls. The percent of theoretical gas produced (%ThGP) was calculated by dividing the cumulative average gas volume of the test material by the theoretical maximum gas production and multiplying by 100. The standard deviation for each replicate set of bottles was also calculated. The sludge medium was analyzed for dissolved organic carbon (DOC) and biomass carbon before and after the experiment to perform mass balance calculations. The total solids (TS) content before and after degradation was also determined in addition to the carbon content. The following equation was used in performing carbon mass balances (C = carbon):

$$C_{input} = C_{output} \tag{3}$$

where:

$$\begin{aligned} C_{input} &= C_{polymer} + C_{biomass} + DOC \\ C_{output} &= C_{polymer} + C_{biomass} + DOC + C_{biogas} \end{aligned} \tag{4}$$

2.2.3.2 Mass Loss Experiments

Two mass loss experiments were performed in parallel to EXP1 and EXP3 using the same sewage sludge medium used in the biogas production experiments. In the first mass loss experiment, PHB melt-pressed plates of three different thicknesses – 0.5 mm, 1.2 mm, and 3.5

mm – were incubated in the medium at 35ºC. Prior to incubation, test pieces had been well-rinsed with nanopure water, oven-dried at 60°C, cooled in a desiccator, and weighed. Five 1-L Erlenmeyer flasks each contained the PHB plates with thicknesses of 0.5 mm (2.5 cm x 2.5 cm; 5 per flask), 1.2 mm (1.5 cm x 7.0 cm; 2 per flask), and 3.5 mm (12.7 mm x 6.4 cm; 5 per flask). The flasks contained the same ratio of initial plastic surface area to sewage sludge volume as the reactors in the parallel biogas production experiment (EXP1) to allow easy comparison of results between the two methods. Calculations for the amount of sludge medium needed per flask in order to meet these conditions were made using Microsoft Excel software and can be found in Appendix A. The flasks were sampled for mass loss determination of the remaining bioplastic at weeks 2, 4, 8, 12 and 19. At each sampling event, one of the flasks was removed from the incubator and the contents sampled. For both mass loss experiments, any remaining plastic was strained from the medium of its flask, rinsed well with nanopure water, oven-dried at 60°C, and cooled in a desiccator prior to mass loss determination by weighing of the remaining plastic. The remaining plastic was then subjected to DSC, Izod pendulum impact testing (first experiment only), FT-IR, SEC, and SEM analyses. These analyses required destructive sampling of the remaining plastic. The mass loss results for different thicknesses of the plastic were used to study an apparent relationship between the degradation rate coefficients and their initial mass-to-surface-area ratios.

In the second mass loss experiment, two additional plate sizes of the PHB bioplastic – those with thicknesses of 0.24 mm and 5 mm – were subjected to degradation in the anaerobic sewage sludge medium to further establish the correlation between the degradation rate coefficients and initial mass-to-surface-area ratio in addition to those with 1.2-mm thickness to serve as a reference between the two mass loss experiments. Like in EXP3, melt-pressed plates

of NatureWorks PLA and the PHB/15% TBC blend were also tested for biodegradation in the second anaerobic mass loss experiment. All plate sizes were degraded in separate flasks and sampled in triplicate. Ninety-nine 250-mL flasks were prepared which contained sewage sludge medium with either the PHB plates with thicknesses of 0.24 mm (2.55 cm x 2.55 cm; 2 per flask), 1.2 mm (1.6 cm x 1.6 cm; 1 per flask), or 5 mm (1.15 cm x 1.15 cm; 1 per flask), or the NatureWorks® PLA plates or PHB/15% TBC blend plates (both 1.2-mm thick plates; 1.6 cm x 1.6 cm; 1 per flask). All flasks contained the same ratio of plastic mass to sewage sludge volume as the reactors in the parallel biogas production experiment (EXP3) to allow easy comparison of results between the two methods. Calculations for the plate dimensions needed in order to meet these conditions were made using Microsoft Excel software and can be found in Appendix A. The sampling schedule for the 0.24-mm PHB plates was 5, 10, 15 days, 3, 4, 6, 8, and 10 weeks of exposure. Sampling times for all other sizes and types of plastic were after 2, 4, 8, 12, 16, and 20 weeks of exposure except that an additional sampling event occurred at 32 weeks for the 5-mm PHB.

Mass loss percentages of materials tested in both mass loss experiments were calculated by dividing the final weight of a specimen by the initial weight and multiplying by 100%. Mass remaining with respect to the initial surface area of specimens was plotted versus time so that degradation rate coefficients could be calculated. Degradation rate coefficients were calculated for all materials tested for biodegradation in both mass loss experiments. Linear regressions were performed for the portion of each degradation curve which showed the maximum rate of mass loss. In most cases, this involved the selection of three data points on the mass loss curve to be used for the linear regression. Diagrams representing these linear regressions can be found in Appendix A. All analyses were performed using SigmaPlot software (v 9.01, ©2004 Systat

Software, Inc.). Additionally an analysis of covariance was performed on the data to show any statistical differences. This was performed using SAS software (v 9.1.3, ©2002-2003 SAS Institute Inc.). Degradation rate coefficients for the three different plate sizes of PHB tested in each experiment were plotted with respect to their initial mass-to-surface-area ratios to form saturation curves as the degradation of the PHB was believed to follow saturation kinetics.

2.3 Results and Discussion

2.3.1 Biogas Production Experiments

In EXP1, peak gas production from biodegradation of the PHB powder and cellulose was observed after 13 and 16 days, respectively (Figure 2.2). Degradation of the PHB plates required much more time (approximately 85 days) due to their lower mass-to-surface-area ratio and the larger amount of mass to be degraded. ASTM D 5210 – 96 states that in order for the test to be valid for reporting biodegradability, the theoretical gas production (ThGP) of the positive control (cellulose) should be 70% or greater. In EXP1, a significant loss of CO_2 gas was expected to have dissolved into the sewage sludge medium since CO_2 gas was not used to sparge the medium and saturate it with CO_2 gas at the beginning of the experiment. Thus, the results have been adjusted for the amount of CO_2 that had dissolved into the media over the course of the experiment using Henry's Law for solubility of CO_2 in water (Table 2.2). Puechner et al. (1995) and Reischwitz et al. (1998) have also used methods to account for dissolved CO_2 in anaerobic biodegradation experiments. Furthermore, Gartiser et al. (1998) evaluated the differences in biogas production for several biopolymers when using the ASTM D 5210 – 96 standard by sparging some reactors with pure N_2 gas and others with a 70% N_2/30% CO_2 gas mixture. The researchers reported significantly more biogas production in the reactors sparged with the 70% N_2/30% CO_2 gas mixture, and although they did not attribute this phenomenon to CO_2 solubility,

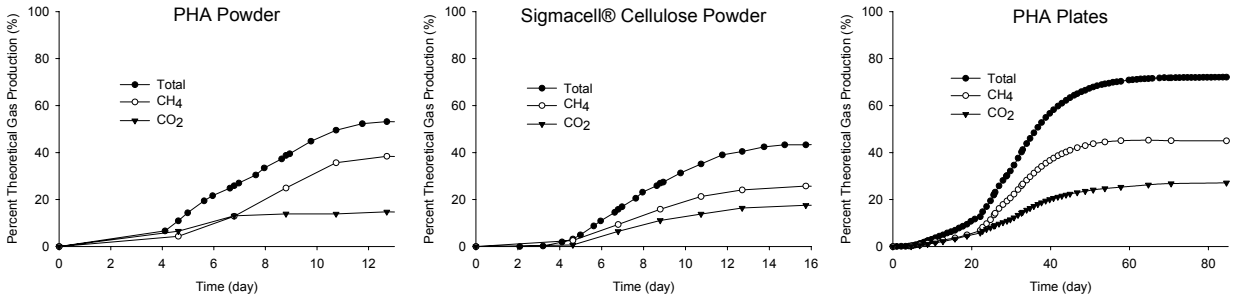

Figure 2.2. Graphs representing the percentage of theoretical gas production (%ThGP) from degradation of the PHB powder, Sigmacell® cellulose powder (positive controls), and the melt-pressed PHB plates in EXP1. The values shown are net values for total gas production, methane (CH_4) production, and carbon dioxide (CO_2) production.

Table 2.2. Percentages of net theoretical gas production (%ThGP) observed for the materials exposed to the anaerobic sludge medium of the three gas production experiments.

	Mean values ± Standard Deviation		
Experiment / Material	**Max. Gas Production (mL)**	**Theor. Gas Production (mL)**	**% ThGP**
EXP1			
PHB powder	88.8 ± 0.5	140 ± 0.1	63.4% ± 0.4%
Cellulose powder	78.1 ± 2.6	140 ± 0.1	55.7% ± 1.8%
PHB plates	1632 ± 157	2235 ± 77.5	73.0% ± 6.2%
EXP2			
PHB powder	191 ± 12.7	280 ± 0.0	68.0% ± 4.5%
Cellulose powder	202 ± 29.2	280 ± 0.0	72.1% ± 10.4%
PHB plates	785 ± 20.7	1170 ± 8.5	67.1% ± 1.3%
EXP3			
PHB plates	1052 ± 99.9	1271 ± 109	82.8% ± 2.3%
Cellulose powder	206 ± 5.6	280 ± 0.1	73.6% ± 2.0%
PHB/15% TBC blend plates	1049 ± 147	1121 ± 46.8	93.8% ± 15.7%
NatureWorks® PLA plates	14 ± 9.8	1162 ± 32.0	1.2% ± 0.9%

it is quite likely that they overlooked that possibility. The assumption that CO_2 had dissolved into the medium in EXP1 is further supported by the fact that the observed percentage of ThGP (%ThGP) from the PHB powder (63.4%) was much less than that for the PHB plates (73.0%).

Since each bottle would lose approximately equal amounts of the biogases, the loss of gases from the bottles with the PHB powder would have a much larger impact on the observed %ThGP than for the PHB plates which had a much larger ThGP. Budwill et al. (1992) conducted a biodegradation experiment of PHB powder in anaerobic sewage sludge and in a similar time frame of 16 days observed a significantly larger %ThGP of 87%, which may somewhat further support the notion that more gas production should have been observed in EXP1 but wasn't possibly due to gas loss, although this could also be attributed to differences in sludges. Puechner et al. (1995) also tested biodegradation of PHB powder in anaerobic sewage sludge and reported more than 80% ThGP after 20 days. One notable observation of EXP1 is that both the PHB powder and plates degraded more thoroughly than the cellulose powder, which is known to be 100% biodegradable, so it can be concluded that the PHB is also 100% biodegradable. Another factor that may have played a role in low levels of gas production in this experiment was that the volatile solids (VS) content of the sewage sludge was 0.74%, slightly below the normal range (approximately 1 to 2%) to ensure proper activity as outlined in ASTM D 5210 – 96.

In EXP2, peak gas production from biodegradation of the PHB and cellulose powders was observed after 12 and 19 days, respectively (Figure 2.3). Once again, gas production from degradation of the PHB plates proceeded much longer (approximately 65 days) than the powders because of the lower mass-to-surface-area ratio and more mass to be degraded. Similar to EXP1, slightly less than 70% ThGP was observed for the positive control (cellulose powder) while again, some loss of CO_2 biogas was believed to have dissolved into the sludge medium since a 70% N_2/30% CO_2 gas mixture had not been used to sparge the medium at the beginning of the experiment; instead, just high purity N_2 gas had been used. For this reason, the results have been

adjusted for the amount of CO_2 that had dissolved into the media over the course of the experiment using Henry's Law for solubility of CO_2 in water (Table 2.2). All materials tested showed approximately 70% of ThGP, showing that all had degraded nearly as well as the cellulose positive control which is presumably 100% degradable. The VS content of the sewage sludge used for EXP2 was 1.57%. A carbon mass balance of EXP2 (Table 2.3) shows that most of the carbon could be re-accounted for and that some of the polymer carbon was converted to new biomass adding to the biodegradation estimates based on only biogases formed. The initial biomass for all bioreactors had been estimated based on the raw sludge solid content and its carbon content and the 1/10 dilution factor used.

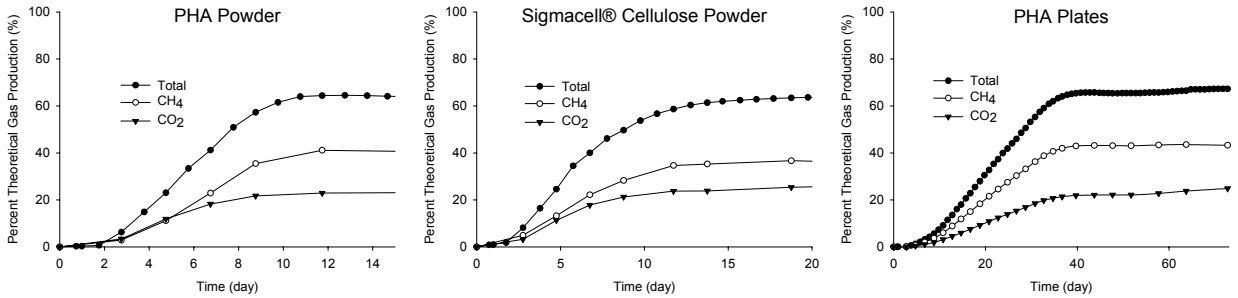

Figure 2.3. Graphs representing the percentage of theoretical gas production (%ThGP) from degradation of the PHB powder, Sigmacell® cellulose powder (positive controls), and the melt-pressed PHB plates in EXP2. The values shown are net values for total gas production, methane (CH_4) production, and carbon dioxide (CO_2) production.

Table 2.3. Carbon mass balance of EXP2 comparing C input (Polymer C + Biomass C + DOC) with C output after incubation (Polymer C + Biomass C + DOC + Biogas C). Values shown are averages for triplicate bioreactors for each polymer tested for biodegradation.

		Polymer	Polymer C	Biomass C	DOC	Biogas C	Total	
	Polymer	(mg/L)	(mg/L)	(mg/L)	(mg/L)	(mg/L)	mg/L	%
Input	Blanks	–	–	799	66.9		866	100.0
Output				734	22.0	65	821	94.8
Input	PHB Powder	1835	1000	799	66.9		1866	100.0
Output			–	878	30.1	704	1612	86.4
Input	Cellulose Powder	2381	998	799	66.9		1864	100.0
Output			–	897	44.0	721	1662	89.2
Input	PHB Plates	7668	4225	799	66.9		5091	100.0
Output			–	864	37.8	2803	3705	72.8

In EXP3, peak gas production from biodegradation of the cellulose positive controls was observed after 30 days (Figure 2.4). The viability of the sludge inoculum was verified for assessing biodegradability since 73.6% ThGP was observed for the positive controls, exceeding the 70% needed as outlined in ASTM D 5210 – 96. Gas production from degradation of the PHB plates and the PHB/15% TBC blend plates reached plateaus by 80 and 190 days, respectively. This data shows that the PHB requires more than twice as long to degrade when blended with 15% TBC. However, the PHB/15% TBC blend exhibited superior biodegradability (93.8%) to the pure PHB (82.8%) on the basis of the observed gas production but with much variability (Table 2.2). The PLA showed no significant gas production in excess of the blank controls, indicating that it had undergone no degradation in the sewage sludge medium throughout the exposure period. This is consistent with results reported by Shin et al. (1997), who did not observe any significant biodegradation of poly-L-lactic during 100 days of exposure to anaerobic sewage sludge using the same ASTM procedure. The longer times required to degrade the materials tested in this experiment indicate that the sewage sludge used was a slower degrading sludge, although it seemed to degrade the substances more thoroughly based on gas evolution; this may be a result of less carbon being assimilated into new biomass of the degrading microorganisms. Presumably, no significant loss of biogases occurred during this experiment since 70% N_2/30% CO_2 gas sparging had been utilized. The VS content of the sewage sludge used for EXP3 was 1.58%. A carbon mass balance of EXP3 (Table 2.4) showed better results than EXP2 with ~100% polymer carbon being re-accounted for in the reactors containing the cellulose powder and the PHB/15% TBC blend plates and 88% for the PHB plates.

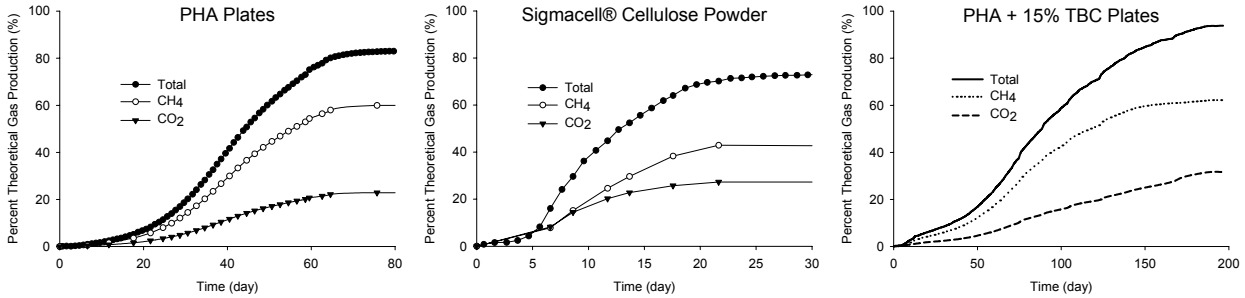

Figure 2.4. Graphs representing the percentage of theoretical gas production (%ThGP) from degradation of the PHB plates, Sigmacell® cellulose powder (positive controls), and PHB/15% TBC blend plates in EXP3. The values shown are net values for total gas production, methane (CH_4) production, and carbon dioxide (CO_2) production.

Table 2.4. Carbon mass balance of EXP3 comparing C input (Polymer C + Biomass C + DOC) with C output after incubation (Polymer C + Biomass C + DOC + Biogas C). Values shown are averages for triplicate bioreactors for each polymer tested for biodegradation.

	Polymer	Polymer (mg/L)	Polymer C (mg/L)	Biomass C (mg/L)	DOC (mg/L)	Biogas C (mg/L)	Total mg/L	Total %
Input	Blanks	–	–	886	13.7		900	100.0
Output				1034	7.4	23	1064	118.0
Input	PHB Plates	8467	4665	886	13.7		5565	100.0
Output			–	1094	21.0	3783	4898	88.0
Input	Cellulose Powder	2381	998	886	13.7		1898	100.0
Output			–	1125	12.2	751	1888	99.5
Input	PHB/15% TBC	7126	4004	886	13.7		4904	100.0
Output	Plates		–	965	157.4	3761	4883	99.6
Input	PLA Plates	8353	4151	886	13.7		5051	100.0
Output			4151	1017	5.7	51	5225	103.4

The reactors containing the PHB/15% TBC blend plates had much larger amounts of DOC remaining at the end of the experiment than the PHB plates, which may indicate that the TBC portion of the blend had not been biodegraded and remained in the sludge medium. In this experiment, the initial biomass of each reactor was estimated based on determined amounts of particulate solids in extra vials that had been filled with 150 mL of the sludge medium during the experimental setup in the same manner as the experimental reactors.

2.3.2 Mass Loss Experiments

The results for the first anaerobic mass loss experiment indicate a 100% mass loss by week 12 for the 0.5-mm and 1.2-mm thick plates, while the 3.5-mm plates were fully biodegraded by week 19 (Table 2.5). For all of the plate sizes in the first anaerobic mass loss experiment, the rate of degradation (g d^{-1}) first increased and then decreased as the end of degradation neared (Appendix A). This resulted in a sigmoidal-shaped mass loss curve for all of the specimens degraded in the experiment which was also seen for most specimens degraded in the second mass loss experiment.

Table 2.5. Percentages of degradation observed for the PHB plates exposed to the anaerobic sewage sludge medium of both the first and second anaerobic mass loss experiments and the PLA and PHB/15% TBC blend plates of the second experiment exposed for the times indicated.

First Experiment	**Plate Thickness**		
Exposure Time	**0.5 mm**	**1.2 mm**	**3.5 mm**
2 weeks	20.3%	12.3%	4.6%
4 weeks	48.4%	46.4%	16.5%
8 weeks	97.3%	97.2%	64.3%
12 weeks	99.5%	100.0%	92.5%
19 weeks	100.0%	100.0%	99.7%

Second Experiment	**PHB**			**PLA**	**PHB/15% TBC**
Exposure Time	**0.24 mm**	**1.2 mm**	**5 mm**	**(1.2 mm)**	**(1.2 mm)**
5 days	6.6%	–	–	–	–
10 days	22.0%	–	–	–	–
2 weeks	–	8.1%	2.2%	-0.2%	6.4%
15 days	54.2%	–	–	–	–
3 weeks	53.7%	–	–	–	–
4 weeks	73.4%	14.5%	7.3%	-0.3%	13.3%
6 weeks	82.9%	–	–	–	–
8 weeks	94.1%	68.2%	22.5%	-9.2%	32.4%
10 weeks	100.0%	–	–	–	–
12 weeks	100.0%	79.1%	26.8%	0.1%	54.4%
16 weeks	100.0%	73.2%	48.8%	0.0%	60.4%
20 weeks	100.0%	100.0%	59.4%	-0.2%	85.5%
32 weeks	100.0%	100.0%	68.9%	–	–

Mass loss with respect to initial surface area increased more rapidly throughout the degradation period for the thicker plates and slower for the thinner plates. This may be attributed to a decrease in the mass-to-surface-area ratio of the thicker plates as the degrading microorganisms burrowed into these plates. Although the same phenomenon would have occurred for the thinner plates, it would be more pronounced for the thicker plates. Mass loss is based on the initial mass of the plates and the final weight of the samples that could be recovered from the medium. Figure 2.5 clearly illustrates the surface deterioration of the plates degraded in the first mass loss experiment. With increasing time, the porosity of the plate surface increased, allowing further colonization of the bacteria deeper into the specimens. A relationship between the degradation rate coefficient and the initial mass-to-surface-area ratios was established during the first anaerobic mass loss study (Figure 2.6, top curve). This relationship expectantly follows saturation kinetics. The maximum degradation rate was estimated to be 4.62 mg cm^{-2} d^{-1}.

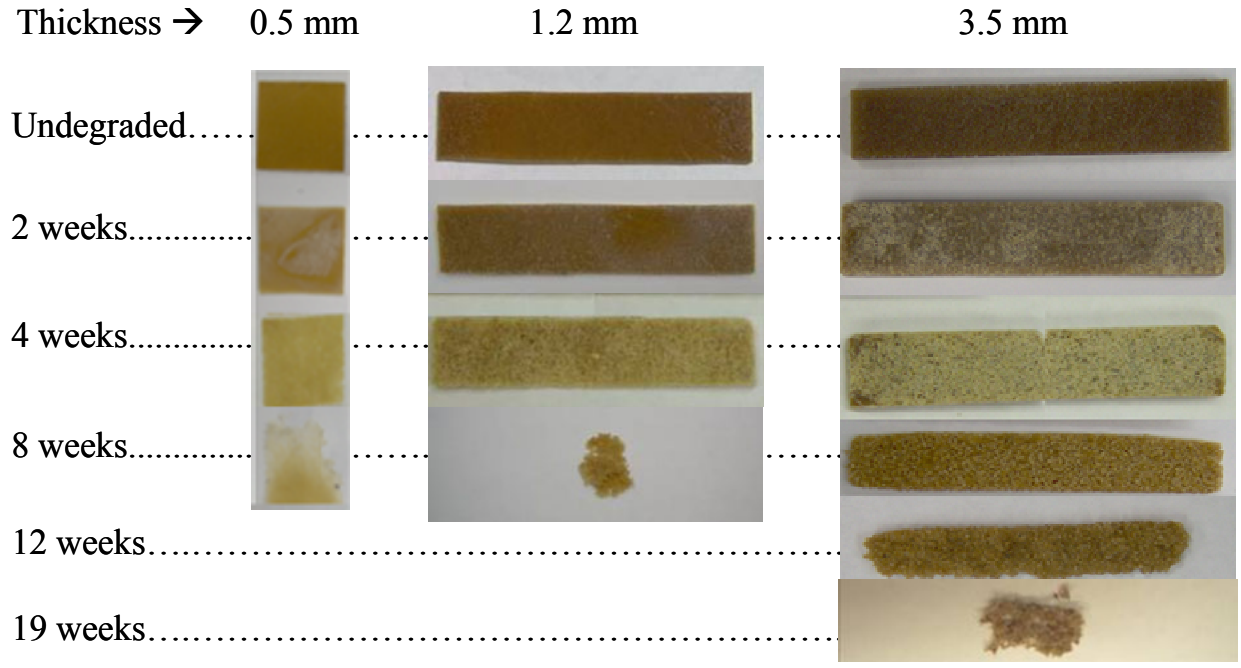

Figure 2.5. Visual comparison of the undegraded and degraded PHB plates with thicknesses of 0.5, 1.2, and 3.5 mm that were degraded in the second anaerobic mass loss experiment. Plate thicknesses and times of exposure are indicated.

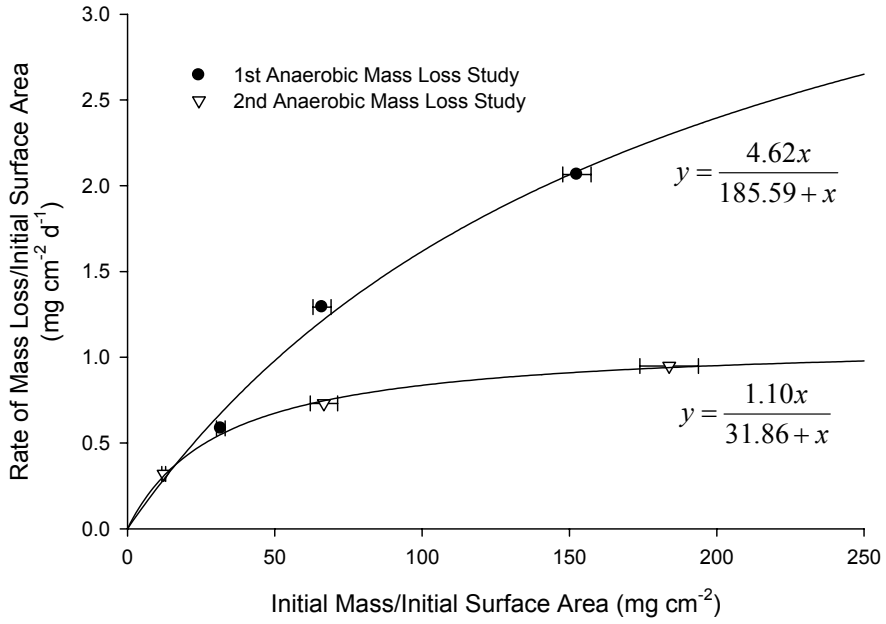

Figure 2.6. Relationships between the degradation rate coefficient (mg cm^{-2} d^{-1}) and the initial mass-to-surface-area ratio (mg cm^{-2}) for the three different plate sizes of PHB degraded in the first anaerobic mass loss study and the three different plate sizes degraded in the second anaerobic mass loss study.

The second anaerobic mass loss experiment was performed in order to further define the relationship between the initial mass-to-surface-area ratio and the degradation rate coefficients of the PHB plates with different thicknesses (Figure 2.6, bottom curve). The 1.2-mm PHB plates were degraded again, thereby, serving as a control between the first and second experiments. The second experiment resulted in a much smaller degradation rate coefficient (25% of the first experiment's rate; 1.10 mg cm^{-2} d^{-1}). The degradation rate of the 1.2-mm PHB plates from the second experiment was approximately 56% of the calculated rate from the first experiment. These results clearly indicate that while the same ASTM standard was used, the activity of the sludge has a tremendous impact on the degradation kinetics. Thus, caution should be used when interpreting and comparing data from various research groups. It can be seen in Figure 2.6 that the sludge in the first anaerobic mass loss study degraded the PHB more quickly than the sludge

in the second study; however, the sludge for the second study seemed to degrade more thoroughly. The photos of Figure 2.7 visually compare the gradual decomposition of all the sizes and types of material tested for biodegradation in the second anaerobic mass loss experiment. The 0.24-mm PHB plates investigated in the second anaerobic mass loss study reached 100% degradation after 10 weeks of exposure (Table 2.5). In the work of Abou-Zeid et al. (2004), PHB films of similar thickness were degraded in an anaerobic sewage sludge medium and reach 100% mass loss within 6 weeks. The 1.2-mm PHB plates showed 100% degradation by 20 weeks, while the 5-mm PHB plates and 1.2-mm PHB/15% TBC blend plates both showed significant degradation but did not show complete biodegradation within the timeframe of the experiment.

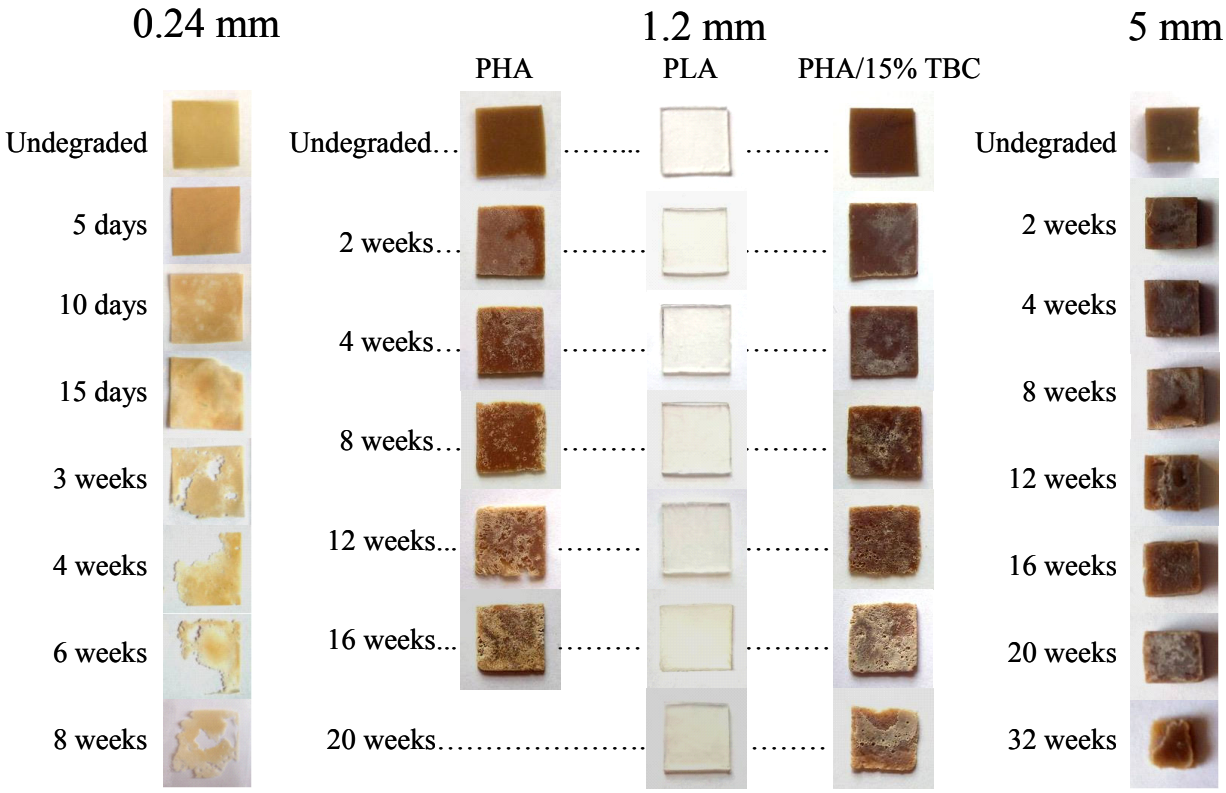

Figure 2.7. Visual comparison of the undegraded and degraded PHB plates with thicknesses of 0.24, 1.2, and 5 mm and the PLA plates and PHB/15% TBC blend plates that were degraded in the second anaerobic mass loss experiment. Plate thicknesses and times of exposure are indicated.

The comparison of the 1.2-mm PHB plates and the 1.2-mm PHB/15% TBC blend plates provides some interesting observations. Within the first month of degradation, no difference was observed in mass loss. During the second month, the PHB degraded twice as fast as the PHB/15% TBC blend, and then the gap closed again thereafter. While the mechanisms are not known at this time, it can be stated that the additives had an effect on the degradation process. However, in practical terms, the difference is only a month or two. No mass loss occurred for the PLA; instead a slight gain of mass was observed throughout most of the experiment except for a slight loss and zero gain at 12 and 16 weeks, respectively. The gain of mass may indicate that the material had absorbed water from the medium that could not be removed by oven-drying of the PLA, a phenomenon also observed previously for bottles made from a polyethylene-starch blend exposed to the natural environment of a freshwater lake by Brandl and Puechner (1992) (Brandl et al., 1995). Shin et al. (1997) also exposed PLA to a sewage sludge environment with no mass loss being observed. The raw data of the mass loss experiments and statistical analyses can be found in Appendix A.

Table 2.6 lists the degradation rate coefficients of all the materials tested for biodegradability in both the first and second anaerobic mass loss experiments. These degradation coefficients were calculated as outlined in the Materials and Methods section. An illustrative example of a degradation curve used to make these calculations is provided in Figure 2.8 and the curves for all thicknesses of plastic in both experiments can be found in Appendix A. These are the same coefficients that were plotted with respect to their initial mass-to-surface-area ratios for the PHB in Figure 2.6. An analysis of covariance on the data for both mass loss experiments was performed to indicate whether these coefficients were statistically different using a significance level of 0.05. The analysis of covariance for the first mass loss experiment

indicated that the degradation coefficients for all three thicknesses of PHB tested were significantly different. For the second mass loss experiment, the analysis of covariance was only able to conclude that the degradation coefficients for the 5-mm PHB and 1.2-mm PHA/15% TBC blend were significantly different. The output of these analyses as reported by the SAS statistical software used can be found in Appendix A.

Table 2.6. The degradation rate coefficients of all materials tested in the first and second anaerobic mass loss experiments.

Experiment/Test Material	**Degradation Rate Coefficient (mg cm^{-2} d^{-1})**
First Anaerobic Mass Loss Experiment	
0.5-mm PHB	0.58
1.2-mm PHB	1.29
3.5-mm PHB	2.07
Second Anaerobic Mass Loss Experiment	
0.24-mm PHB	0.32
1.2-mm PHB	0.73
5-mm PHB	0.95
1.2-mm PHB/15% TBC blend	0.38
1.2-mm PLA	0.00

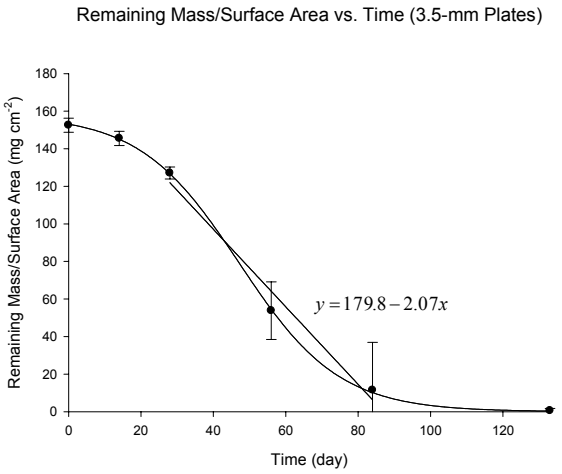

Figure 2.8. An illustrative example of a degradation curve used to perform a linear regression in the determination of degradation coefficients of plastics biodegraded in the anaerobic mass loss experiments. The example shown is for the 3.5-mm PHB plates degraded in the first mass loss experiment. A linear regression was performed for the three data points in the middle of the degradation curve. The equation for that line is shown.

2.3.3 Characterization Analyses

2.3.3.1 Chemical Properties

The results of the FT-IR analyses for the melt-pressed PHB plates with 1.2-mm and 3.5-mm thickness degraded in the first anaerobic mass loss study and the melt-pressed PHB plates of all thicknesses including the PHB/15% TBC blend degraded in the second anaerobic mass loss study are presented in Figures 2.9 and 2.10, respectively. Degradation appeared to have no effect on the spectrograms of the PHB bioplastic. This indicates that the cleavage of the many different types of bonds occurs proportionally equal throughout the polymer during the degradation process. These findings are consistent with those of Day et al. (1994) who degraded PHBV in an anaerobic sewage sludge medium for 40 days. One of the more notable indications of the data is the appearance of peaks specific to peptide groups, most likely from proteins of the degrading bacteria in the sludge medium. Figure 2.11 shows an enlarged view of these peaks for the 3.5-mm PHB plates degraded in the first anaerobic mass loss experiment.

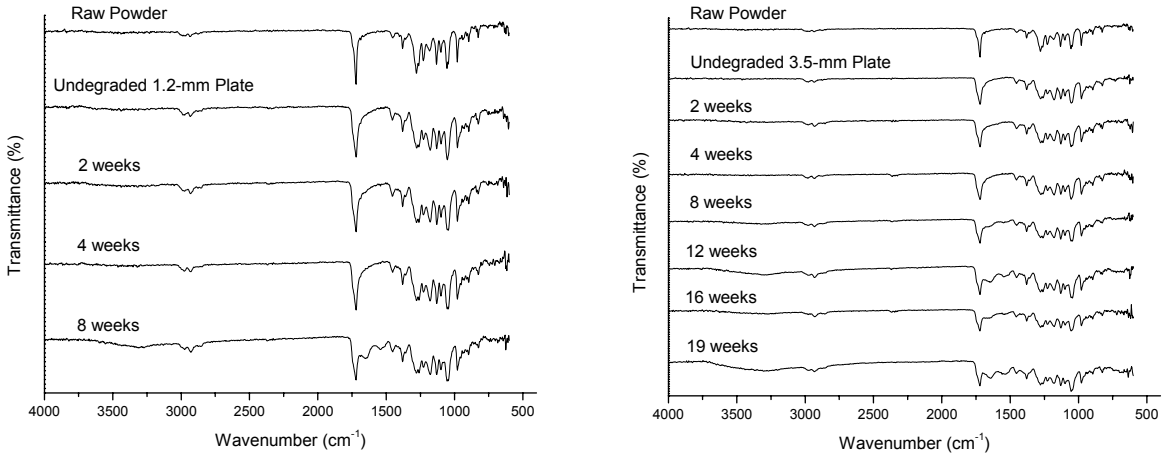

Figure 2.9. Spectrograms obtained by FT-IR of the PHB melt-pressed plates with 1.2-mm thickness (left graph) and 3.5-mm thickness (right graph) before and after degradation in the first anaerobic mass loss experiment. The spectrogram for the raw-powder form of the plastic is included for comparison.

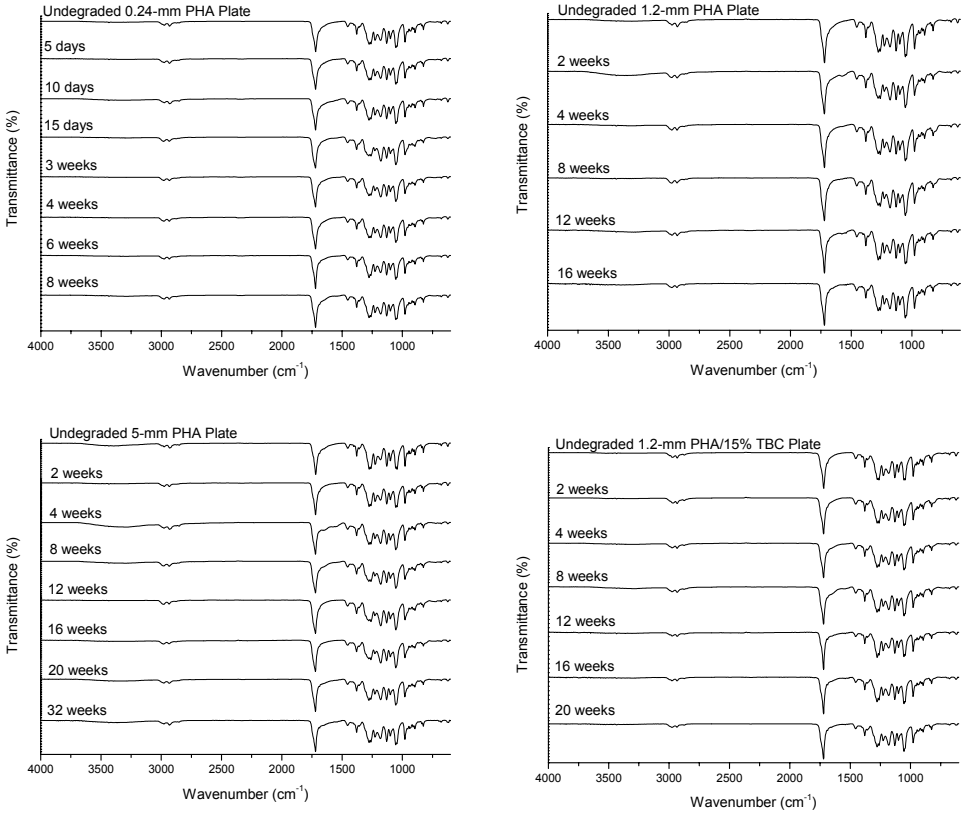

Figure 2.10. Spectrograms obtained by FT-IR of the PHB plates with 0.24-mm (top left), 1.2-mm (top right), 5-mm thickness (bottom left), and the 1.2-mm PHB/15% TBC plates (bottom right) before and after degradation in the second anaerobic mass loss experiment.

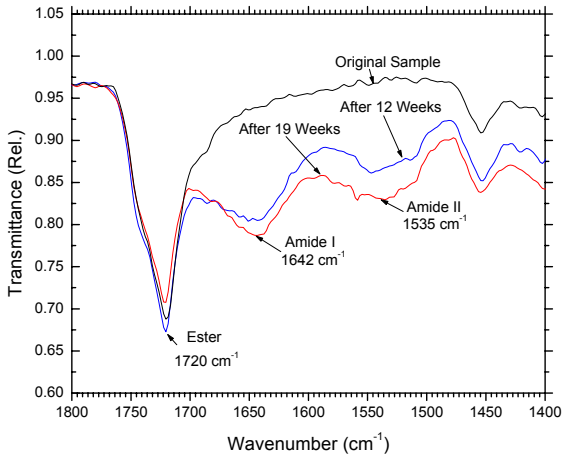

Figure 2.11. An enlarged view of the FT-IR spectrograms for the original (undegraded) 3.5-mm PHB plates and those that had been degraded for 12 and 19 weeks in the first anaerobic mass loss experiment showing build-up of amides.

Molecular weight determinations of the undegraded PHB plates and those with 0.5-mm, 1.2-mm, and 3.5-mm thickness degraded in the first anaerobic mass loss experiment (Figure 2.12) show that biodegradation had little to no effect on the molecular weight of the PHB bioplastic. Many other degradation experiments have little to no decrease in molecular weight as a result of degradation (Day et al., 1994; Mergaert et al., 1994; Mergaert et al., 1993; Doi et al., 1990; Kanesawa and Doi, 1990) and usually, when a decrease in molecular weight is observed, it can be attributed to some other phenomenon such as abiotic hydrolysis (Gilmore et al., 1992). This has led researchers to believe that the polymer is degraded enzymatically at the surface to lower-molecular-weight fragments that are rapidly metabolized by the degrading microorganisms causing mass loss but no effect on the molecular weight of the remaining polymer.

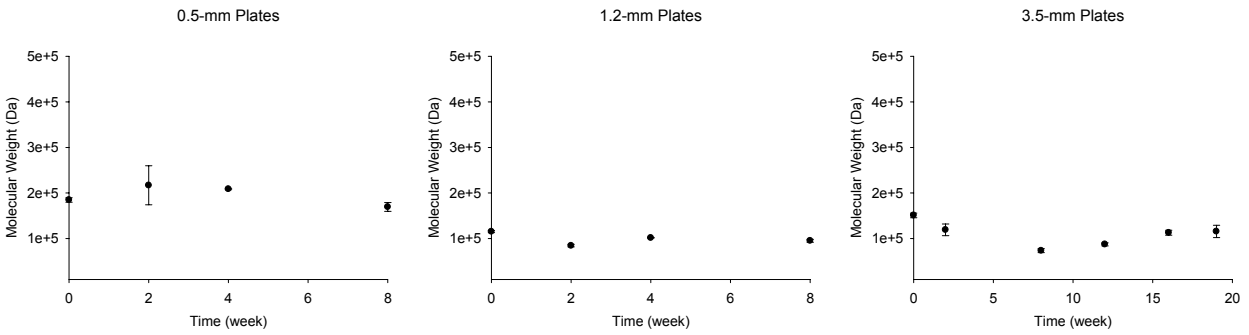

Figure 2.12. Molecular weight data obtained by Size Exclusion Chromatography of the PHB plates degraded in the first anaerobic mass loss experiment. Error bars indicate standard deviation of duplicate measurements and the x-axis refers to time of degradation.

2.3.3.2 Thermal Properties

Figure 2.13 shows the graphical representation of the DSC data for the undegraded 1.2-mm PHB plates as analyzed using the TA Universal Analysis V3.9A software. An interesting trend was noticed in the ΔH_m values for the PHB samples which had been formed into plates of different thicknesses. The thinner plates seemed to have lesser values of ΔH_m during the first heatings than the thicker plates, ranging from approximately 90 J g^{-1} for the 0.24-mm plates to

104 J g^{-1} for the 5-mm plates (Table 2.7). This means the crystallinity of the PHB was dependent on the plate thickness and ranged from approximately 62% for the 0.24-mm plates to 71% for the 5-mm plates determined from the ratio $\Delta H_f/\Delta H_f^0$, where ΔH_f and ΔH_f^0 are the observed enthalpy of fusion and the enthalpy of fusion of perfect PHB crystal (146 J g^{-1}) (El-Hadi et al., 2002; Yoshie et al., 2000; Barham and Keller, 1986; Barham et al., 1984), respectively. The difference in degrees of crystallinity can be attributed to the differences in cooling rates from the melt during melt-pressing of the plates. It can be stated that during preparation, the thinner plates cooled more quickly than the thicker plates. It is known that the crystallization rate of PHB increases with increasing heating/cooling rates, while the half-time of crystallization decreases (An et al., 1998) and as a result, the crystallinity decreases (Chen et al., 2005).

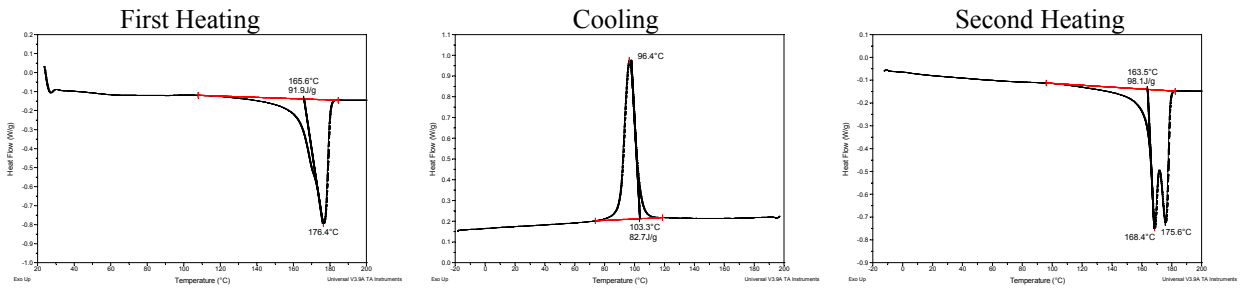

Figure 2.13. Graphical representations of the DSC data for the undegraded 1.2-mm PHB plates as analyzed using the TA Universal Analysis V3.9A software.

Table 2.7. DSC thermal data of the undegraded bioplastics.

	1st Heating				Cooling			2nd Heating			
	1st Peak (°C)	2nd Peak (°C)	T_m (°C)	ΔH_m (J g^{-1})	Peak (°C)	T_c (°C)	ΔH_c (J g^{-1})	1st Peak (°C)	2nd Peak (°C)	T_m (°C)	ΔH_m (J g^{-1})
PHB Powder	-	175.4	165.0	106.1	97.0	104.1	82.9	168.4	175.0	165.1	98.6
0.24-mm PHB	-	173.0	167.6	89.9	94.3	102.2	74.3	167.9	175.3	162.9	96.0
1.2-mm PHB	-	176.4	165.6	91.9	96.4	103.3	82.7	168.4	175.6	163.5	98.2
3.5-mm PHB	-	174.0	168.4	99.2	97.4	103.6	82.4	167.9	175.5	163.6	98.7
5-mm PHB	172.1	180.4	163.5	104.1	95.3	103.3	73.3	166.2	174.8	160.9	92.3
PHB/15 % TBC	161.4	170.4	153.4	81.9	83.9	101.7	59.2	154.1	167.4	144.5	82.2

It's interesting to note that the DSC endotherms often showed two distinct peaks, especially during the second heating period, which could be attributed to melting andrecrystallization of thin, unstable crystals during the DSC scan, a phenomenon observed by Renstad et al. (1997). The melting peak at the lower temperature was attributed to melting of the crystals formed during isothermal and non-isothermal crystallization, while the melting peak at the higher temperature was a result of recrystallization that took place during the heating process as was observed by Chen et al. (2005). The PHB/15% TBC blend appears to have lowered values of ΔH_m and ΔH_c compared to those of the pure PHA. This indicates a lower degree of crystallinity for the blend due to the addition of TBC. Lowered values of T_m also seem to occur for the PHA/15% TBC blend, which was also observed by Labrecque et al. (1997) who blended TBC with PLA, although an increase in crystallinity was observed in their blends with PLA, which had a very low crystallinity (less than 1%).

Biodegradation appeared to have only minor effects on the thermal properties of the PHB (Appendix B). It can be seen that for some samples from both experiments, the exotherms of the PHB plates during the cooling period became slightly smaller, indicating a decrease in the crystallization enthalpy (ΔH_c). It also appears that the endotherms during the melting period sometimes showed a slight decrease, indicating a decrease in the melting enthalpy (ΔH_m). This phenomenon was especially true for the 1.2-mm PHB plates in the first anaerobic mass loss experiment and the 0.24-mm PHB plates degraded in the second anaerobic mass loss experiment at 8 weeks, just before biodegradation was complete. This is most likely due to proteins from the degrading microorganisms and possibly other debris becoming incorporated into the polymer. The observed decreases in the endotherms is consistent with data reported in literature by

Tercjak et al. (2003), who degraded blends of a commercial plastic (Biopol) and polyamide 11 in compost. They also observed a decrease in ΔH_m after degradation.

2.3.3.3 Mechanical Properties

Tensile testing of the PHB melt-pressed plates (1.2-mm thick) showed that the mean stress at maximum load was 32.6 ± 0.73 MPa. This value is only slightly less than that (35 MPa) reported for PHB by El-Hadi and coworkers (2002) but much larger than that (21 MPa) reported by El-Taweel and coworkers (2004). However, it can be hard to compare the tensile properties of PHB as determined by others because they can depend on many factors, especially the aging time of the polymer. PHB is known to undergo secondary crystallization during storage at room temperature (El-Hadi et al., 2002) leading to an increase in brittleness of the polymer (Scandola et al., 1989). During aging, the modulus increases while the extension to break decreases (Barham and Organ, 1994). The storage time of the tensile test specimens for this research was approximately one week.

The 3.5-mm PHB plates that had been degraded for 2, 4, and 8 weeks were subjected to Izod pendulum impact testing (Table 2.8). The impact resistance of PHB seems to vary greatly based on what has been reported in literature (El-Hadi et al., 2002; Luzier, 1992; Barham and Keller, 1986). Luzier (1992) reports that the impact strength of PHB should be 60 J m^{-1} (~5.9 kJ m^{-2}) for PHB with 80% crystallinity while El-Hadi et al. (2002) reported 3 kJ m^{-2} (~30.5 J m^{-1}) for PHB with 60% crystallinity. So, it seems that the crystallinity greatly influences the impact strength. The PHB used in this research had a crystallinity of ~67%, so the strength value found (Table 2.8) for the undegraded material was similar to the results found by El-Hadi et al. although it showed a lesser strength value but higher crystallinity. From Figure 2.14, it can be seen that some of the samples were not normally broken when they were subjected to the Izod

pendulum impact test. Thus, when analyzing the results, only the samples which showed normal breakage were considered to have provided good data. The samples degraded for 8 weeks didn't fit the size requirements of the ASTM standard, but the results were presented, nonetheless.

Table 2.8. Summarized results of Izod pendulum impact testing of 3.5-mm melt-pressed plates of PHB degraded in the first anaerobic mass loss experiment. The strength data is shown in the units of both kJ/m2 and J/m. Standard deviations are also reported.

Degradation Time	Strength (kJ m^{-2})	Strength (J m^{-1})
Undegraded	2.45 ± 0.1	24.9 ± 0.7
2 weeks	2.31 ± 0.3	23.5 ± 3.0
4 weeks	2.19 ± 0.1	22.3 ± 0.6
8 weeks	0.53 ± 0.2	5.4 ± 1.9

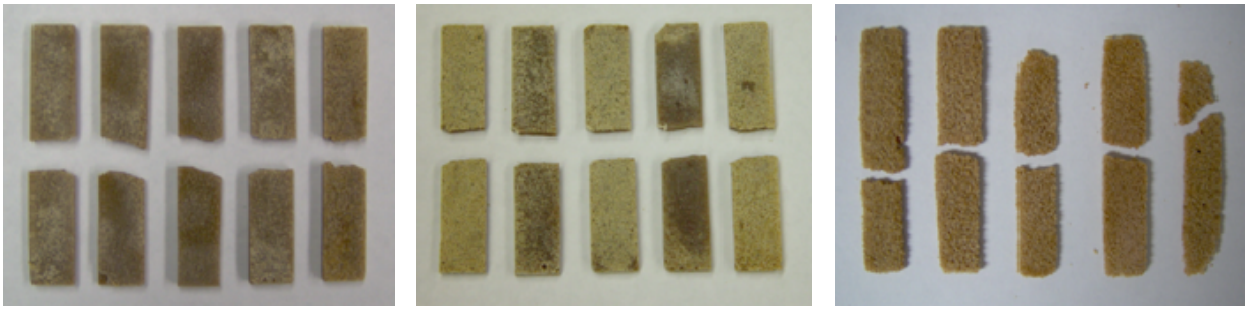

Figure 2.14. Samples after Izod pendulum impact testing. Plates with 3.5-mm thickness that were subjected to this test after 2, 4, and 8 weeks of degradation are shown here in that order from left to right.

The viscosity of the PHB in molten state at 180°C (considered as the temperature used for molding or extruding the material) decreased in time, e.g., from 28.3 Pa-s after 25 min (and an angular velocity of 10 s^{-1}) to 3.5 Pa-s after 70 min (reading @ 10 s^{-1}), pointing to a rather severe thermal degradation at this temperature. The viscosity after 70 min at 180°C was less than that read after 25 min at 190°C (7.2 Pa-s @ 10 s^{-1}). The data obtained is summarized in Figure 2.15. By comparison, Verhoogt et al. (1996) reported viscous stability only at 160ºC for P(3HB-*co*-12%-3HV). At 170ºC, they observed a 10% reduction in the complex viscosity was already

obtained after 200 s while a residence time of only 2 min resulted in a decrease in viscosity of almost 10% at 180ºC and of more than 20% at 200ºC.

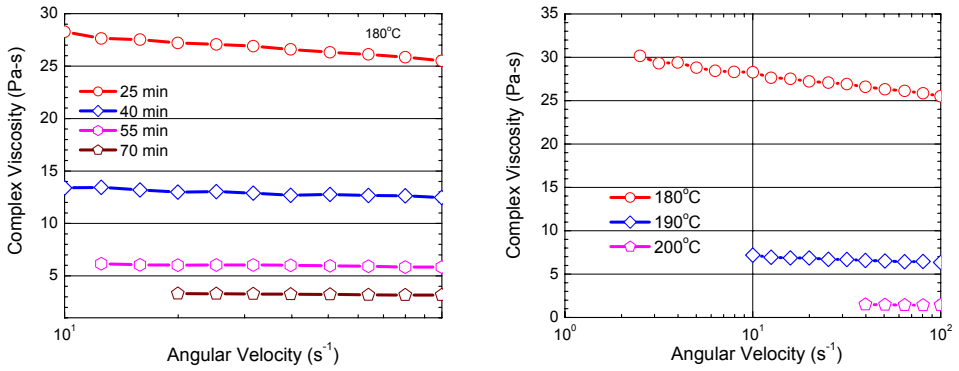

Figure 2.15. Rheological characterization of the PHB in molten state: Dependence of complex viscosity on angular velocity and temperature.

2.3.3.4 Physical Properties

Scanning electron micrographs were taken of the degraded melt-pressed PHB plates of all thicknesses from both anaerobic mass loss experiments and of 3.5-mm plates that were degraded in separate vials parallel to those of the EXP2 biogas experiment. Figure 2.16 below presents SEM images of the 3.5-mm PHB plates that were degraded parallel to EXP2 and Figure 2.17 contains images of the degrading microorganisms found on the plate that had been degraded for 2 weeks. Figure 2.18 contains SEM images of the plates of various thicknesses degraded in the first anaerobic mass loss experiment showing the gradual decomposition of the plates throughout the 19 weeks of the experiment. Figures 2.19 – 2.23 illustrate the gradual decomposition and increasing porosity of the plates of each thickness degraded in the second anaerobic mass loss experiment. An extensive discussion of the images from the second anaerobic mass loss experiment can be found after the figures.

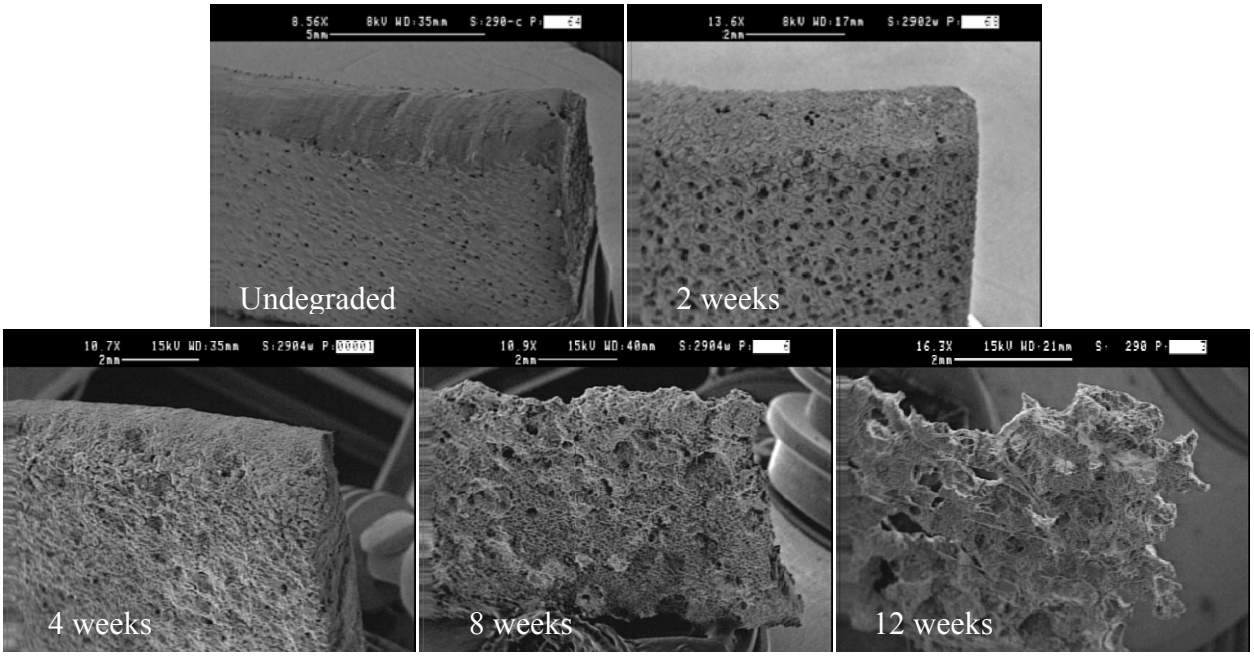

Figure 2.16. SEM photographs of an undegraded 3.5-mm thick melt-pressed PHB plate compared to those after 2, 4, 8, and 12 weeks of anaerobic degradation in the ASTM-defined sewage sludge medium. Captions indicate time of degradation.

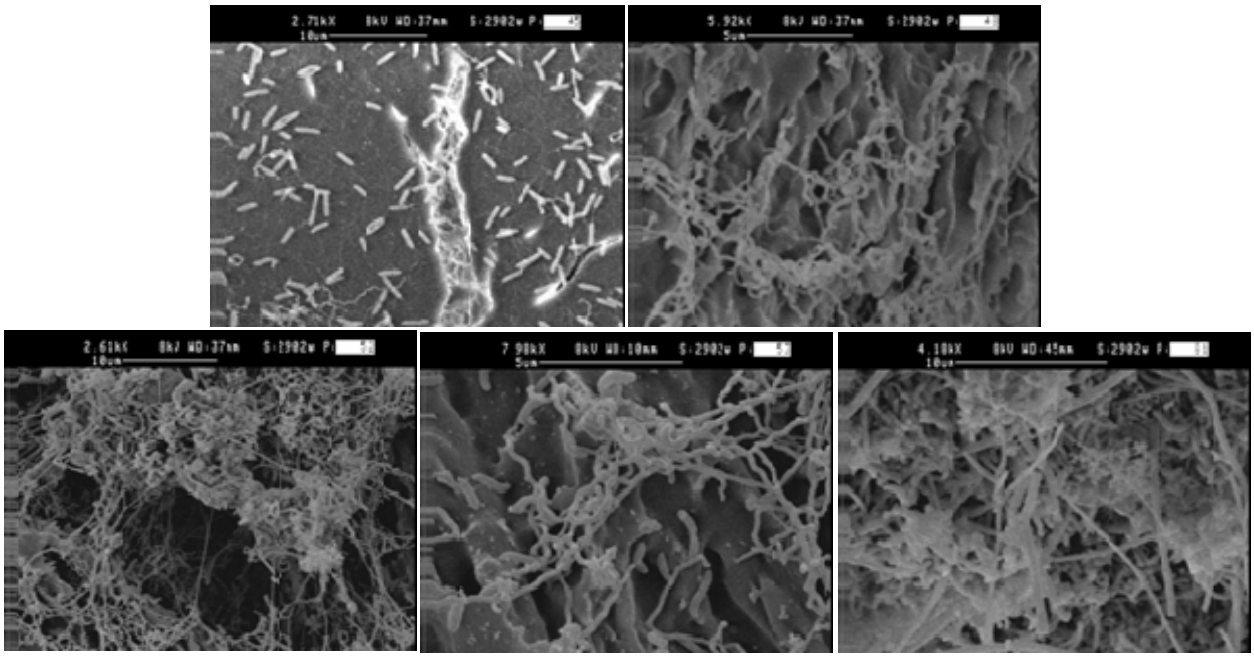

Figure 2.17. Various SEM images of the degrading microorganisms found on a melt-pressed plate of PHB after 2 weeks of degradation in the ASTM-sludge medium parallel to EXP2.

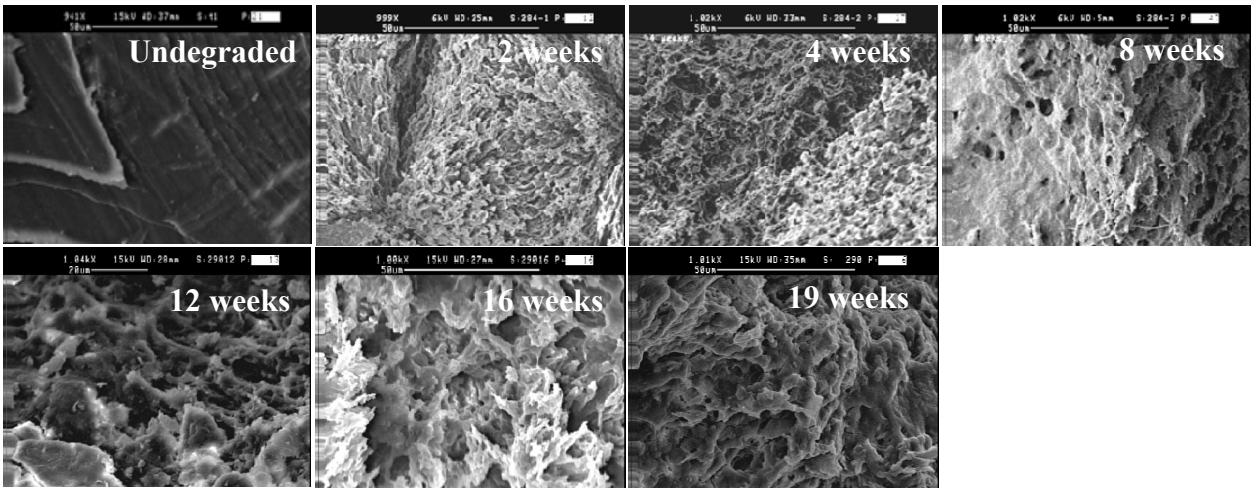

Figure 2.18. SEM images (~1000X magnification) of 1.2-mm melt-pressed PHB plates undegraded and after 2, 4, 8, 12, 16, and 19 weeks of biodegradation in the first anaerobic mass loss experiment. Times of degradation are indicated in the upper-right corner of each picture.

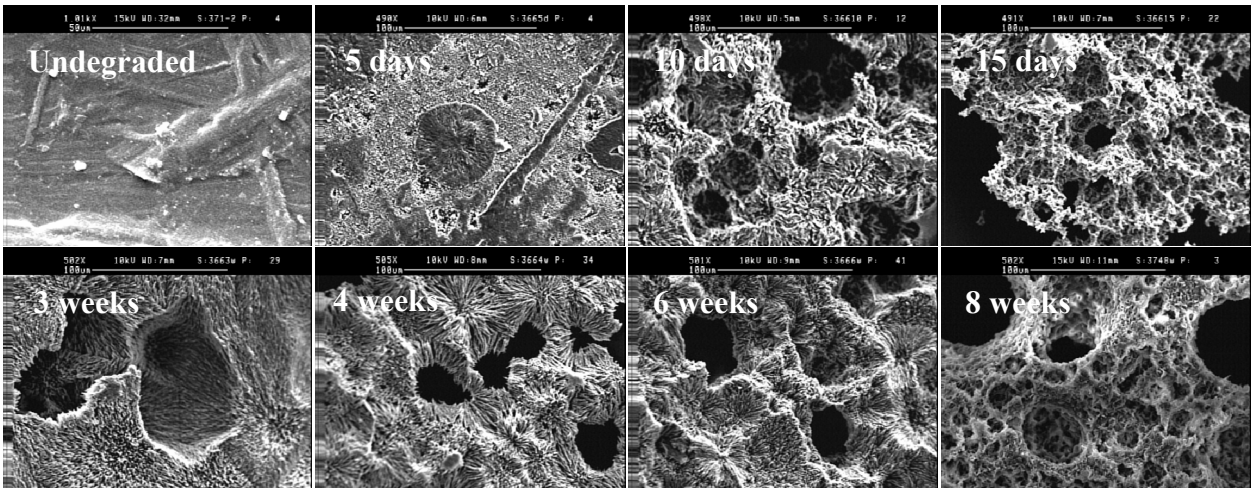

Figure 2.19. SEM images (~500X magnification) of 0.24-mm melt-pressed PHB plates undegraded and after 5, 10, and 15 days, and 3, 4, 6, 8 weeks of biodegradation in the second anaerobic mass loss experiment. Times of degradation are indicated in the upper-left corner of each picture.

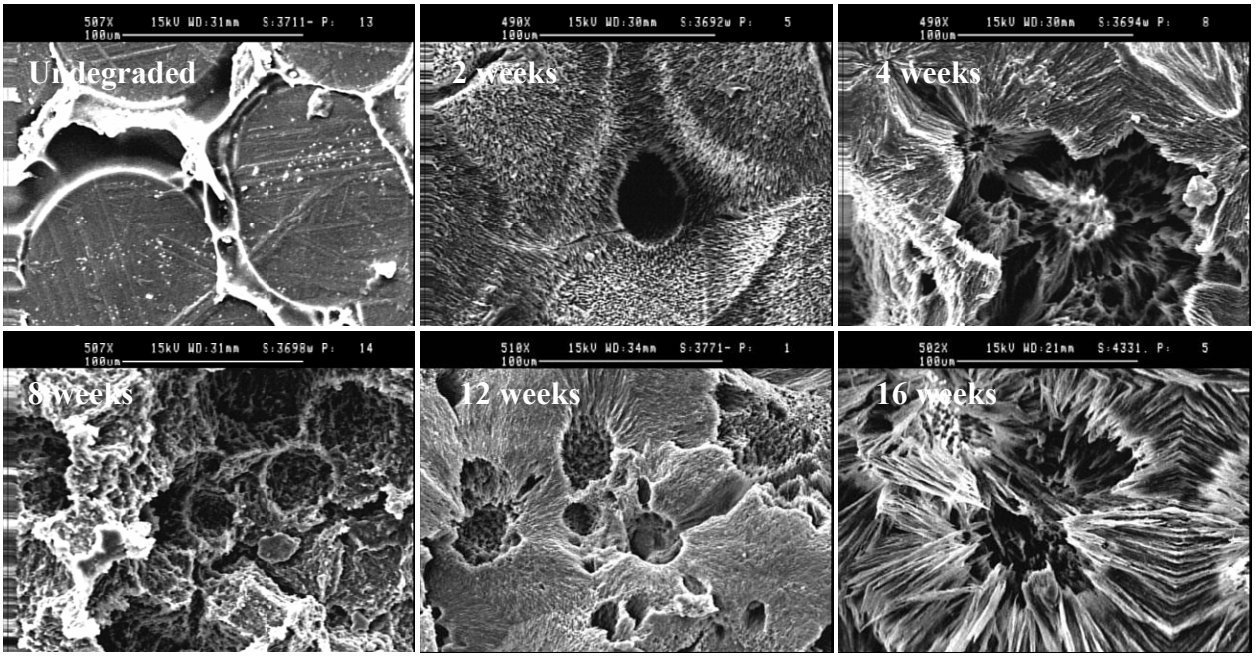

Figure 2.20. SEM images (~500X magnification) of 1.2-mm melt-pressed PHB plates undegraded and after 2, 4, 8, 12, and 16 weeks of exposure in the second anaerobic mass loss experiment. Times of degradation are indicated in the upper-left corner of each picture.

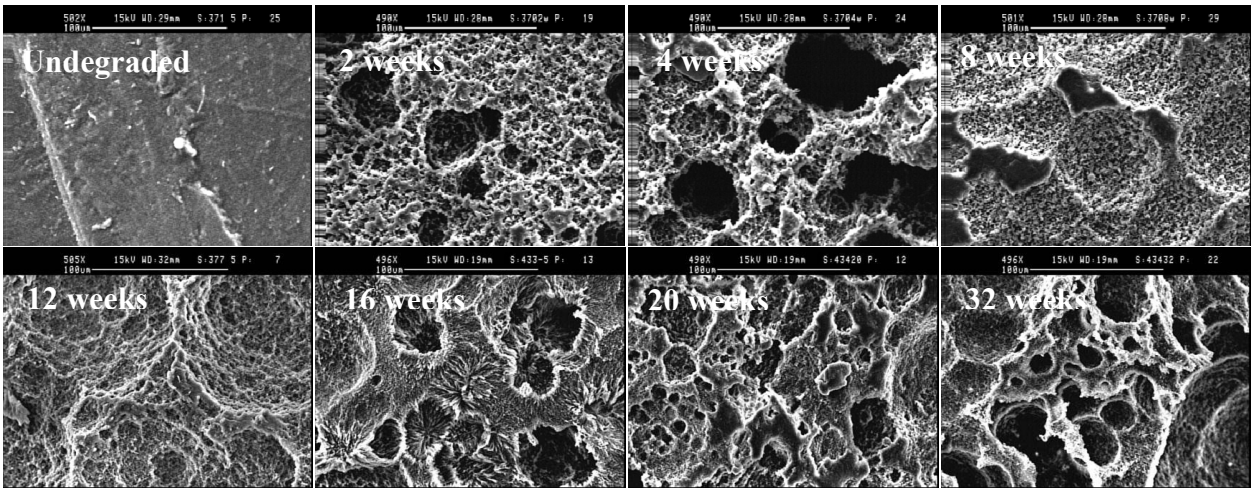

Figure 2.21. SEM images (~500X magnification) of 5-mm melt-pressed PHB plates undegraded and after 2, 4, 8, 12, 16, 20, and 32 weeks of biodegradation in the second anaerobic mass loss experiment. Times of degradation are indicated in the upper-left corner of each picture.

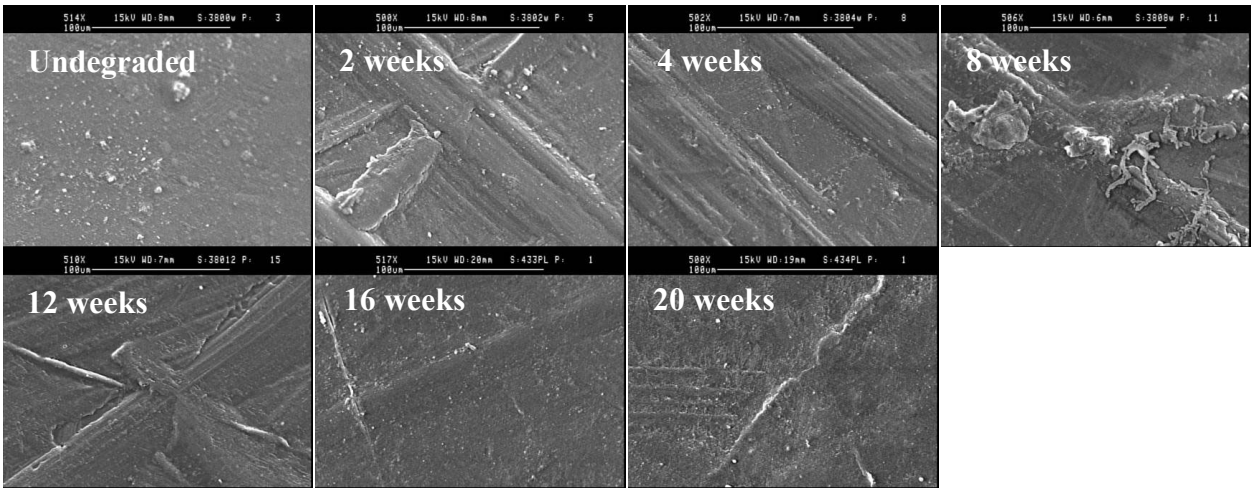

Figure 2.22. SEM images (~500X magnification) of 1.2-mm melt-pressed PLA plates undegraded and after 2, 4, 8, 12, 16, and 20 weeks of biodegradation in the second anaerobic mass loss experiment. Times of degradation are indicated in the upper-left corner of each picture.

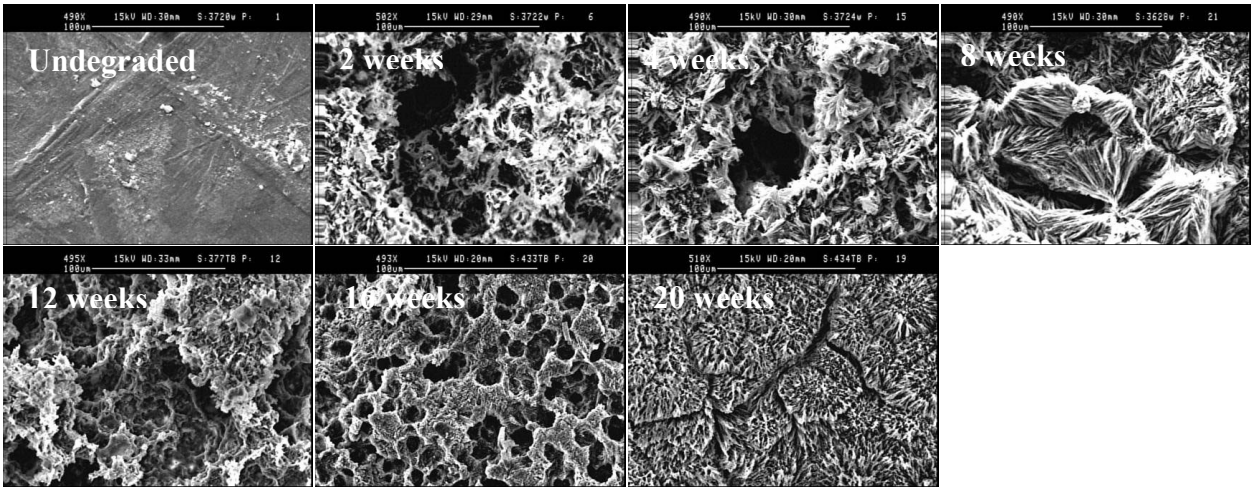

Figure 2.23. SEM images (~500X magnification) of 1.2-mm melt-pressed PHB/15% TBC blend plates undegraded and after 2, 4, 8, 12, 16, and 20 weeks of biodegradation in the second anaerobic mass loss experiment. Times of degradation are indicated in the upper-left corner of each picture.

The 0.24-mm PHB plates degraded in the second anaerobic mass loss experiment (Figure 2.19) initially lost their luster and became very matte showing only small lesions after 5 days. Within 10 days, numerous holes and gullies could be seen which became larger and more abundant throughout the degradation process. After only 15 days, holes could be seen in the SEM micrographs that protruded through the entire thickness of the plates and by 10 weeks, no plastic remained. The 1.2-mm PHB plates degraded in the second anaerobic mass loss experiment (Figure 2.20) showed some holes in the surface of the plates after 2 weeks which were most likely remnants of the large crevasses seen on the undegraded material which surrounded spherulitic structures within the material; most degradation at this point appeared to have occurred primarily at the surface, which became very matte, as usual. By 4 weeks, microbial attack within the material was apparent with lesions becoming larger, more abundant, and more scattered throughout the degradation process. By 16 weeks, though, the remaining surface structures had changed their appearance to a network of narrow and scattered "sickles," most likely due to either a shift in the microbial consortia or maybe crystalline regions of the material left behind by microbes which favored the more amorphous regions; this would be consistent with the findings of Spyros and Kimmich (Spyros et al., 1997) whose work provides evidence for the preferential degradation of the amorphous phase by PHB depolymerase B from *Pseudomonas lemoignei*. The 5-mm PHB plates degraded in the second anaerobic mass loss experiment (Figure 2.21) showed numerous holes and lesions in the surface of the material that did not show very much change in appearance throughout the degradation process due to the extreme thickness of the plates which seemed to inhibit microbial attack from occurring within the greater depths of the material. The surfaces of the 1.2-mm PLA plates (Figure 2.22) did not show any significant changes throughout the exposure period in the second anaerobic mass loss

experiment as was expected since no degradation of the PLA was observed. The 1.2-mm PHB/ 15% TBC blend plates degraded in the second anaerobic mass loss experiment (Figure 2.23) showed surface morphology much different than that for the pure PHB throughout the degradation process. At 2 and 4 weeks, it appeared the microbes had begun to attack the inner parts of the material but later appeared to prefer microbial attack at just the surface which would partly explain why the blend required more time to degrade than the pure PHB.

2.4 Conclusions

The degradation studies in anaerobic sewage sludge have shown that the PHB bioplastic is completely biodegradable. More than 80% biogas recovery was observed in the gas production experiments while 100% mass loss was observed in the mass loss experiments, meaning that up to 20% of the polymer mass could be expected to assimilate into new biomass of the degrading microorganisms. This observation along with the data showing that the degradation rate coefficient is dependent upon the initial mass-to-surface-area ratio and follows saturation kinetics should provide useful information for PHA waste treatment design in anaerobic waste treatment processes. The combined characterization analyses of the degraded PHB have shown that it undergoes a rather uniform degradation with respect to molecular attributes of the material (i.e. no change in relative composition of molecular bonds as measured by FT-IR and no significant changes in molecular weight as measured by SEC). These observations show that commercial products made from PHA bioplastics would maintain their integrity for a useful lifespan despite the fact that the material is degradable since PHAs are known to remain inert in ambient air and environments that would not facilitate biodegradation. Furthermore, the fact that the presence of thermal history had no significant effects on thermal properties in the DSC experiments shows that the PHB could potentially be recyclable and

undergo the involved re-melting processes without compromising material characteristics. All of these data provide useful insight regarding the lifecycle design of PHAs to ease the transition from commodity plastics to their biodegradable alternatives.

Chapter 3: Aerobic Biodegradation of Polyhydroxybutyrate (PHB) in Compost

3.1 Introduction

The biodegradation of bio-based plastics has become a growing topic of interest due to the environmental issues associated with the production and disposal of petroleum-based plastics and the finite supply of and reliance on foreign oil to produce these commodity plastics. "Bioplastics" are thermoplastic materials that can be naturally made from renewable resources and will biodegrade in natural environments. To be classified as biodegradable, more than 60% of a material's organic carbon must be converted within a maximum of six months in laboratory experiments. In real-life conditions of composting, more than 90% of the plastic is required to be degraded to fragments not more than 2 mm in size (Mecking, 2004). The end products of bioplastic degradation are non-toxic and already occur naturally in the environment: carbon dioxide (CO_2) gas and water (H_2O) in aerobic environments and CO_2 and methane (CH_4) gas in anaerobic environments. The degradation of bioplastic additives, such as plasticizers, could potentially release toxic by-products, but this could be avoided by using natural additives such as tributyl citrate (TBC). The manufacture of plastic products that enter the waste stream from biodegradable materials would significantly reduce the negative environmental impact caused by the previously mentioned methods of disposal used for petroleum-based plastics.

Biodegradation of PHAs is often studied using isolated microorganisms *in vitro* that have been identified as PHA degraders (Lee et al., 2005; Elbanna et al., 2004; Handrick et al., 2004; Kim and Rhee, 2003; Jendrossek and Handrick, 2002; Sang et al., 2002; Jendrossek, 2001; Scherer et al., 1999; Iwata et al., 1997; Hocking et al., 1996; Jendrossek et al., 1996; Molitoris et al., 1996). The types of microorganisms used and the environmental conditions will greatly affect the degradation rate, which under controlled conditions can be determined with very

reproducible results. However, only very few studies have studied the biodegradation of PHAs in natural environments or waste-degrading environments consisting of mixed cultures of species. It is very important that more research be performed in such environments so that more can be understood about how to increase confidence that PHAs will degrade at a certain rate under given conditions in a mixed-culture environment or to at least better understand what other factors will affect those results. One municipal waste environment that has attracted great interest for biodegradation of PHAs is compost under aerobic conditions. Several research groups have published work involving biodegradation of PHAs in aerobic compost (Grima et al., 2000; Manna and Paul, 2000; Ohtaki and Nakasaki, 2000a; Ohtaki and Nakasaki, 2000b; Imam et al., 1998; Eldsäter et al., 1997; Yue et al., 1996; Mergaert et al., 1994; Gilmore et al., 1992) and in similar soil environments (Song et al., 2003; Mergaert et al., 1993). Some of these works have studied the biodegradation behavior of PHAs through characterization of the degraded polymers but usually only focus on a limited number of aspects of the material characteristics. This work has combined the results from several different characterization analyses of a PHA degraded in aerobic compost to provide further insight to PHA degradation with focus on the characteristics of the material that have more implications concerning the life-cycle design of the polymer. The overall goals of this research thrust were to assess the aerobic biodegradation of a bioplastic obtained from a commercial producer in compost and determine how biodegradation affects the characteristics of the material. Additionally, a blend of the bioplastic with a natural additive was also tested for biodegradation to gain insight to the impact of such additives.

3.2 Materials and Methodology

The methodology consisted of three major sections: (1) material characterization and preparation, (2) characterization analyses, and (3) biodegradation studies. The characterization

analyses consisted of chemical properties, thermal properties, mechanical properties, and physical properties. The biodegradation studies consisted of one experiment assessing biodegradation based on biogas production monitored via respirometry and two mass loss experiments. The materials tested for biodegradation in the both the respirometric and mass loss experiments were PHB melt-pressed plates and PHB/15% TBC blend melt-pressed plates. In one biogas production experiment, low-density polyethylene (LDPE) melt-pressed plates were tested as a negative control.

3.2.1 Material Preparation

The bioplastic was obtained from Metabolix, Inc. whom identified it as a blend of polyhydroxybutyrate (PHB), the most prevalent PHA. Wide-angle X-ray diffraction (WAXD) performed on the raw material confirmed that the bioplastic was PHB (Figure 3.1). The material in its raw form was a fine, white plastic powder produced and extracted from the aerobic fermentation of recombinant *E. coli*. The PHB was also blended with 15% tributyl citrate (TBC) as an additive and degraded for comparison and to determine the impact of the

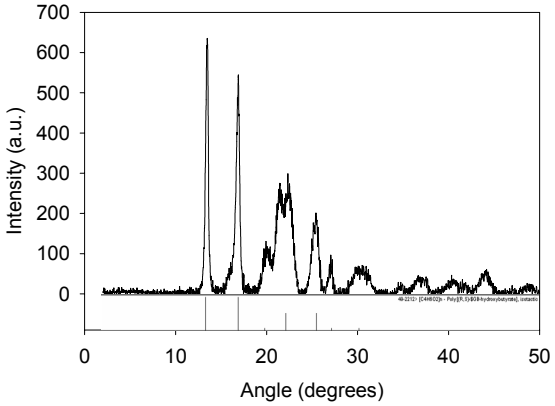

Figure 3.1. The WAXD spectrogram of the bioplastic obtained from Metabolix, Inc. The spectrogram was used to identify the material as PHB when compared to a database of many known spectrograms. The legend under the spectrogram shows where the peaks that are characteristic of isotactic polyhydroxybutyrate should appear and their relative intensity. Any additional peaks of the spectrogram were considered to be caused by impurities or other remnants from the extraction process after intracellular production in *E. coli*.

additive on the biodegradation of the material. Lastly, for the respirometric experiment, LDPE was tested for biodegradation as a negative control.

The PHB powder was melted at 179°C (355°F) for 5 – 10 min (longer for thicker plates), and pressed with a hydraulic jack into plates of different thicknesses (0.24 mm, 0.5 mm, 1.2 mm, 3.5 mm, and 5 mm) using a Carver Laboratory Press. The plates were allowed to cool to room temperature while still enclosed in the steel plates and mold or spacers used. The prepared plates were then cured for at least 7 days to allow for complete chemical equilibrium and crystallization prior to use in the degradation experiments and characterization analyses. Plates of the PHB/15% TBC blend and the low-density polyethylene (LDPE; negative controls in biodegradation experiments) were prepared in the same way except that the melting temperature of the LDPE was 121°C (250°F).

3.2.2 Material Characterization

3.2.2.1 Chemical Properties

Wide angle X-ray diffraction (WAXD) was performed on the PHB raw powder to identify its chemical composition. Two-dimensional wide angle X-ray diffraction images of the samples were obtained using an X-ray diffractometer (Siemens/Bruker D5000 XRD) equipped with KEVEX solid state detector. The Siemens D5000 XRD has a large diameter goniometer (600 mm), low divergence collimator, and Soller slits. The X-ray source was Copper radiation generated at 40 kV and 30 mA. The collected data were analyzed using the Siemens Kristalloflex V3.1 software application and compared to a database of many known spectrograms to identify the chemical composition.

Molecular bonding characteristics were investigated by Fourier Transform Infrared Spectroscopy (FT-IR) for the raw powder form of the PHB bioplastic, undegraded and degraded

melt-pressed plates (0.24-mm, 1.2-mm, 3.5-mm, and 5-mm thick) of the bioplastic, and of PHB/15% TBC blend melt-pressed plates (1.2-mm thick). IR determinations were performed using a Bruker Tensor 27 microspectrometer. Both the sample scan time and the background scan time were 16 scans at a resolution of 4 cm^{-1}. Spectrograms were processed using OPUS Version 4.2 software.

Molecular weight was measured by Size Exclusion Chromatography (SEC) for the raw powder form of the PHB bioplastic, undegraded and degraded melt-pressed plates (0.24-mm, 0.5-mm, 1.2-mm, 3.5-mm, and 5-mm thick) of the bioplastic, and of PHB/15% TBC blend melt-pressed plates (1.2-mm thick). For all samples, the plastic was dissolved in solution at an approximate concentration of 5 mg mL^{-1} in chloroform ($CHCl_3$). For the separation, three Phenogel 300 x 7.8 mm columns (Phenomenex, Torrance, CA), connected in series were used: (1) 5 μ, 500 Å (1 K – 15 K); (2) 5 μ, 10-4Å (5K – 500 K); (3) 10μ, MXM (100 – 10,000 K) and a guard column (5 μ, 50 x 7.8 mm) was used. The SEC instrumentation consisted of an Agilent 1100 pump, and an Agilent 1100 autosampler. For detection, three detectors connected on series were used: A Wyatt Heleos Multi Angle Light Scattering (MALS) detector equipped with a QUELS DLS detector, a Wyatt ViscoStar viscosity detector, and a Wyatt rEX Differential Refractive Index detector. All separations were performed using an injection volume of 100 μL. Chloroform (1 mL min^{-1}) was used as the solvent.

3.2.2.2 Thermal Properties

Thermal analyses were performed by Differential Scanning Calorimetry (DSC) using a TA Instruments DSC 2920 for the raw powder form of the PHB bioplastic, undegraded and degraded melt-pressed plates (0.24-mm, 1.2-mm, 3.5-mm, and 5-mm thick) of the bioplastic, and PHB/15% TBC blend melt-pressed plates (1.2-mm thick) in accordance with ASTM D 3418 –

03 (Standard Test Method for Transition Temperatures and Enthalpies of Fusion and Crystallization of Polymers by Differential Scanning Calorimetry). A heating rate of 5°C min^{-1} in a liquid nitrogen atmosphere was utilized. Sample sizes of approximately 5-10 mg were used for all analyses. The samples were heated to 200°C and held for 0.5 min, then cooled to –20°C for 1 min and reheated to 200°C. Melting temperature (T_m), melting enthalpy (ΔH_m), crystallization temperature (T_c) and crystallization enthalpy (ΔH_c) were obtained from the thermograms. T_m and T_c were taken as the onset points of melting or crystallization, respectively, as determined using the TA Universal Analysis V3.9A software.

3.2.2.3 Mechanical Properties

The mechanical strength of the undegraded PHB melt-pressed plates was determined using an Instron 4301 tensile test machine and in accordance with ASTM D 638 – 03 (Standard Test Method for Tensile Properties of Plastics). Specimens with a thickness of 1.2 mm were tested at a crosshead speed of 3.0 mm min^{-1} and sample rate of 6.667 points s^{-1}. The specimens were cured at room temperature for at least 7 days after the plates were melt-pressed and then for three additional days at 23°C (73°F) and relative humidity of 50% prior to testing.

Impact resistance was measured by notched Izod pendulum impact testing using a Tinius Olsen Model 892 Pendulum Impact tester for undegraded and degraded specimens of the PHB melt-pressed plates (3.5-mm thick) and in accordance with ASTM D 256 – 06a (Standard Test Methods for Determining the Izod Pendulum Impact Resistance of Plastics). Plates with a thickness of 3.5 mm were used for this analysis.

Dynamic Shear Rheometry (DSR) was performed on the raw PHB powder to determine rheological properties of the material. This analysis was performed by Dr. Simioan Petrovan at the University of Tennessee.

3.2.2.4 Physical Properties

To examine surface morphology, Scanning Electron Microscopy (SEM) images were recorded of undegraded and degraded melt-pressed plates of the PHB and the PHB/15% TBC blend using a Stereoscan 260 scanning electron microscope. Samples were sputter-coated with gold. Some samples were prepared so that the degrading microorganisms attached were fixated and could be recorded by SEM. These samples were removed from the degrading medium to a 2% glutaraldehyde, 1% formaldehyde, 0.1M cacodylate buffer solution for 30 min to fixate the sample. Then, samples were rinsed with 0.1M cacodylate buffer and transferred to a 1:1 mixture of distilled water and 95% ethanol, replacing half of the mixture with 95% ethanol every 5 min for 30 min to gradually dehydrate the sample. Then, the entire mixture was replaced with 95% ethanol every 5 min for 15 min before critical point drying with CO_2 and sputter-coating with gold.

3.2.3 Biodegradation Study

3.2.3.1 Respirometric Experiment

An aerobic biodegradation experiment was performed via respirometry using a Micro-Oxymax respirometer (Columbus Instruments; Columbus, OH). The instrument is controlled by a computer with Micro-Oxymax V5.06 software. The Micro-Oxymax respirometer measures and records O_2 and CO_2 levels in the headspace of reactors with respect to time to compute O_2 consumption and CO_2 production rates in addition to the cumulative amounts of gases consumed/produced. A schematic of this experimental setup and the system air flow during a sampling event is provided in Appendix C. The data reported by the respirometer was recorded as ASCII data files, which were later analyzed using Microsoft Excel software. The respirometric experiment was performed parallel to the second mass loss experiment and in

accordance with ASTM D 5338 – 98 (Standard Test Method for Determining Aerobic Biodegradation of Plastic Materials Under Controlled Composting Conditions; Reapproved 2003).

For the respirometric experiment, the compost inoculum was an aged (~4 months) and mature compost (retained on a 9.5-mm sieve) consisting of horse bedding, tree trimmings, wood shavings, and bark obtained from LSU AgCenter's Callegari Environmental Center. Ammonium chloride (NH_4Cl) was added to the compost to lower the C:N ratio to 30:1. Ten 2-L reactors (one for each available channel of the respirometer) containing the compost were prepared and were either used as controls or test material was added. Thus, the experimental setup consisted of controls in triplicate, PHB bioplastic in triplicate, SigmaCell® cellulose powder (20 μm particle size) as positive control in triplicate, and a single reactor containing LDPE as a negative control. The PHB bioplastic and the LDPE (negative controls) were in the form of melt-pressed plates and were of the same size (1.2 mm x 1.6 cm x 1.6 cm) and quantity in each reactor (35 per reactor). The reactors with cellulose powder or PHB plates each received an amount of test material that was roughly one-sixth of the dry weight of the compost as outlined in the ASTM standard. Since each reactor had an initial compost weight of approximately 195 g with a moisture content of 63.1%, then each reactor had approximately 72 g of dry compost and received approximately 12 g of polymer except for blanks and the negative control. The negative control reactor received plates of LDPE that were in the same physical size, shape, and number as the PHB plates in their reactors. The reactors were maintained at 58ºC as outlined in ASTM D 5338 – 98. Reactors were frequently monitored by visual observation and distilled water added as necessary to maintain appropriate moisture content (~55%).

When the experiments were concluded, actual amounts of gas produced could be compared to the theoretical amounts to assess biodegradation of the test materials. All biogas produced during the biodegradation process was expected to be CO_2 gas since aerobic conditions had been maintained. Maximum ThGP was calculated based on the original mass of test material as follows:

$$ThGP(mg) = mass(mg) \times (\%\ by\ weight\ carbon) \times \frac{1\ mmol\ CO_2\ gas}{12\ mg\ Carbon} \times \frac{44\ mg\ CO_2\ gas}{1\ mmol\ CO_2\ gas} \quad (1)$$

Theoretical oxygen uptake (ThOU) was calculated using an equation found in ASTM D 5929 – 96 (Standard Test Method for Determining Biodegradability of Materials Exposed to Municipal Solid Waste Composting Conditions by Compost Respirometry; Reapproved 2004) based on the percent by weight of carbon (C), hydrogen (H), nitrogen (N), phosphorus (P), sulfur (S), and oxygen (O) present in the test material. Both the PHB and cellulose contain only carbon, hydrogen, and oxygen in their chemical formulas, so the equation reduced to:

$$ThOU\left(\frac{mg\ O_2}{mg}\right) = \frac{C}{37.5} + \frac{H}{12.5} + \frac{O}{100} \quad (2)$$

In the data analysis, the cumulative-average (of triplicate results) gas volumes from anaerobic biodegradation of the test materials was calculated by subtracting the cumulative-average gas volume production of the blank controls. The percent of theoretical gas produced (%ThGP) was calculated by dividing the cumulative average gas volume of the test material by the theoretical maximum gas production and multiplying by 100. The standard deviation for each replicate set of bottles was also calculated. The compost mixture was analyzed for mass and carbon content before and after the experiment to perform mass balance calculations. The following equation was used in performing carbon mass balances (C = carbon):

$$C_{input} = C_{output} \tag{3}$$

where:

$$\begin{aligned} C_{input} &= C_{polymer} + C_{biomass} \\ C_{output} &= C_{polymer} + C_{biomass} + C_{biogas} \end{aligned} \tag{4}$$

3.2.3.2 Mass Loss Experiments

Two mass loss experiments were performed with the second experiment being performed in parallel to the respirometric experiment. For the first mass loss experiment, a synthetic municipal solid waste (MSW) was prepared according to ASTM D 5929 – 96 (Standard Test Method for Determining Biodegradability of Materials Exposed to Municipal Solid Waste Composting Conditions by Compost Respirometry; Reapproved 2004) and consisted of shredded virgin newsprint, pine bark, corn starch, corn oil, bovine casein, urea, and a buffer/nutrient solution. A mature compost mixture of sugar cane and bagasse was obtained from LSU AgCenter's Callegari Environmental Center as an inoculum. Urea was added to the mixture to lower the C:N ratio to 35:1. In 2-L Erlenmeyer flasks, PHB plates of three different thicknesses (0.5 mm, 1.2 mm, 3.5 mm) were exposed to the ASTM-defined synthetic MSW and periodically sampled for remaining plastic for mass loss determination and to perform characterization analyses (some requiring destructive sampling) for the remaining plastic (if any). Each of the seven flasks prepared contained three 0.5-mm plates (0.5 mm x 2.5 cm x 2.5 cm), one 1.2-mm plate (1.2-mm x 1.5 cm x 7 cm), and five 3.5-mm plates (3.5 mm x 12.7 mm x 6.4 cm). Each flask contained roughly 132 g of solid ingredients for the compost mixture, 133 mL of the ASTM-defined buffer solution, and 8.6 mL of corn oil. The amount of plastic in each flask was approximately 19 g. Prior to incubation, test pieces had been well-rinsed with nanopure water, oven-dried at 60°C, cooled in a desiccator, and weighed. The flasks were maintained at 40ºC for

the duration of the experiment until using a water bath. The contents of each flask were aerated with humidified air using an aquarium air pump to maintain appropriate moisture levels (~55%) and moisture was added as needed. Sampling events occurred at 2, 4, 6, 12, 18, 26, and 50 weeks of exposure. At each sampling event, one of the flasks was removed from the experiment and the remaining plastic (if any) was separated from the compost mixture. After mass loss determination, the remaining plastic was then subjected to DSC, Izod pendulum impact testing, FT-IR, SEC, and SEM analyses. These analyses required destructive sampling of the remaining plastic.

In the second aerobic mass loss experiment, 250-mL Erlenmeyer flasks each containing PHB plates of three different thicknesses and 1.2-mm plates of the PHB/15% TBC blend were exposed to the same compost mixture prepared for the respirometric experiment and using the same ratio of plastic to compost. Calculations for the plate dimensions needed in order to meet these conditions were made using Microsoft Excel software and can be found in Appendix C. The purpose of testing plates with different thicknesses was to determine the relationship between the mass-to-surface-area ratio of the plates and their degradation rates. The PHB/15% TBC blend was tested for the purpose of evaluating the impact of additives on the biodegradation of the PHB. Twenty-one mass-loss flasks were incubated and sampled in triplicate at 3, 6, 9, 12, 16, 20, and 30 weeks of exposure for mass loss determination and to perform characterization analyses for the remaining plastic (if any). Each flask contained three 0.24-mm PHB plates (0.24 mm x 2.55 cm x 2.55 cm), two 1.2-mm plates (1.2 mm x 1.6 cm x 1.6 cm), two 5-mm plates (5 mm x 1.15 cm x 1.15 cm), and two 1.2-mm PHB/15% TBC blend plates (1.2 mm x 1.4 cm x 1.8 cm). These flasks were also maintained at 58ºC for the duration of the experiment using an incubator. The contents of each flask were aerated with humidified using an aquarium air pump

to maintain moisture content of approximately 55% and distilled water was added as needed. Like the first mass loss experiment, initial weights of test pieces had been determined after rinsed with distilled water, dried at 60°C, and cooled in a desiccator. After being sampled, mass loss determinations were made for these test pieces before they were subjected to DSC, FT-IR, SEC, and SEM analyses.

Mass loss percentages of materials tested in both mass loss experiments were calculated by dividing the final weight of a specimen by the initial weight and multiplying by 100%. Mass remaining with respect to the initial surface area of specimens was plotted versus time so that degradation rate coefficients could be calculated. Degradation rate coefficients were calculated for all materials tested for biodegradation in both mass loss experiments. Linear regressions were performed for the portion of each degradation curve which showed the maximum rate of mass loss. In most cases, this involved the selection of three data points on the mass loss curve to be used for the linear regression. Diagrams representing these linear regressions can be found in Appendix C. All analyses were performed using SigmaPlot software (v 9.01, ©2004 Systat Software, Inc.). Additionally an analysis of covariance was performed on the data to show any statistical differences. This was performed using SAS software (v 9.1.3, ©2002-2003 SAS Institute Inc.). Degradation rate coefficients for the three different plate sizes of PHB tested in each experiment were plotted with respect to their initial mass-to-surface-area ratios to form saturation curves as the degradation of the PHB was believed to follow saturation kinetics.

3.3 Results and Discussion

3.3.1 Respirometric Experiment

In the respirometric experiment, the O_2 uptake and CO_2 production data did not seem to agree (Table 3.1). After 150 days, less than 30% theoretical CO_2 production (ThCDP) was

observed for both the PHB plates and the cellulose powder while slightly more than 100% theoretical O_2 uptake (ThOU) was observed. This may indicate that anaerobiosis may have unavoidably occurred throughout the experiment causing much of the degraded carbon to be converted to CH_4 gas instead of the CO_2 gas which the respirometer was equipped to measure. However, this assumption does not seem to be supported by the large amounts of ThOU that occurred, which would not be indicative of anaerobiosis. Grima et al. (2000) lists anaerobiosis as one of many potential problems that may occur in aerobic biodegradation tests. Perhaps it is for reasons such as this that most of the literature involving biodegradation tests of bioplastics in aerobic compost reports biodegradation in terms of mass loss. Several literature papers have evaluated methods used for assessing biodegradation of polymers including the ASTM standard used. Jayasekara et al. (2005) stated that one of the main problems with the ASTM D 5338-92 standard is that the percent biodegradation does not include the carbon converted to cell biomass and not metabolized to CO_2 during the course of the test, while Gu and Gu (2005) have stated that results may mislead the environmental fate of the materials tested because negative results may be due to the insensitivity of the test methods.

Table 3.1. Percentages of net theoretical CO_2 production (ThCDP) and theoretical O_2 uptake (ThOU) observed for the materials exposed to the aerobic compost of the second respirometric experiment.

	Mean values ± Standard Deviation		
Material	**Max. CO_2 Production (mg)**	**Theor. CO_2 Production (mg)**	**% ThCDP**
PHB plates	7,427 ± 630	26,018 ± 256	28.5% ± 2.3%
Cellulose powder	4,814 ± 513	19,888 ± 10.7	24.2% ± 2.6%
Material	**Max. O_2 Uptake (mg)**	**Theor. O_2 Uptake (mg)**	**% ThOU**
PHB plates	22,308 ± 3340	21,873 ± 215	101.9% ± 14.3%
Cellulose powder	16,602 ± 604	15,368 ± 8.3	108.0% ± 4.0%

The O_2 uptake due to biodegradation of the PHB plates showed an apparent lag phase of ~30 days (Figure 3.2) while the cellulose powder showed a much shorter lag phase of ~5 days, most likely due to the high mass-to-surface-area ratio of the cellulose powder. While most researchers often report biodegradation in aerobic compost on the basis of mass loss, in a rare study by Ohtaki and Nakasaki (2000b), polymer conversion to CO_2 was reported for several unnamed bioplastics in an experiment that proceeded for just 8 days. That experiment showed significantly more carbon conversion (up to 65%) than this one and in a much shorter timeframe. However, very few studies report polymer conversion based on ThOU, although this is outlined as a feasible approach in ASTM D 5929 – 96.

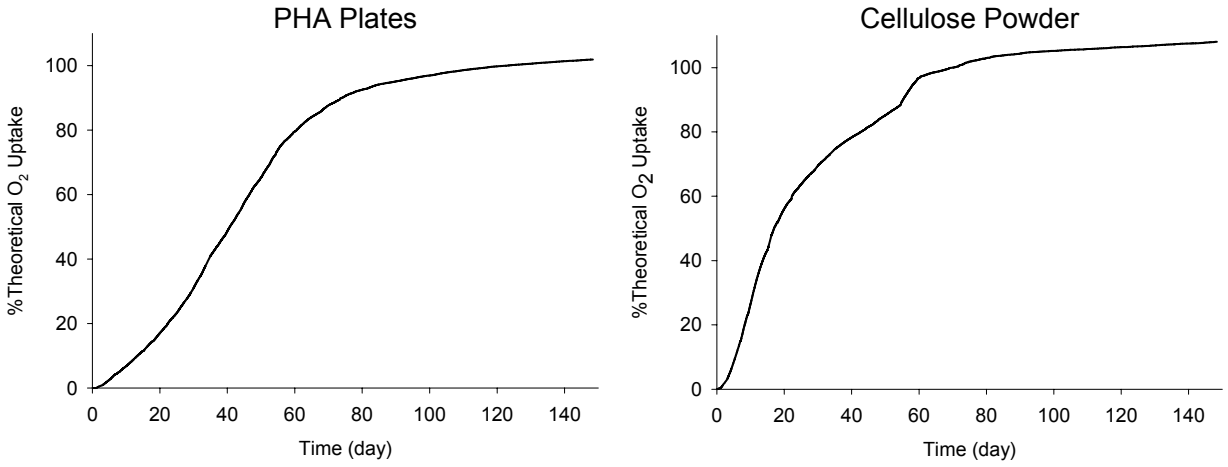

Figure 3.2. Graphs representing the percentage of theoretical O_2 uptake from degradation of the PHB plates and cellulose powder with respect to time. CO_2 production data has been excluded due to possible uncertainty in those results.

A carbon mass balance of the respirometric experiment (Table 3.2) shows that some carbon could not be re-accounted for in the test reactors at the end of the experiment. This may support the possibility that some CO_2 biogas had gone unaccounted for maybe due to system leaks or anaerobiosis. This would explain why the O_2 uptake and CO_2 production data from the

experiment did not agree. In the carbon mass balance, the initial and final compost for all bioreactors had been estimated based on measured weights and carbon content of the compost. The biogas reported was that measured as CO_2 gas by the respirometer.

Table 3.2. Carbon mass balance of the respirometric experiment comparing C input (Polymer C + Compost C) with C output after incubation (Polymer C + Compost C + Biogas C). Values shown are averages for triplicate bioreactors for each polymer tested for biodegradation except for the LDPE negative control which had only one replicate.

		Polymer	Polymer C	Compost C	Biogas C	Total	
	Polymer	**(g)**	**(g)**	**(g)**	**(g)**	**g**	**%**
Input	Blanks	0.0	0.0	22.5		22.5	100.0
Output			0.0	19.9	0.7	20.6	91.5
Input	PHB Plates	13.0	7.2	23.0		30.1	100.0
Output			0.0	20.4	2.7	23.1	76.8
Input	Cellulose Powder	12.9	5.4	23.0		28.4	100.0
Output			0.0	19.0	2.0	21.0	74.0
Input	LDPE	9.4	8.0	22.6		30.6	100.0
Output			8.0	19.9	0.6	28.6	93.5

3.3.2 Mass Loss Experiments

The mass loss of all three PHB plate sizes proceeded very slowly in the first 12 weeks of exposure to the synthetic MSW during experiment one (Table 3.3). At 18 weeks of exposure, a significant increase in degradation rate was observed and at 26 weeks, complete degradation of the 0.5-mm and 1.2-mm plates was observed, while the 3.5-mm plates had achieved nearly 70% mass loss. By 18 weeks of exposure, samples showed significant colonization by fungi, which became even more apparent by 26 weeks. By 50 weeks, the 3.5-mm plates had exhibited almost complete biodegradation. Manna and Paul (2000) also degraded sheets of PHB (0.25-mm thickness) in compost but observed less biodegradation. After 200 days, only 23.4% mass loss was observed at the same incubation temperature of 40°C, while complete biodegradation was observed for the 0.5-mm and 1.2-mm plates in this experiment after just 182 days (26 weeks).

Table 3.3. Percentages of degradation observed for the PHB plates exposed to the aerobic compost mixtures of the first and second aerobic mass loss experiments and for the PHB/15% TBC blend plates of the second experiment exposed for the times indicated.

First Experiment	Plate Thickness		
Exposure Time	**0.5-mm**	**1.2-mm**	**3.5-mm**
2 weeks	0.1%	0.0%	0.0%
4 weeks	3.1%	0.3%	0.5%
6 weeks	4.0%	4.5%	0.9%
12 weeks	16.7%	7.7%	2.1%
18 weeks	40.8%	38.2%	9.6%
26 weeks	100.0%	100.0%	67.8%
50 weeks	100.0%	100.0%	94.4%

Second Experiment	PHB			PHB/15% TBC
Exposure Time	**0.24-mm**	**1.2-mm**	**5-mm**	**(1.2-mm)**
3 weeks	35.0%	16.7%	4.0%	3.1%
6 weeks	N/A	31.7%	4.2%	3.2%
9 weeks	81.9%	66.3%	16.4%	5.3%
12 weeks	95.7%	98.3%	29.1%	8.0%
16 weeks	98.9%	100.0%	35.0%	N/A
20 weeks	100.0%	100.0%	36.9%	N/A
30 weeks	100.0%	100.0%	45.2%	13.9%

A relationship between the degradation rate coefficient and the corresponding initial mass-to-surface-area ratio was established (Figure 3.3). For the three mass-to-surface-area ratios investigated, the correlation to the degradation rate coefficient is linear. From a theoretical perspective, this relationship would be expected to plateau at a maximum degradation rate, which would be defined as the point where enzymatic activity of the microorganisms is at its maximum level. This correlation provides a practical tool for estimating the degradation time for various products, which will be of varying thickness. Figure 3.4 shows a visual comparison of the PHB plates degraded in the first aerobic mass loss experiment and illustrates the gradual deterioration of the specimens.

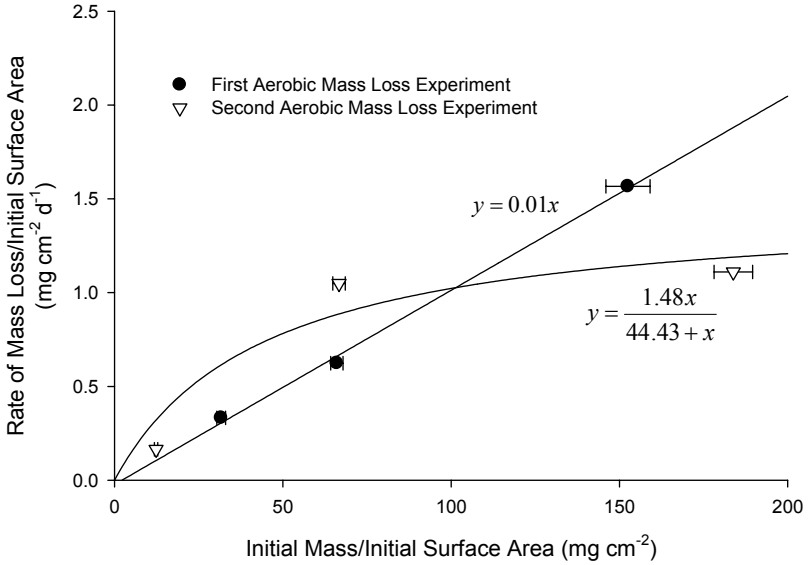

Figure 3.3 Relationships between the degradation rate coefficient (mg cm^{-2} d^{-1}) and the initial mass-to-surface-area ratio for the three different plate sizes of PHB degraded in the first aerobic mass loss experiment and those degraded in the second aerobic mass loss experiment.

The second aerobic mass loss experiment was performed in order to further define the relationship between the initial mass-to-surface-area ratio and the degradation rate coefficients of the PHB plates with different thicknesses (Figure 3.3). The 1.2-mm PHB plates were degraded again, thereby, serving as a control between the first and second experiments. The second experiment seemed to show a curve that follows saturation kinetics, as would be expected, unlike the first mass loss experiment. This difference may be attributed to the different compost mixtures that were used which may indicate that different degradation mechanisms had occurred. However, the second experiment showed very unusual amounts of variability of results among different mass loss flasks in the experiment. Extra flasks that had been incorporated into the experiment were not used in the results since some showed hardly any degradation of the plastic while others showed significantly more degradation of the bioplastic. This is believed to be a result of some of the flasks receiving excessive aeration causing the compost mixture to dry out

and hinder the degradation process. The maximum degradation rate for the second mass loss experiment was estimated to be 1.48 mg cm^{-2} d^{-1}.

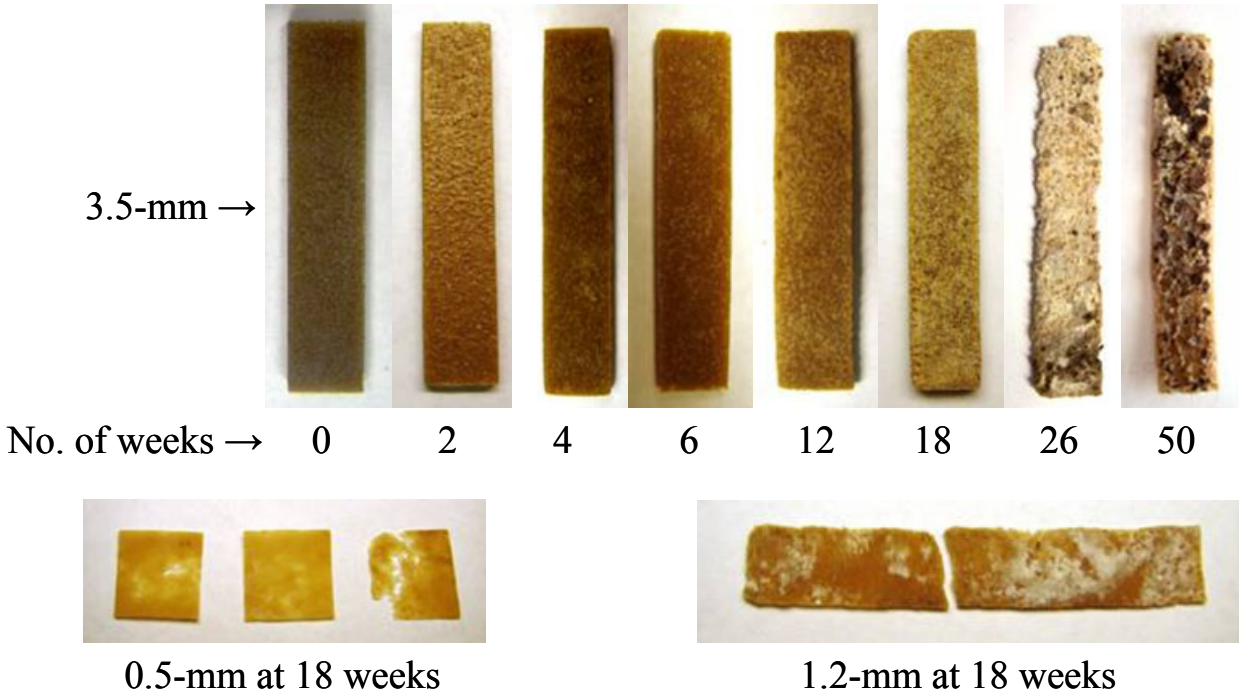

Figure 3.4. Visual comparison of the undegraded and degraded PHB plates with thicknesses of 3.5 mm that were degraded in the first aerobic mass loss experiment. Additional images show plates of 0.5-mm and 1.2-mm thickness after 18 weeks of degradation. Plate thicknesses and times of exposure are indicated.

In the second aerobic mass loss experiment, polymer degradation proceeded rapidly for the 0.24-mm and 1.2-mm PHB plates with complete biodegradation being observed for the 1.2-mm plates within 16 weeks and only ~1% of polymer remaining for the 0.24-mm plates (Table 3.3). The degradation of the 5-mm plates appeared to be hindered by their low mass-to-surface-area ratio while the TBC in the PHB/15% TBC blend appeared to hinder its degradation. Mass loss with respect to initial surface area reached greater peaks for the thicker PHB plates than for the thinner plates (Appendix C). This may be attributed to a decrease in the mass-to-surface-area

ratio of the thicker plates as the degrading microorganisms burrowed into these plates. Although the same phenomenon would have occurred for the thinner plates, it would be more pronounced for the thicker plates. Figure 3.5 clearly illustrates the surface deterioration of the plates due to biodegradation. Table 3.4 lists the degradation rate coefficients of all materials tested in both aerobic mass loss experiments. These degradation coefficients were calculated as outlined in the Materials and Methods section. An illustrative example of a degradation curve used to make these calculations is provided in Figure 3.6 and the curves for all thicknesses of plastic in both

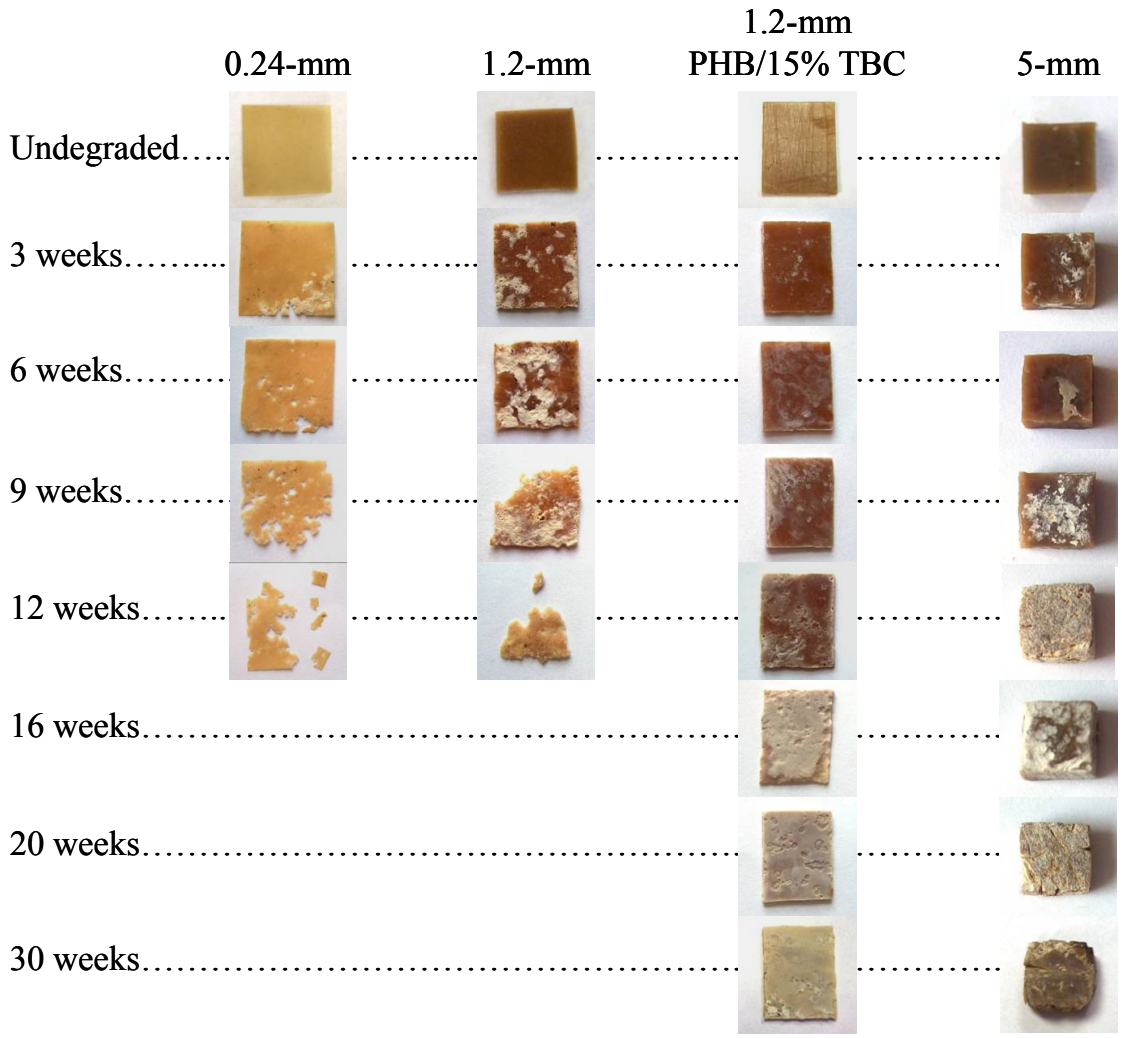

Figure 3.5. Visual comparison of the undegraded and degraded PHB plates with thicknesses of 0.24, 1.2, and 5 mm and the PHB/15% TBC blend plates that were degraded in the second aerobic mass loss experiment. Plate thicknesses and times of exposure are indicated.

experiments can be found in Appendix C. These are the same coefficients that were plotted with respect to their initial mass-to-surface-area ratios for the PHB in Figure 3.2. An analysis of covariance on the data for both mass loss experiments was performed to indicate whether these coefficients were statistically different using a significance level of 0.05. The analysis of

Table 3.4. The degradation rate coefficients of all materials tested in the first and second aerobic mass loss experiments.

Experiment/Test Material	**Degradation Rate Coefficient (mg cm^{-2} d^{-1})**
First Aerobic	
0.5-mm PHB	0.33
1.2-mm PHB	0.62
3.5-mm PHB	1.57
Second Aerobic	
0.24-mm PHB	0.16
1.2-mm PHB	1.05
5-mm PHB	1.11
1.2-mm PHB/15% TBC Blend	0.04

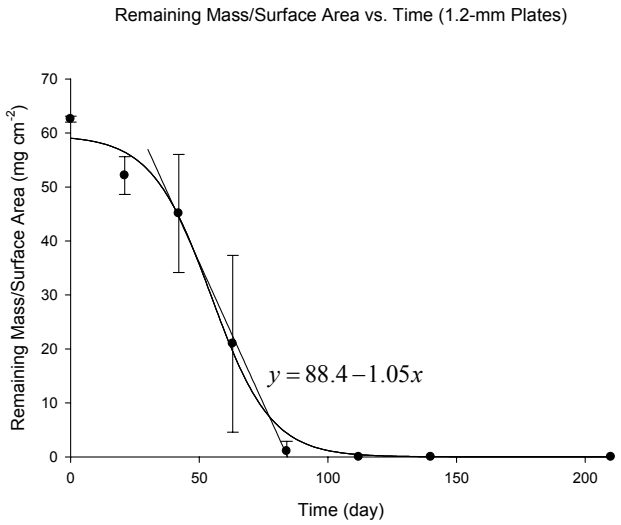

Figure 3.6. An illustrative example of a degradation curve used to perform a linear regression in the determination of degradation coefficients of plastics biodegraded in the aerobic mass loss experiments. The example shown is for the 1.2-mm PHB plates degraded in the second mass loss experiment. A linear regression was performed for the three data points in the middle of the degradation curve. The equation for that line is shown.

covariance for the first mass loss experiment indicated that the degradation coefficient for the 3.5-mm PHB plates was statistically different than that for both the 0.5-mm and 1.2-mm plates. However, the degradation coefficients for the 0.5-mm plates and 1.2-mm plates were not shown to be statistically different. For the second mass loss experiment, all comparisons in the analysis of covariance showed significant difference between the degradation coefficients except for the comparison of the 0.24-mm PHB plates and 1.2-mm PHB/15% TBC blend plates and of the 1.2-mm and 5-mm PHB plates. The output of these analyses as reported by the SAS statistical software used can be found in Appendix C.

3.3.3 Characterization Analyses

3.3.3.1 Chemical Properties

The results of the FT-IR analyses for undegraded plastics and those degraded in the first and second mass loss experiments are presented in Figures 3.7 and 3.8, respectively. Degradation appeared to have no effect on the spectrograms of the PHB bioplastic. This indicates that the cleavage of the many different types of bonds occurs proportionally equal throughout the polymer during the degradation process. These findings are consistent with those

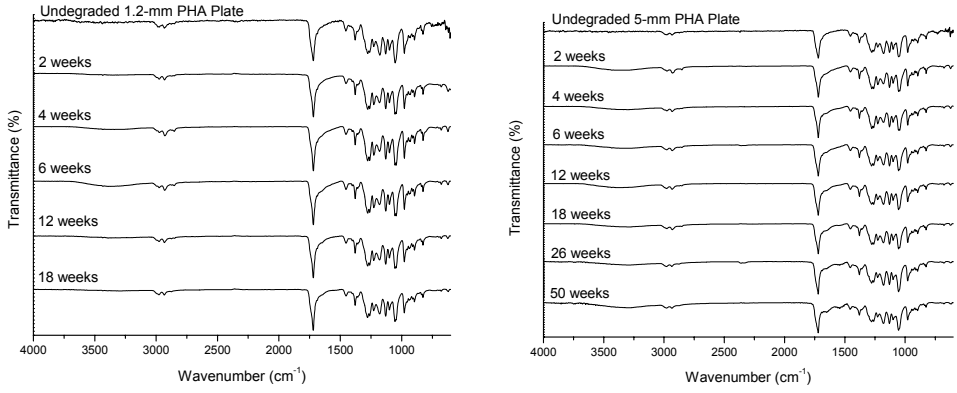

Figure 3.7. Spectrograms obtained by FT-IR of the PHB melt-pressed plates with 1.2-mm thickness (left) and 3.5-mm thickness (right) before and after degradation in the first aerobic mass loss experiment.

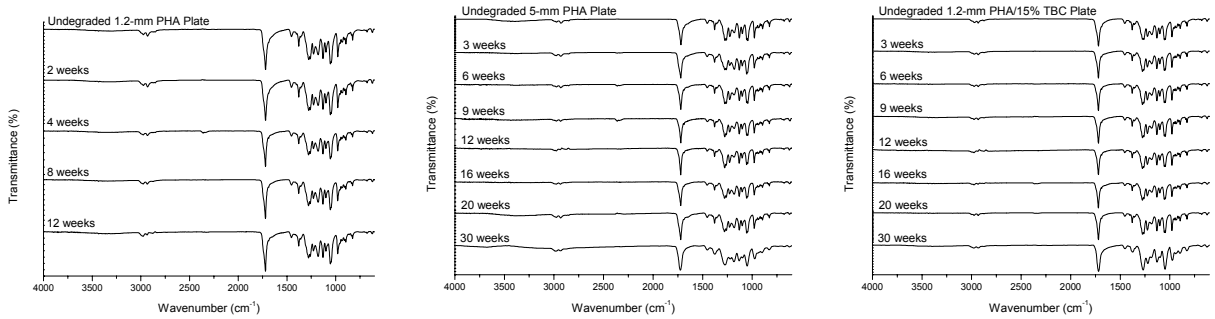

Figure 3.8. Spectrograms obtained by FT-IR of the PHB plates with 1.2-mm (left) and 5-mm (middle) thickness, and the 1.2-mm PHB/15% TBC plates (bottom right) before and after degradation in the second aerobic mass loss experiment.

of Day et al. (1994) who degraded PHBV in an anaerobic sewage sludge medium for 40 days. However, some spectrograms did show an appearance of peaks specific to peptide groups at wavenumbers of ~1642 cm^{-1} and 1535 cm^{-1}, most likely from proteins of the degrading bacteria in the compost that accumulated on the surface of the plates.

Molecular weight determinations of the undegraded PHB plates and those with 0.5-mm and 1.2-mm thickness degraded in the first aerobic mass loss experiment (Figure 3.9) show that biodegradation had little to no effect on the molecular weight of the PHB bioplastic. Many other degradation experiments have shown little to no decrease in molecular weight as a result of degradation (Day et al., 1994; Mergaert et al., 1994; Mergaert et al., 1993; Doi et al., 1990; Kanesawa and Doi, 1990). In most cases, when a decrease in molecular weight is observed, it can be attributed to some other phenomenon such as abiotic hydrolysis (Gilmore et al., 1992). This has led researchers to believe that the polymer is degraded enzymatically at the surface to lower-molecular-weight fragments that are rapidly metabolized by the degrading microorganisms resulting in mass loss but having no effect on the molecular weight of the remaining polymer.

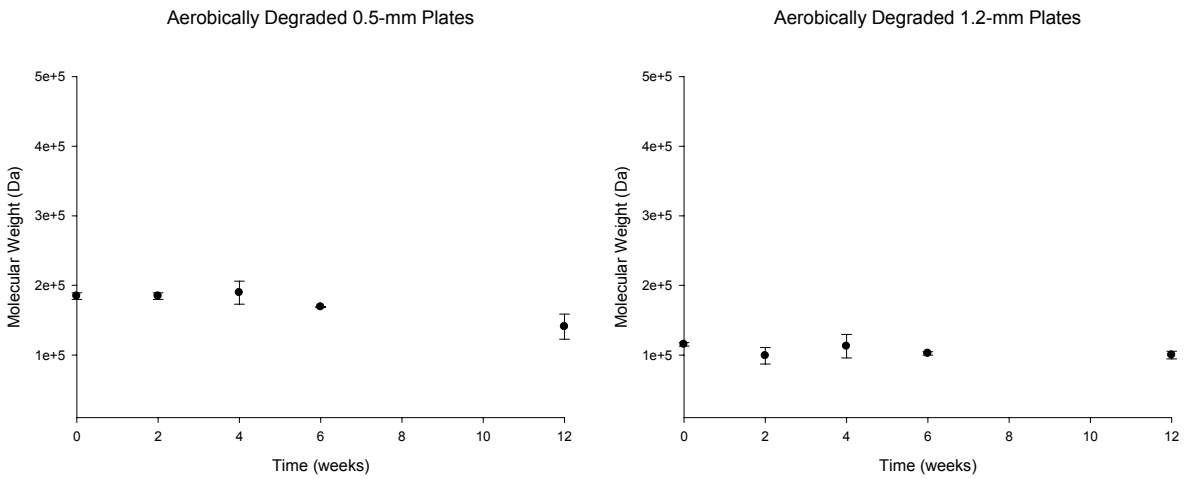

Figure 3.9. Molecular weight data obtained by Size Exclusion Chromatography of the 0.5-mm and 1.2-mm PHB plates degraded in the first aerobic mass loss experiment. Error bars indicate standard deviation of duplicate measurements and the x-axis refers to time of degradation.

3.3.3.2 Thermal Properties

Figure 3.10 shows the graphical representation of the DSC data for the undegraded 1.2-mm PHB plates as analyzed using the TA Universal Analysis V3.9A software. An interesting trend was noticed in the ΔH_m values for the PHB samples which had been formed into plates of different thicknesses. The thinner plates seemed to have lesser values of ΔH_m during the first heatings than the thicker plates, ranging from approximately 90 J g^{-1} for the 0.24-mm plates to 104 J g^{-1} for the 5-mm plates (Table 3.5). This means the crystallinity of the PHB may have had a slight dependency on the plate thickness as it ranged from approximately 62% for the 0.24-mm plates to 71% for the 5-mm plates determined from the ratio $\Delta H_f/\Delta H_f^0$, where ΔH_f and ΔH_f^0 are the observed enthalpy of fusion and the enthalpy of fusion of perfect PHB crystal (= 146 J g^{-1}) (El-Hadi et al., 2002; Yoshie et al., 2000; Barham and Keller, 1986; Barham et al., 1984), respectively. The difference in degrees of crystallinity can be attributed to the differences in cooling rates from the melt during melt-pressing of the plates. It can be stated that during preparation, the thinner plates cooled more quickly than the thicker plates. It is known that the crystallization rate of PHB increases with increasing heating/cooling rates, while the half-time of

crystallization decreases (An et al., 1998) and as a result, the crystallinity decreases (Chen et al., 2005).

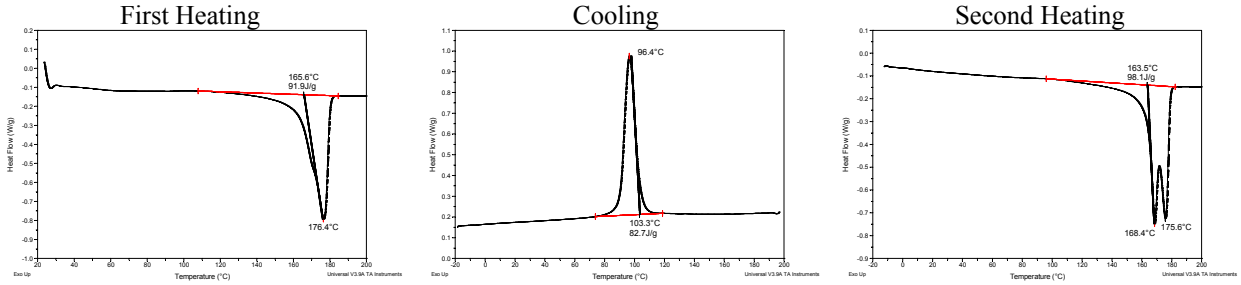

Figure 3.10. Graphical representations of the DSC data for the undegraded 1.2-mm PHB plates as analyzed using the TA Universal Analysis V3.9A software.

Table 3.5. DSC thermal data of the undegraded bioplastics.

	1st Heating				Cooling			2nd Heating			
	1st Peak (°C)	2nd Peak (°C)	T_m (°C)	ΔH_m (J g^{-1})	Peak (°C)	T_c (°C)	ΔH_c (J g^{-1})	1st Peak (°C)	2nd Peak (°C)	T_m (°C)	ΔH_m (J g^{-1})
PHB Powder	-	175.4	165.0	106.1	97.0	104.1	82.9	168.4	175.0	165.1	98.6
0.24-mm PHB	-	173.0	167.6	89.9	94.3	102.2	74.3	167.9	175.3	162.9	96.0
1.2-mm PHB	-	176.4	165.6	91.9	96.4	103.3	82.7	168.4	175.6	163.5	98.2
3.5-mm PHB	-	174.0	168.4	99.2	97.4	103.6	82.4	167.9	175.5	163.6	98.7
5-mm PHB	172.1	180.4	163.5	104.1	95.3	103.3	73.3	166.2	174.8	160.9	92.3
PHB/15 % TBC	161.4	170.4	153.4	81.9	83.9	101.7	59.2	154.1	167.4	144.5	82.2

It's interesting to note that the DSC endotherms often showed two distinct peaks, especially during the second heating period, which could be attributed to melting and recrystallization of thin, unstable crystals during the DSC scan, a phenomenon observed by Renstad et al. (1997). The melting peak at the lower temperature was attributed to melting of the crystals formed during isothermal and non-isothermal crystallization, while the melting peak at the higher temperature was a result of recrystallization that took place during the heating process as was observed by Chen et al. (2005). The PHB/15% TBC blend appears to have lowered values of ΔH_m and ΔH_c compared to those of the pure PHB. This indicates a lower degree of crystallinity for the blend due to the addition of TBC. Lowered values of T_m also seem to occur

for the PHB/15% TBC blend, which was also observed by Labrecque et al. (1997) who blended TBC with PLA, although an increase in crystallinity was observed in their blends with PLA, which had a very low crystallinity (less than 1%).

Biodegradation appeared to have only minor effects on the thermal properties of the PHB during the first mass loss experiment (Appendix D). In the second mass loss experiment, one interesting observation was that the ΔH_m values for the 5-mm PHB plates and the PHB/15% TBC blend plates showed significant increases with degradation. This may indicate preferential attack of the amorphous part of the polymer, which could cause ΔH_m values to be higher due to a higher proportion of crystalline polymer remaining. This is a phenomenon which has also been observed in other literature.

3.3.3.3 Mechanical Properties

Tensile testing of the PHB melt-pressed plates (1.2-mm thick) showed that the mean stress at maximum load was 32.6 ± 0.73 MPa. This value is only slightly less than that (35 MPa) reported for PHB by El-Hadi and coworkers (2002) but much larger than that (21 MPa) reported by El-Taweel and coworkers (2004). However, it can be hard to compare the tensile properties of PHB as determined by others because they can depend on many factors, especially the aging time of the polymer. PHB is known to undergo secondary crystallization during storage at room temperature (El-Hadi et al., 2002) leading to an increase in brittleness of the polymer (Scandola et al., 1989). During aging, the modulus increases while the extension to break decreases (Barham and Organ, 1994). The storage time of the tensile test specimens for this research was approximately one week.

The 3.5-mm PHB plates that had been degraded for 2, 4, 6, 12, and 18 weeks were subjected to Izod pendulum impact testing (Table 3.6). The impact resistance of PHB seems to

vary greatly based on what has been reported in literature (El-Hadi et al., 2002; Luzier, 1992; Barham and Keller, 1986). Luzier (1992) reports that the impact strength of PHB should be 60 J m^{-1} (~5.9 kJ m^{-2}) for PHB with 80% crystallinity while El-Hadi et al. (2002) reported 3 kJ m^{-2} (~30.5 J m^{-1}) for PHB with 60% crystallinity. So, it seems that the crystallinity greatly influences the impact strength. The PHB used in this research had a crystallinity of ~67%, so the strength value found (Table 3.6) for the undegraded material was similar to the results found by El-Hadi et al. although it showed a lesser strength value but higher crystallinity. However, the high variability of the strength just among the PHB used for this study can be seen with the test pieces being degraded for 12 weeks showing a higher strength value than the undegraded test pieces. It was not until the test pieces began to lose their overall structure that the strength value significantly decreased at 18 weeks.

Table 3.6. Summarized results of Izod pendulum impact testing of 3.5-mm melt-pressed plates of PHB degraded in the first aerobic mass loss experiment. The strength data is shown in the units of both kJ/m^2 and J/m. Standard deviations are also reported.

Degradation Time	Strength (kJ m^{-2})	Strength (J m^{-1})
Undegraded	2.45 ± 0.7	24.9 ± 0.7
2 weeks	2.12 ± 0.8	21.3 ± 5.6
4 weeks	2.38 ± 0.5	22.7 ± 4.6
6 weeks	2.19 ± 0.7	22.2 ± 8.2
12 weeks	2.78 ± 0.46	28.2 ± 4.6
18 weeks	1.76 ± 0.46	17.9 ± 7.0

The viscosity of the PHB in molten state at 180°C (considered as the temperature used for molding or extruding the material) decreased in time, e.g., from 28.3 Pa-s after 25 min (and an angular velocity of 10 s^{-1}) to 3.5 Pa-s after 70 min (reading @ 10 s^{-1}), pointing to a rather severe thermal degradation at this temperature (Figure 3.11). The viscosity after 70 min at 180°C was less than that read after 25 min at 190°C (7.2 Pa-s @ 10 s^{-1}). By comparison, Verhoogt et al.

(1996) reported viscous stability only at 160ºC for P(3HB-*co*-12%-3HV). At 170ºC, they observed a 10% reduction in the complex viscosity was already obtained after 200 s while a residence time of only 2 min resulted in a decrease in viscosity of almost 10% at 180ºC and of more than 20% at 200ºC.

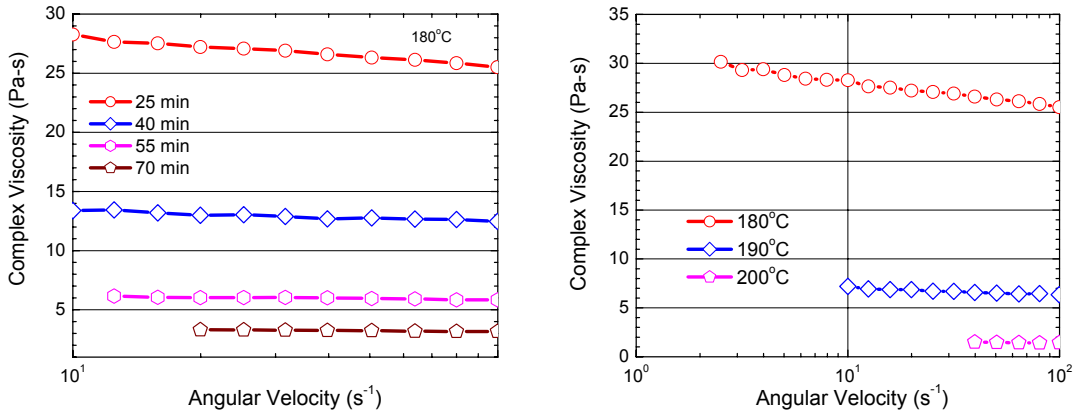

Figure 3.11. Rheological characterization of PHB in molten state: Dependence of complex viscosity on angular velocity and temperature.

3.3.3.4 Physical Properties

Scanning electron micrographs were recorded for degraded melt-pressed PHB plates of all thicknesses from both aerobic mass loss experiments. Figures 3.12 – 3.18 illustrate the gradual decomposition and increasing porosity of the plates of each thickness degraded in the second aerobic mass loss experiment. An extensive discussion of the images from the aerobic mass loss experiments can be found after the figures.

Both the 0.5-mm PHB plates (Figure 3.12) and 1.2-mm PHB plates (Figure 3.13) degraded in the first aerobic mass loss experiment had spherulitic structures with surrounding crevasses that appeared to smooth out in the first 2 weeks of exposure. Then, small distinct holes began to appear in the surface which became gradually larger and more widespread throughout the degradation process. By 12 weeks, crystalline formations could be seen at the surface

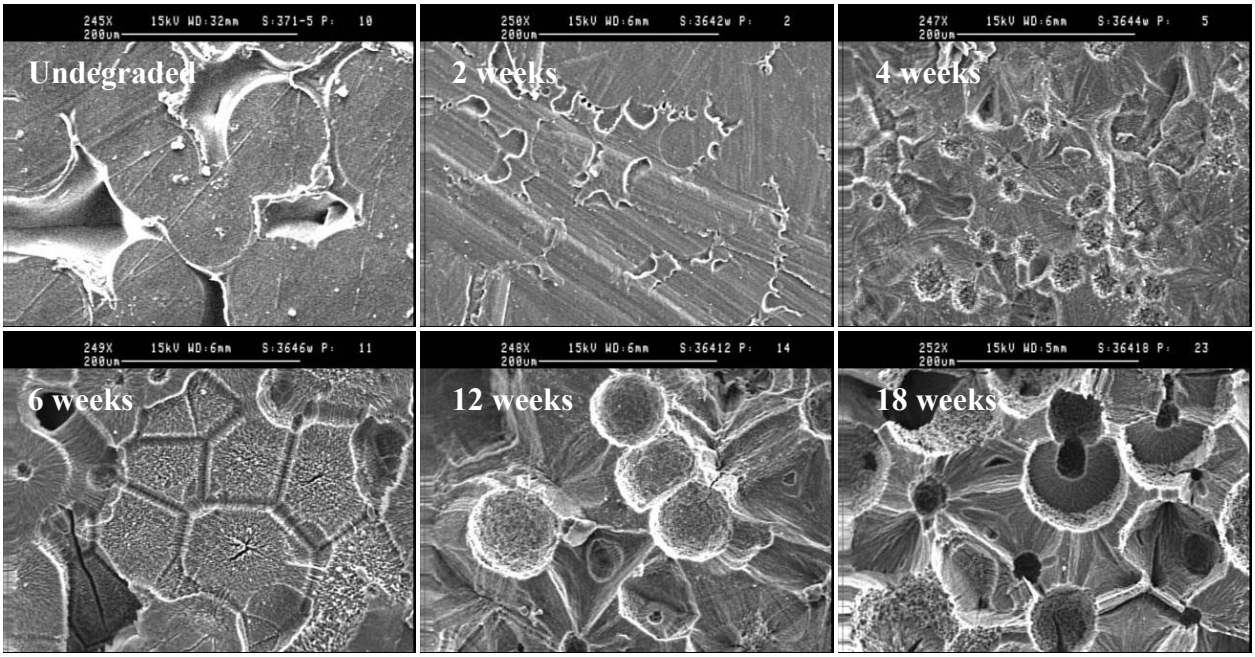

Figure 3.12. SEM images (~250X magnification) of 0.5-mm melt-pressed PHB plates undegraded and after 2, 4, 6, 12, and 18 weeks of exposure in the first aerobic mass loss experiment. Captions indicate time of degradation.

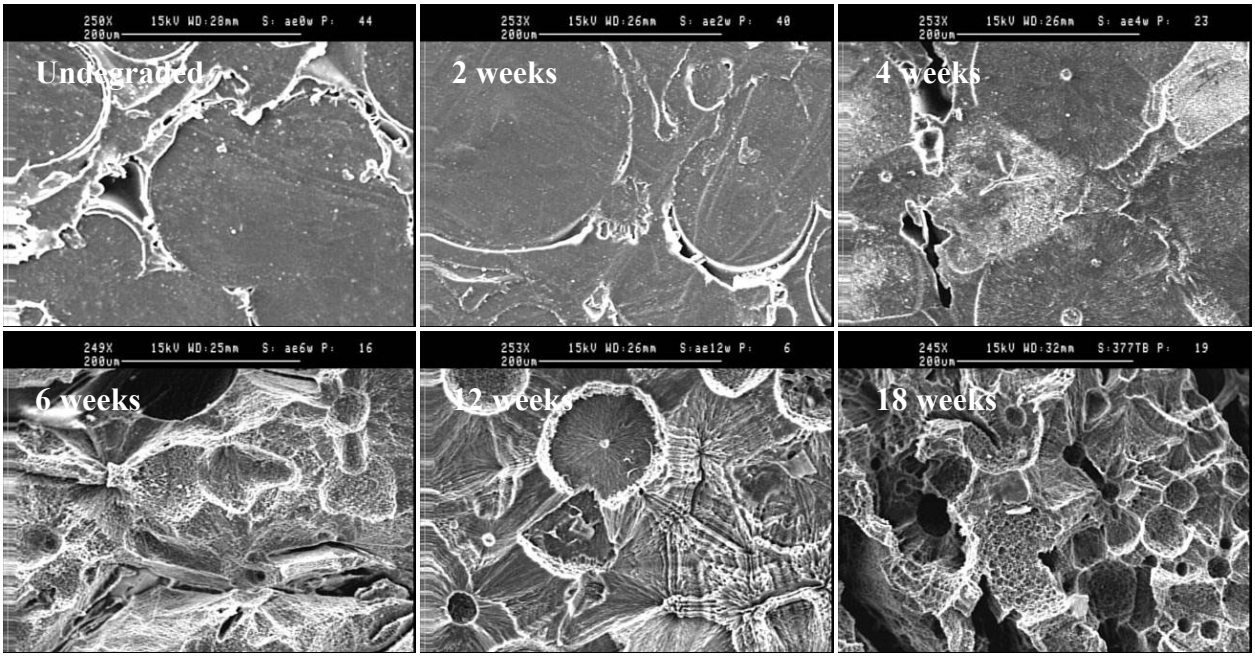

Figure 3.13. SEM images (~250X magnification) of 1.2-mm melt-pressed PHB plates undegraded and after 2, 4, 6, 12, and 18 weeks of exposure in the first aerobic mass loss experiment. Captions indicate time of degradation.

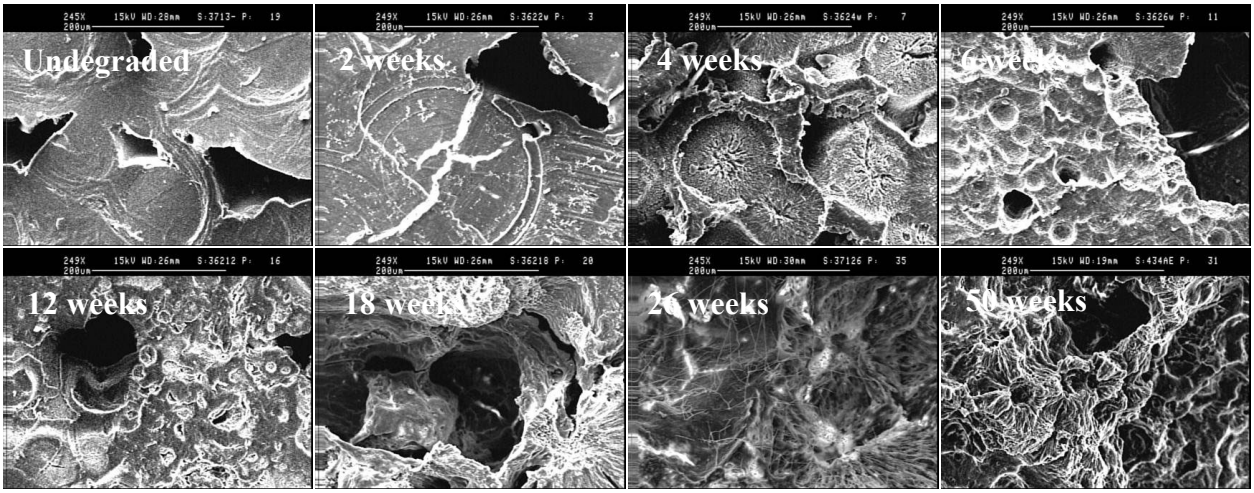

Figure 3.14. SEM images (~250X magnification) of 3.5-mm melt-pressed PHB plates undegraded and after 2, 4, 6, 12, 18, and 26 weeks of exposure in the first aerobic mass loss experiment. Captions indicate time of degradation.

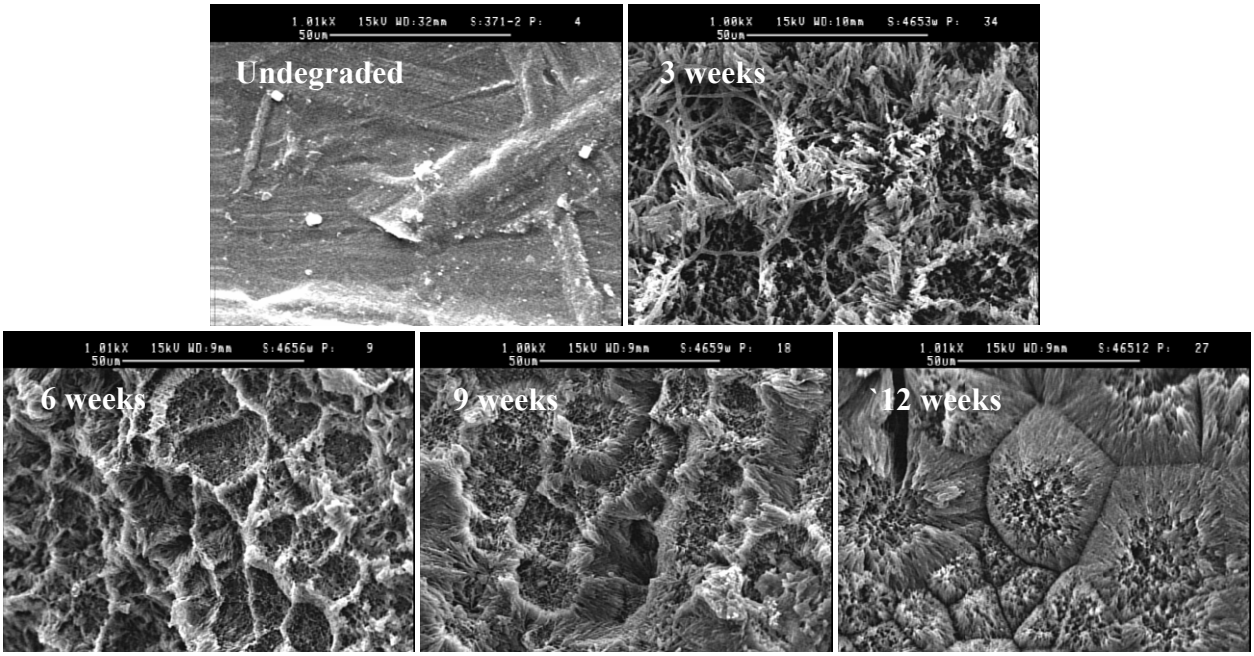

Figure 3.15. SEM images (~1,000X magnification) of 0.24-mm melt-pressed PHB plates undegraded and after 3, 6, 9, and 12 weeks of exposure in the second aerobic mass loss experiment. Captions indicate time of degradation.

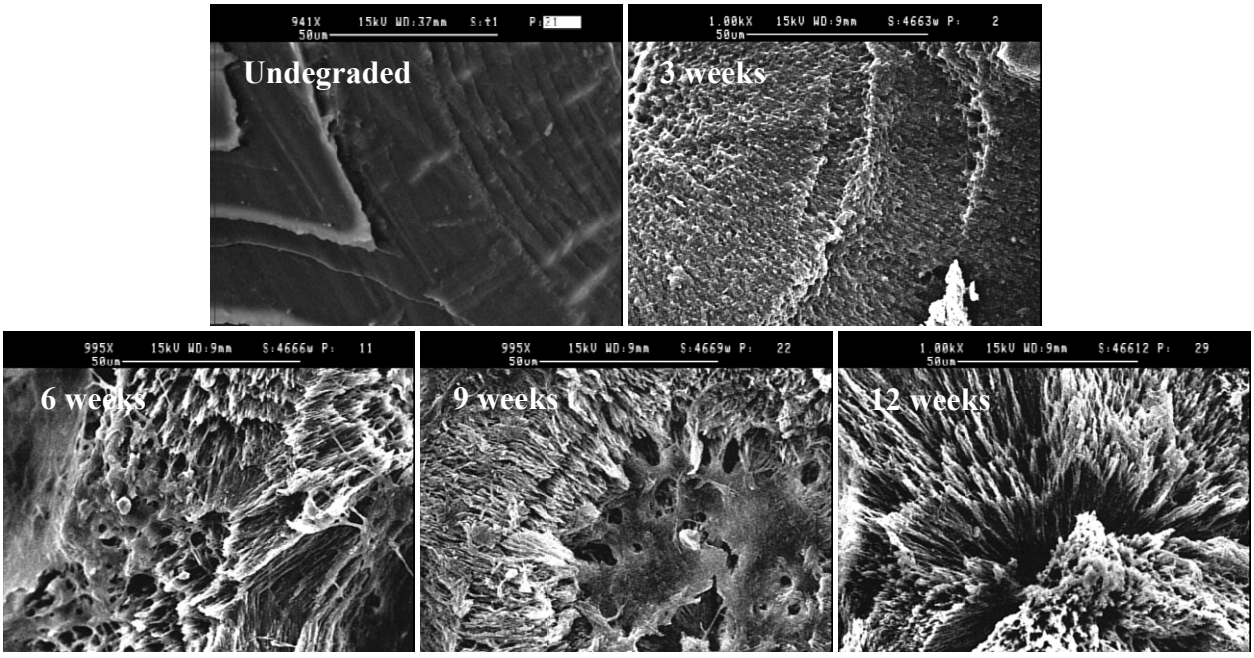

Figure 3.16. SEM images (~1,000X magnification) of 1.2-mm melt-pressed PHB plates undegraded and after 3, 6, 9, and 12 weeks of exposure in the second aerobic mass loss experiment. Captions indicate time of degradation.

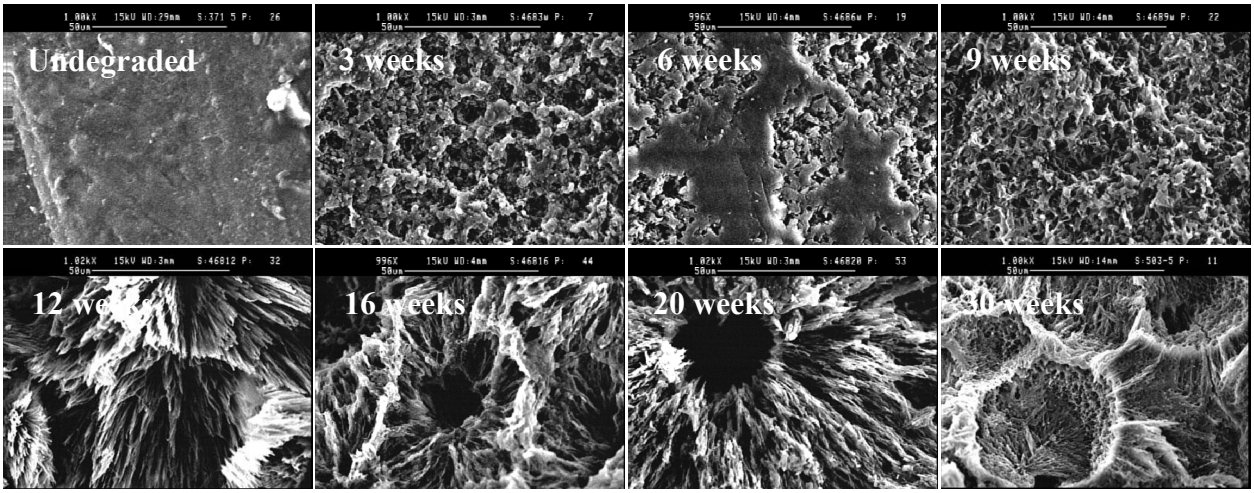

Figure 3.17. SEM images (~1,000X magnification) of 5-mm melt-pressed PHB plates undegraded and after 3, 6, 9, 12, 16, 20, and 30 weeks of exposure in the second aerobic mass loss experiment. Captions indicate time of degradation.

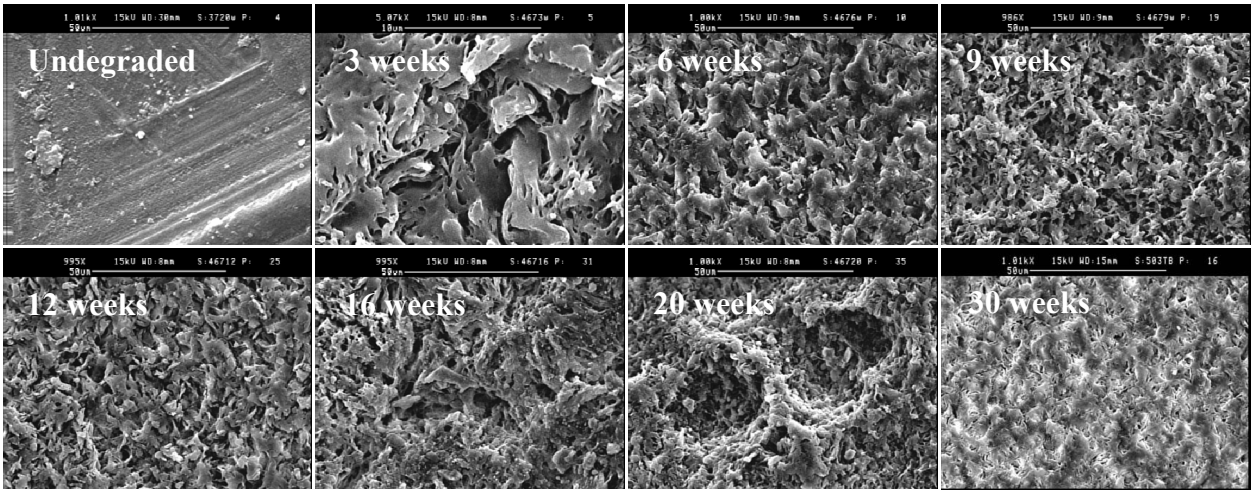

Figure 3.18. SEM images (~1,000X magnification) of 1.2-mm melt-pressed PHB/15% TBC blend plates undegraded and after 3, 6, 9, 12, 16, 20, and 30 weeks of exposure in the second aerobic mass loss experiment. Captions indicate time of degradation.

indicating the preference for microbial attack of the amorphous part of the polymer. However, the 3.5-mm PHB plates degraded in the first aerobic mass loss experiment (Figure 3.14) required longer for the spherulitic structures to smooth out (~4 weeks) and showed much more microbial attack within the material as indicated by the presence of larger holes that protrude deep into the material.

Samples degraded in second aerobic experiment seem to show much more erosion than those degraded in the first aerobic experiment due to the many different types of pits and the much rougher surfaces that can be seen. However, the pits on the first aerobic specimens appear much larger (hence the lesser magnification used) probably due to a dominance of fungi as the degrading microorganisms believed to have been present as evidenced by the white fibrous material attached to the surface of some specimens which could be seen by the naked eye. Fungi also are believed to have played a large role in the degradation process of the second experiment as some samples showed whitening of the surfaces with degradation and fibrous structures could be seen in some of the scanning electron micrographs.

The 0.24-mm PHB plates degraded in the second aerobic mass loss experiment (Figure 3.15) showed significant erosion within 3 weeks which progressed into many gullies and crevasses in the material throughout the degradation period. The 1.2-mm PHB plates (Figure 3.16) initially lost their luster and became very matte showing only small lesions after 3 weeks. Within 6 weeks, scattered lesions could be seen which became larger and more abundant throughout the degradation process. By 12 weeks, the remaining surface structures had changed their appearance to a network of narrow and scattered "sickles," most likely due to either a shift in the microbial consortia or maybe crystalline regions of the material left behind by microbes which favored the more amorphous regions. This would be consistent with the findings of Spyros et al. (1997) whose work provides evidence for the preferential degradation of the amorphous phase by PHB depolymerase B from *Pseudomonas lemoignei*. The 5-mm PHB plates degraded in the second anaerobic mass loss experiment (Figure 3.17) showed numerous lesions at the surface of the material within 3 weeks that did not show very much change in appearance for the first 9 weeks due to the extreme thickness of the plates which seemed to inhibit microbial attack from occurring within the greater depths of the material. Within 12 weeks, numerous "sickle" structures appeared as did for the 1.2-mm plates. These "sickle" structures persisted throughout the degradation process with large gaping holes also appearing after 16 weeks. The 1.2-mm PHB/15% TBC blend plates degraded in the second aerobic mass loss experiment (Figure 3.18) showed surface morphology much different than that for the pure PHB throughout the degradation process. The lesions and other structures left on the surface seemed much curvier. These structures seemed to become much smaller and more scattered between 3 and 6 weeks. The microorganisms did not seem to burrow into the inner parts of the

material as they did for the pure PHB which would indicate a preference for microbial attack at the surface. However, slight gullies did begin to appear after 20 weeks.

3.4 Conclusions

The degradation studies in aerobic compost have shown that the PHB bioplastic is completely biodegradable. Although less than 30% biogas recovery was observed in the respirometric experiments, slightly more than 100% ThOU uptake was observed while 100% mass loss was observed in the mass loss experiments. These observations along with the data showing the relationship between the degradation rate coefficients and the initial mass-to-surface-area ratio should provide useful information for PHA waste treatment in municipal aerobic compost piles. The combined characterization analyses of the degraded PHB have shown that it undergoes a rather uniform degradation with respect to molecular attributes of the material (i.e. no change in relative composition of molecular bonds as measured by FT-IR and no significant changes in molecular weight as measured by SEC). These observations show that commercial products made from PHA bioplastics would maintain their integrity for a useful lifespan despite the fact that the material is degradable since PHAs are known to remain inert in ambient air and environments that would not facilitate biodegradation. Furthermore, the fact that the presence of thermal history had only minor effects on thermal properties in the DSC experiments shows that the PHB could potentially be recyclable and undergo the involved remelting processes without compromising material characteristics. All of these data provide useful insight regarding the lifecycle design of PHAs to ease the transition from commodity plastics to their biodegradable alternatives.

Chapter 4: Global Discussion

PHB is a bioplastic that has long been known to be biodegradable. What this work has shown is how long it takes for the material to degrade in the environments of anaerobic municipal sludge and aerobic compost. The research has also shown that the results can vary greatly depending on the chosen source of the degrading environment. The form and bulk size of the material (i.e. fine powder/thinner films/thicker plates) will affect the degradation rate due to the relationship between the exposed surface area available for microbial attack and the mass of specimens. Furthermore, a natural citrate ester plasticizing additive (tributyl citrate) slowed the degradation of the PHB, but did not seem to hinder complete degradation of the material. The study of these and other phenomenon in this research thrust will provide valuable insight for future studies of PHAs and other bioplastics in addition to data that can be considered during the development of degradation models involving disposal of these materials in municipal wastewater digesters and compost piles. Manufacturers of plastic products made from PHB will also be able to use the data in their lifecycle design and estimate how long their products will last in the researched environments.

This work has also supported the findings of many other works: that PHB undergoes a very uniform degradation at the molecular level. This means that the molecular weight of the material remains relatively unchanged with biodegradation (Eldsäter et al., 1997; Day et al., 1994; Mergaert et al., 1994; Mergaert et al., 1993; Gilmore et al., 1992; Doi et al., 1990; Kanesawa and Doi, 1990), which directly affects other properties of the material, so those properties remain relatively unaffected, as well. Although in most cases, the degrading microorganisms preferentially attack the amorphous regions of the polymer leaving behind more of the crystalline regions (Spyros et al., 1997), re-melting and subsequent cooling of the polymer

would return it to its normal state of crystallinity. This means that in addition to the benefit of being biodegradable and eco-friendly, PHB would potentially be recyclable like commodity plastics even after being partially biodegraded as long as remnants of the degrading microbes and any other debris are separated from the remaining material to prevent unwanted impurities. This could prove to be important due to the high cost of PHA production by the methods currently used. Recycling of PHAs would reduce the demand to produce new polymer by those processes. Regardless of the preferential attack of amorphous polymer, biodegradation seems to occur uniformly starting at lesions on the surface and proceeding inward (Rossini et al., 2001; Molitoris et al., 1996).

Globally, a transition to the use of bioplastics such as PHB would significantly reduce the strain on the world's oil supply, which is currently used to make the petroleum-based commodity plastics. However, the major hurdle for the widespread use of bioplastics is their production costs and methods (Choi and Lee, 1999; Lee and Choi, 1999; Lee et al., 1999). The methods used to ferment PHB in bacteria and then separate and extract the polymer from those cells require much more time and expenses than the production processes of their petroleum-based counterparts. Although many improvements are being made to these processes to drive down production costs, there is still much more to be done to make PHAs and other bioplastics cost-competitive with petroleum-based plastics. The prospect of growing PHAs in many different types of plants is being researched and attempts to increase polymer yield from those plants are being made (Petrasovits et al., 2007; Kourtz et al., 2005; Wróbel et al., 2004; Lössl et al., 2003; Poirier and Gruys, 2002; Bohmert et al., 2000; Houmiel et al., 1999; Valentin et al., 1999; Williams et al., 1999; Nawrath et al., 1994). Also, growing these polymers in large-scale batch reactors may prove to be more cost-effective than the small-scale processes that have been

implemented so far. Other setbacks in the development of PHAs have been their limited processability (Mecking, 2004) and mismatches between their physical properties and certain applications. These are two problems that seem to hold the same solution – additives such as plasticizers can improve their physical properties making them more suitable for certain applications and also lower their melting temperature and increase their thermal degradation temperature, therefore widening their processing window. However, this also leads to the issue that most plasticizers in use are synthetic and toxic in contrast to the naturally occurring PHAs, so it is necessary to develop or identify more natural and eco-friendly plasticizers. Lastly, since more PHAs with varying thermoplastic properties are still being identified, it may become unnecessary to add plasticizers.

Chapter 5: Conclusions and Future Recommendations

This research thrust has shown that PHB will fully biodegrade in the appropriate disposal environment, specifically those that were evaluated – anaerobic municipal sludge and aerobic compost. While the PHB biodegrades, no significant changes occur in the overall physical, thermal, and chemical properties of the polymer. Changes in mechanical properties and discoloration are the obvious results polymer loss during biodegradation. Although some analyses of the degraded bioplastic did show slight changes in properties, these changes could most likely be attributed to remnants of the degrading microorganisms and other debris that were difficult to remove from the remaining material. Any changes that may not have occurred for this reason were most likely a result of the crystalline regions of the polymer which more abundantly remained after the degrading microorganisms preferentially attacked the amorphous regions; the change in crystallinity would easily be reversed by re-melting/re-processing of the material. In some cases though, it seems that not all of the weight loss of the polymer may have been a result of microbial degradation, but possibly hydrolytic degradation due to high moisture levels. In future studies, it may be beneficial to distinguish how much polymer degradation occurs as a result of microbial attack of the polymer and how much is a result of other phenomena such as hydrolytic degradation or chemical means. It is also recommended that more emphasis be placed on research of other environments that facilitate PHA degradation and are common disposal sites of plastic degradation such as soil and fresh/marine water. Litter is a major concern in this country meaning soil would be a common disposal site of plastic products, which is why in a transition to bioplastics, some of the main products to be made from PHAs or other bioplastics should be the types of articles most commonly seen as litter such as plastic grocery bags, cigarette backs, and plastic bottles.

The TBC additive tested in this research thrust seemed to slow degradation of the PHB but did not hinder its complete biodegradation. The TBC is a naturally occurring citrate ester, but its environmental impact should probably be evaluated more thoroughly. In the mass balance calculations of the degradation experiments in anaerobic municipal sludge, it was noticed that a much higher dissolved organic carbon (DOC) content remained for the reactors in which the PHB/TBC blend was degraded. The remaining DOC was most likely remnants of the TBC which had not degraded. However, it cannot be said for sure whether the TBC had degraded into other potentially toxic compounds. This aspect of the biodegradation process should be further evaluated for TBC and other potential additives to PHAs.

Lastly, the ASTM test methods should be further evaluated for their efficiency. The methods do not seem to account for the causes of what may seem to be negative results from an experiment, especially for the experiments in aerobic compost. In the respirometric experiments, complete mass loss of the PHB was occurred but only ~30% theoretical CO_2 production was observed. However, when assessing biodegradation on the basis of theoretical O_2 production, ~100% degradation was observed. Obviously, a lot of carbon was unaccounted for that may have been lost as CH_4 gas due to anaerobiosis, which can be very difficult to avoid. Although that experiment was intended to be purely aerobic process, if anaerobiosis occurred on the lab scale then it would most likely also occur in a compost pile at a municipal waste facility that the experiment is intended to simulate. So, the ASTM standards shouldn't be written with the presumption that the process would be completely aerobic, because in practice, that just may not always be practical.

References

American Public Health Association (APHA), 1998. Standard Methods for the Examination of Water and Wastewater, 20th ed., APHA, Washington, D.C., 1220 pp.

ASTM D 256 – 06a. Standard Test Methods for Determining the Izod Pendulum Impact Resistance of Plastics. ASTM International.

ASTM D 638 – 03. Standard Test Method for Tensile Properties of Plastics. ASTM International.

ASTM D 3418 – 03. Standard Test Method for Transition Temperatures and Enthalpies of Fusion and Crystallization of Polymers by Differential Scanning Calorimetry. ASTM International.

ASTM D 5210 – 92 (Reapproved 2000). Standard Test Method for Determining the Anaerobic Biodegradation of Plastic Materials in the Presence of Municipal Sewage Sludge. ASTM International.

ASTM D 5338 – 98 (Reapproved 2003). Standard Test Method for Determining Aerobic Biodegradation of Plastic Materials Under Controlled Composting Conditions. ASTM International.

ASTM D 5929 – 96 (Reapproved 2004). Standard Test Method for Determining Biodegradability of Materials Exposed to Municipal Solid Waste Composting Conditions by Compost Respirometry. ASTM International.

Abou-Zeid, D.-M., Müller, R.-J., Deckwer, W.-D., 2001. Degradation of Natural and Synthetic Polyesters under Anaerobic Conditions. *J. Biotechnol.* 86, 113-126.

Abou-Zeid, D.-M., Müller, R.-J., Deckwer, W.-D., 2004. Biodegradation of Aliphatic Homopolyesters and Aliphatic-Aromatic Copolyesters by Anaerobic Microorganisms. *Biomacromolecules*. 5, 1687-1697.

Abou-Zeid, D. M., 2004. Anaerobic Biodegradation of Natural and Synthetic Polyesters. Ph.D. Dissertation, TU-Braunschweig, Germany.

Amor, S. R., Raymont, T., Sanders, J. K. M., 1991. Poly(hydroxybutyrate) in Vivo: NMR and X-ray Characterization of the Elastomeric State. *Macromol.* 24, 4583-4588.

An, Y., Dong, L., Mo, Z., Liu, T., Feng, Z., 1998. Nonisothermal Crystallization Kinetics of Poly(β-hydroxybutyrate). *J. Polym. Sci. B: Polym. Phys.* 36, 1305-1312.

Anderson, A. J., Dawes, E. A., 1990. Occurrence, Metabolism, Metabolic Role, and Industrial Uses of Bacterial Polyhydroxyalkanoates. *Microbiol. Rev.* 54, 450-472.

Baptist, J. N. 1962a. U. S. Patent 3036959.

Baptist, J. N. 1962b. U. S. Patent 3044942.

Barham, P. J., Keller, A., 1986. The Relationship between Microstructure and Mode of Fracture in Polyhydroxybutyrate. *J. Polym. Sci.: Polym. Phys. Ed.* 24, 69-77.

Barham, P. J., Keller, A., Otun, E. L., Holmes, P. A., 1984. Crystallization and Morphology of a Bacterial Thermoplastic: Poly-3-Hydroxybutyrate. *J. Mater. Sci.* 19, 2781-2794.

Barham, P. J., Organ, S. J., 1994. Mechanical Properties of Polyhydroxybutyrate-hydroxybutyrate-hydroxyvalerate Copolymer Blends. *J. Mater. Sci.* 29, 1676-1679.

Bauer, H., Owen, A. J., 1988. Some Structural and Mechanical Properties of Bacterially Produced Poly-β-hydroxybutyrate-co-β-hydroxyvalerate. *Colloid Polym. Sci.* 266, 241-247.

Bohmert, K., Balbo, I., Kopka, J., Mittendorf, V., Nawrath, C., Poirier, Y., Tischendorf, G., Trethewey, R. N., Willmitzer, L., 2000. Transgenic *Arabidopsis* Plants Can Accumulate Polyhydroxybutyrate to up to 4% of their Fresh Weight. *Planta*. 211, 841-845.

BP, 2006. Statistical Review of World Energy - Proved Oil Reserves. Accessed May 2007. http://www.bp.com/liveassets/bp_internet/globalbp/globalbp_uk_english/reports_and_publications/statistical_energy_review_2006/STAGING/local_assets/downloads/pdf/table_of_proved_oil_reserves_2006.pdf.

Brandl, H., Bachofen, R., Mayer, J., Wintermantel, E., 1995. Degradation and Applications of Polyhydroxyalkanoates. *Can. J. Microbiol.* 41, 143-153.

Brandl, H., Püchner, P., 1992. Biodegradation of Plastic Bottles Made from 'Biopol' in an Aquatic Ecosystem under *In Situ* Conditions. *Biodegrad.* 2, 237-243.

Budwill, K., Fedorak, P. M., Page, W. J., 1992. Methanogenic Degradation of Poly(3-hydroxyalkanoates). *Appl. Environ. Microbiol.* 58, 1398-1401.

Buswell, A. M., Mueller, H. F., 1952. Mechanism of Methane Fermentation. *Ind. Eng. Chem.* 44, 550-552.

Byrom, D., 1987. Polymer Synthesis by Microorganisms: Technology and Economics. *Trends Biotechnol.* 5, 246-250.

Calmon-Decriaud, A., Bellon-Maurel, V., Silvestre, F., 1998. Standard Methods for Testing the Aerobic Biodegradation of Polymeric Materials. Review and Perspectives. *Adv. Polym. Sci.* 135, 207-226.

Carrasco, T., Dionisi, D., Martinelli, A., Majone, M., 2006. Thermal Stability of Polyhydroxyalkanoates. *J. Appl. Polym. Sci.* 100, 2111-2121.

Chan, C. H., Kummerlöwe, C., Kammer, H.-W., 2004. Crystallization and Melting Behavior of Poly(3-hydroxybutyrate)-Based Blends. *Macromol. Chem. Phys.* 205, 664-675.

Chen, C., Cheung, M. K., Yu, P. H. F., 2005. Crystallization Kinetics and Melting Behaviour of Microbial Poly(3-hydroxybutyrate-*co*-3-hydroxyhexanoate). *Polym. Int.* 54, 1055-1064.

Chen, G. Q., Zhang, G., Park, S. J., Lee, S. Y., 2001. Industrial Scale Production of Poly(3-hydroxybutyrate-co-3-hydroxyhexanoate). *Appl. Microbiol. Biotechnol.* 57, 50-55.

Chiu, H.-J., Shu, W.-J., 2005. Lamellar Morphology of Poly(3-hydroxybutyrate-co-3-hydroxyvalerate)/Poly(methyl methacrylate) Blends Probed by Small Angle X-ray Scattering. *J. Polym. Res.* 12, 149-157.

Choi, G. G., Kim, H. W., Rhee, Y. H., 2004. Enzymatic and Non-enzymatic Degradation of Poly (3-hydroxybutyrate-*co*-3-hydroxyvalerate) Copolyesters Produced by *Alcaligenes* sp. MT-16. *J. Microbiol.* 42, 346-352.

Choi, J.-i., Lee, S. Y., 1999. Factors Affecting the Economics of Polyhydroxyalkanoate Production by Bacterial Fermentation. *Appl. Microbiol. Biotechnol.* 51, 13-21.

Chun, Y. S., Kim, W. N., 2000. Thermal Properties of Blends of Poly(hydroxybutyrate-*co*-hydroxyvalerate) and Poly(styrene-*co*-acrylonitrile). *J. Appl. Polym. Sci.* 77, 673-679.

Cyras, V. P., Vázquez, A., Rozsa, C., Fernanández, N. G., Torre, L., Kenny, J. M., 2000. Thermal Stability of P(HB-*co*-HV) and Its Blends with Polyalcohols: Crystallinity, Mechanical Properties, and Kinetics of Degradation. *J. Appl. Polym. Sci.* 77, 2889-2900.

Day, M., Shaw, K., Cooney, D., 1994. Biodegradability: An Assessment of Commercial Polymers According to the Canadian Method for Anaerobic Conditions. *J. Environ. Polym. Deg.* 2, 121-127.

de Koning, G. J. M., Lemstra, P. J., 1993. Crystallization Phenomena in Bacterial Poly [(R)-3-hydroxybutyrate]: 2. Embrittlement and Rejuvenation *Polym.* 34, 4089-4094.

Doi, Y., Kanewasa, Y., Kunioka, M., 1990. Biodegradation of Microbial Copolyesters Poly(3-hydroxybutyrate-*co*-3-hydroxybutyrate) and Poly(3-hydroxybutyrate-*co*-4-hydroxybutyrate). *Macromol.* 23, 26-31.

El-Hadi, A., Schnabel, R., Straube, E., Müller, G., Henning, S., 2002. Correlation Between Degree of Crystallinity, Morphology, Glass Temperature, Mechanical Properties and Biodegradation of Poly (3-hydroxyalkanoate) PHAs and Their Blends. *Polym. Test.* 21, 665-674.

El-Taweel, S. H., Stoll, B., Höhne, G. W. H., Mansour, A. A., Seliger, H., 2004. Stress-Strain Behavior of Blends of Bacterial Polyhydroxybutyrate. *J. Appl. Polym. Sci.* 94, 2528-2537.

Elbanna, K., Lutke-Eversloh, T., Jendrossek, D., Luftmann, H., Steinbüchel, A., 2004. Studies on the Biodegradability of Polythioester Copolymers and Homopolymers by Polyhydroxyalkanoate (PHA)-Degrading Bacteria and PHA Depolymerases. *Arch. Microbiol.* 182, 212-225.

Eldsäter, C., Albertsson, A.-C., Karlsson, S., 1997. Impact of Degradation Mechanisms on Poly(3-hydroxybutyrate-*co*-3-hydroxyvalerate) During Composting. *Acta Polym.* 48, 478-483.

Encyclopedia of Chemical Technology, 1986. Vol. 6, 3rd ed., New York, Wiley and Sons, p. 170.

Federle, T. W., Barlaz, M. A., Pettigrew, C. A., Kerr, K. M., Kemper, J. J., Nuck, B. A., Schechtman, L. A., 2002. Anaerobic Biodegradation of Aliphatic Polyesters: Poly(3-hydroxybutyrate-co-3-hydroxyoctanoate) and Poly(ϵ-caprolactone). *Biomacromolecules*. 3, 813-822.

Ferreira, B. M. P., Duek, E. A. R., 2005. Pins Composed of Poly(L-lactic acid)/poly(3-hydroxybutyrate-co-hydroxyvalerate) PLLA/PHBV Blends: Degradation *In Vitro*. *J. Appl. Biomater. Biomech.* 3, 50-60.

Fulghum, R. S., Worthington, J. M., 1977. Butyl Rubber Stoppers Increase the Shelf Life of Prereduced, Anaerobically Sterilized Media. *Appl. Environ. Microbiol.* 33, 1220-1221.

Gage, P., 1990. Degradable Polyethylene Film–The Fact. *Tappi J.* 73,

Gartiser, S., Wallrabenstein, M., Stiene, G., 1998. Assessment of Several Test Methods for the Determination of the Anaerobic Biodegradability of Polymers. *J. Polym. Environ.* 3, 159-173.

Gerngross, T. U., Martin, D. P., 1995. Enzyme-catalyzed Synthesis of Poly[(*R*)-(–)-3-hydroxybutyrate]: Formation of Macroscopic Granules *in vitro*. *Proc. Natl. Acad. Sci. USA*. 92, 6279-6283.

Gilmore, D. F., Antoun, S., Lenz, R. W., Goodwin, S., Austin, R., Fuller, R. C., 1992. The Fate of 'Biodegradable' Plastics in Municipal Leaf Compost. *J. Indust. Microbiol.* 10, 199-206.

Grima, S., Bellon-Maurel, V., Feuilloley, P., Silvestre, F., 2000. Aerobic Biodegradation of Polymers in Solid-State Conditions: A Review of Environmental and Physicochemical Parameter Settings in Laboratory Simulations. *J. Polym. Environ.* 8, 183-195.

Gu, J.-G., Gu, J.-D., 2005. Methods Currently Used in Testing Microbiological Degradation and Deterioration of a Wide Range of Polymeric Materials with Various Degree of Degradability: A Review. *J. Polym. Environ.* 13, 65-74.

Hakkarainen, M., 2001. Aliphatic Polyesters: Abiotic and Biotic Degradation and Degradation Products. *Adv. Polym. Sci.* 157, 113-138.

Handrick, R., Reinhardt, S., Schultheiss, D., Reichart, T., Schüler, D., Jendrossek, V., Jendrossek, D., 2004. Unraveling the Function of the *Rhodospirillum rubrum* Activator of Polyhydroxybutyrate (PHB) Degradation: the Activator Is a PHB-Granule-Bound Protein (Phasin). *J. Bacteriol.* 186, 2466-2475.

He, J.-D., Cheung, M. K., Yu, P. H., Chen, G.-Q., 2001. Thermal Analyses of Poly(3-hydroxybutyrate), Poly(3-hydroxybutyrate-*co*-3-hydroxyvalerate), and poly(3-hydroxybutyrate-*co*-3-hydroxyhexanoate). *J. Appl. Polym. Sci.* 82, 90-98.

Hocking, P. J., Marchessault, R. H., Timmins, M. R., Lenz, R. W., Fuller, R. C., 1996. Enzymatic Degradation of Single Crystals of Bacterial and Synthetic Poly(*β*-hydroxybutyrate). *Macromol.* 29, 2472-2478.

Holmes, P. A., 1985. Applications of PHB – A Microbially Produced Biodegradable Thermoplastic. *Phys. Technol.* 16, 32-36.

Horowitz, D. M., Sanders, J. K., 1994. Phase Separation within Artificial Granules from a Blend of Poyhydroxybutyrate and Polyhydroxyoctanoate: Biological Implications. *Polymer*. 35, 5079-5083.

Houmiel, K. L., Slater, S., Broyles, D., Casagrande, L., Colburn, S., Gonzalez, K., Mitsky, T. A., Reiser, S. E., Shah, D., Taylor, N. B., Tran, M., Valentin, H. E., Gruys, K. J., 1999. Poly(β-hydroxybutyrate) Production in Oilseed Leukoplasts of *Brassica napus*. *Planta*. 209, 547-550.

Hungate, R. E., Smith, W., Clarke, R. T. J., 1966. Suitability of Butyl Rubber Stoppers for Closing Anaerobic Roll Culture Tubes. *J. Bacteriol.* 91, 908-909.

ICIS, 2006. Chemical Price Reports - Chemical Industry - ICIS Pricing. Accessed Nov 2006. http://www.icispricing.com/il_shared/il_splash/chemicals.asp?

Ikejima, T., Yagi, K., Inoue, Y., 1999. Thermal Properties and Crystallization Behavior of Poly(3-hydroxybutyric acid) in Blends with Chitin and Chitosan. *Macromol. Chem. Phys.* 200, 413-421.

Imam, S. H., Chen, L., Gordon, S. H., Shogren, R. L., Weisleder, D., Greene, R. V., 1998. Biodegradation of Injection Molded Starch-Poly (3-hydroxybutyrate-*co*-3-hydroxyvalerate) Blends in a Natural Compost Environment. *J. Environ. Polym. Deg.* 6, 91-98.

Imam, S. H., Gordon, S. H., Shogren, R. L., Greene, R. V., 1995. Biodegradation of Starch-Poly(β-hydroxybutyrate-Co-valerate) Composites in Municipal Activated Sludge. *J. Polym. Environ.* 3, 205-213.

Iwata, T., Doi, Y., Tanaka, T., Akehata, T., Teramachi, M. S. S., 1997. Enzymatic Degradation and Adsorption on Poly{(*R*)-3-hydroxybutyrate] Single Crystals with Two Types of Extracellular PHB Depolymerases from *Comamonas acidovorans* YM1609 and *Alcaligenes faecalis* T1. *Macromol.* 30, 5290-5296.

Iwata, T., Shiromo, M., Doi, Y., 2002. Surface Structures of Poly[(R)-3-hydroxybutyrate] and Its Copolymer Single Crystals Before and After Enzymatic Degradation with an Extracellular PHB Depolymerase. *Macromol. Chem. Phys.* 203, 1309-1316.

Jayasekara, R., Harding, I., Bowater, I., Lonergan, G., 2005. Biodegradability of a Selected Range of Polymers and Polymer Blends and Standard Methods for Assessment of Biodegradation. *J. Polym. Environ.* 13, 231-251.

Jendrossek, D., 2001. Microbial Degradation of Polyesters. *Adv. Biochem. Eng./Biotechnol.*

Jendrossek, D., Handrick, R., 2002. Microbial Degradation of Polyhydroxyalkanoates. *Annu. Rev. Microbiol.* 56, 403-432.

Jendrossek, D., Schirmer, A., Schlegel, H. G., 1996. Biodegradation of Polyhydroxyalkanoic Acids. *Appl. Microbiol. Biotechnol.* 46, 451-463.

Kadouri, D., Jurkevitch, E., Okon, Y., 2005. Ecological and Agricultural Significance of Bacterial Polyhydroxyalkanoates. *Crit. Rev. Microbiol.* 31, 55-67.

Kanesawa, Y., Doi, Y., 1990. Hydrolytic Degradation of Microbial Poly(3-hydroxybutyrate-co-3-hydroxyvalerate) Fibers. *Makromol. Chem.* 11, 679-682.

Kawaguchi, Y., Doi, Y., 1990. Structure of Native Poly(3-hydroxybutyrate) Granules Characterized by X-Ray Difffraction. *Microbiol. Lett.* 70, 151-156.

Kemnitzer, J. E., Gross, R. A., McCarthy, S. P., Liggat, J., Blundell, D. J., Cox, M., 1995. Crystallization Behavior of Predominantly Syndiotactic Poly(β-hydroxybutyrate). *J. Environ. Polym. Degrad.* 3, 37-47.

Kessler, B., Witholt, B., 2001. Factors Involved in the Regulatory Network of Polyhydroxyalkanoate Metabolism. *J. Bacteriol.* 86, 97-104.

Kim, D. Y., Rhee, Y. H., 2003. Biodegradation of Microbial and Synthetic Polyesters by Fungi. *Appl. Microbiol. Biotechnol.* 61, 300-308.

Kim, Y. B., Lenz, R. W., 2001. Polyesters from Microorganisms. *Adv. Biochem. Eng.* 71, 51-79.

Kourtz, L., Dillon, K., Daughtry, S., Madison, L. L., Peoples, O., Snell, K. D., 2005. A Novel Thiolase–Reductase Gene Fusion Promotes the Production of Polyhydroxybutyrate in *Arabidopsis*. *Plant Biotechnol. J.* 3, 435-447.

Labrecque, L. V., Kumar, R. A., Dave, V., Gross, R. A., McCarthy, S. P., 1997. Citrate esters as plasticizers for poly(lactic acid). *J. Appl. Polym. Sci.* 66, 1507-1513.

Lee, K.-M., Gilmore, D. F., Huss, M. J., 2005. Fungal Degradation of the Bioplastic PHB (Poly-3-hydroxybutyric acid). *J. Polym. Environ.* 13, 213-219.

Lee, S. Y., 1996. Bacterial Polyhydroxyalkanoates. *Biotechnol. Bioeng.* 49, 1-14.

Lee, S. Y., Chang, H. N., 1995. Production of Poly(hydroxyalkanoic acid). *Adv. Biochem. Eng. Biotechnol.* 52, 27-58.

Lee, S. Y., Choi, J.-I., 1999. Production and Degradation of Polyhydroxyalkanoates in Waste Environment. *Waste Manage.* 19, 133-139.

Lee, S. Y., Choi, J.-i., Wong, H. H., 1999. Recent Advances in Polyhydroxyalkanoate Production by Bacterial Fermentation: Mini-review. *J. Biol. Macromol.* 25, 31-36.

Lemoigne, M., 1926. Products of Dehydration and of Polymerization of β-hydroxybutyric Acid. *Bull. Soc. Chem. Biol.* 8, 770-782.

Li, S.-D., Yu, P. H., Cheung, M. K., 2001. Thermogravimetric Analysis of Poly(3-hydroxybutyrate) and Poly(3-hydroxybutyrate-*co*-3-hydroxyvalerate). *J. Appl. Polym. Sci.* 80, 2237-2244.

Lössl, A., Eibl, C., Harloff, H.-J., Jung, C., Koop, J.-U., 2003. Polyester Synthesis in Transplastomic Tobacco (*Nicotiana tabacum* L.): Significant Contents of Polyhydroxybutyrate are Associated with Growth Reduction. *Plant Cell Rep.* 21, 891-899.

Luzier, W. D., 1992. Materials Derived from Biomass/Biodegradable Materials. *Proc. Natl. Acad. Sci. USA.* 89, 839-842.

Madison, L. L., Huisman, G. W., 1999. Metabolic Engineering of Poly(3-hydroxyalkanoates): From DNA to Plastic. *Microbiol. Molec. Biol. Rev.* 63, 21-53.

Manna, A., Paul, A. K., 2000. Degradation of Microbial Polyester Poly(3-hydroxybutyrate) in Environmental Samples and in Culture. *Biodegradation*. 11, 323-329.

Mecking, S., 2004. Nature or Petrochemistry? – Biologically Degradable Materials. *Angew. Chem. Int. Ed.* 43, 1078-1085.

Mergaert, J., Anderson, C., Wouters, A., Swings, J., 1994. Microbial Degradation of Poly(3-hydroxybutyrate) and Poly(3-hydroxybutyrate-co-3-hydroxyvalerate) in Compost. *J. Environ. Polym. Degrad.* 2, 177-183.

Mergaert, J., Webb, A., Anderson, C., Wouters, A., Swings, J., 1993. Microbial Degradation of Poly(3-hydroxybutyrate) and Poly(3-hydroxybutyrate-co-3-hydroxyvalerate) in Soils. *Appl. Environ. Microbiol.* 59, 3233-3238.

Metabolix, 2002. Metabolix Brochure. http://www.metabolix.com/resources/brochure.pdf.

Metabolix, 2006. ADM and Metabolix Announce First Commercial Plant for PHA Natural Plastics. http://www.metabolix.com/publications/pressreleases/PR20060213.html.

Mitomo, H., Barham, P. J., Keller, A., 1987. Crystallization and Morphology of Poly(β-hydroxybutyrate) and Its Copolymer. *Polym. J.* 19, 1241-1253.

Molitoris, H. P., Moss, S. T., de Konig, G. J. M., Jendrossek, D., 1996. Scanning Electron Microscopy of Polyhydroxyalkanoate Degradation by Bacteria. *Appl. Microbiol. Biotechnol.* 46, 570-579.

Nawrath, C., Poirier, Y., Somerville, C., 1994. Targeting of the Polyhydroxybutyrate Biosynthetic Pathway to the Plastids of *Arabidopsis thaliana* Results in High Levels of Polymer Accumulation. *Proc. Natl. Acad. Sci. USA*. 91, 12760-12764.

Ohtaki, A., Nakasaki, K., 2000a. Comparison of the Weight-Loss Degradability of Various Biodegradable Plastics under Laboratory Composting Conditions. *J. Mater. Cycles Waste Manag.* 2, 118-124.

Ohtaki, A., Nakasaki, K., 2000b. Report: Ultimate Degradability of Various Kinds of Biodegradable Plastics Under Controlled Composting Conditions. *Waste Manage. Res.* 18, 184-189.

Petrasovits, L. A., Purnell, M. P., Nielsen, L. K., Brumbley, S. M., 2007. Production of Polyhydroxybutyrate in Sugarcane. *Plant Biotechnol. J.* 5, 162-172.

Phillip, S., Keshavarz, T., Roy, I., 2007. Polyhydroxyalkanoates: Biodegradable Polymers with a Range of Applications. *J. Chem. Technol. Biotechnol.* 82, 233-247.

Poirier, P. D. Y., Gruys, D. K. J., 2002. Production of Polyhydroxyalkanoates in Transgenic Plants. *Biopolymers, Volume 3a: Polyesters I – Biological Systems and Biotechnological Production*. 401-435.

Puechner, P., Mueller, W.-R., Bardtke, D., 1995. Assessing the Biodegradation Potential of Polymers in Screening- and Long-Term Test Systems. *J. Environ. Polym. Deg.* 3, 133-143.

Reddy, C. S. K., Ghai, R., Rashmi, Kalia, V. C., 2003. Polyhydroxyalkanoates: An Overview. *Bioresour. Technol.* 87, 137-146.

Reischwitz, A., Stoppok, E., Klaus, B., 1998. Anaerobic Degradation of Poly-3-hydroxybutyrate and Poly-3-hydroxybutyrate-co-3-hydroxyvalerate. *Biodegradation.* 8, 313-319.

Renstad, R., Karlsson, S., Albertsson, A.-C., Werner, P.-E., Westdahl, M., 1997. Influence of Processing Parameters of the Mass Crystallinity of Poly(3-hydroxybutyrate-*co*-3-hydroxyvalerate). *Polym. Int.* 43, 201-209.

Rossini, C. J., Arceo, J. F., McCarney, E. R., Augustine, B. H., 2001. Use of In-situ Atomic Force Microscopy to Monitor the Biodegradation of Polyhydroxyalkanoates (PHAs). *Macromol. Symp.* 167, 139-151.

Sang, B.-I., Hori, K., Tanji, Y., Unno, H., 2002. Fungal Contribution to In Situ Biodegradation of Poly(3-hydroxybutyrate-*co*-3-hydroxyvalerate) Film in Soil. *Appl. Microbiol. Biotechnol.* 58, 241-247.

Scandola, M., Ceccorulli, G., Pizzoli, M., 1989. The Physical Aging of Bacterial Poly (D-β-hydroxybutyrate). *Die Makromolekulare Chemie*. 10, 47-50.

Scherer, T. M., Fuller, R. C., Lenz, R. W., Goodwin, S., 1999. Hydrolase Activity of an Extracellular Depolymerase from *Aspergillus fumigatus* with Bacterial and Synthetic Polyesters. *Polym. Degrad. Stab.* 64, 267-275.

Shelton, D. R., Tiedje, J. M., 1984. General Method for Determining Anaerobic Biodegradation Potential. *Appl. Environ. Microbiol.* 47, 850-857.

Shin, P. K., Kim, M. H., Kim, J. M., 1997. Biodegradability of Degradable Plastics Exposed to Anaerobic Digested Sludge and Simulated Landfill Conditions. *J. Environ. Polym. Degrad.* 5, 33-39.

Snell, K. D., Feng, F., Zhong, L., Martin, D., Madison, L. L., 2002. YfcX Enables Medium-Chain-Length Poly(3-hydroxyalkanoate) Formation from Fatty Acids in Recombinant *Escherichia coli fadB* strains. *J. Bacteriol.* 184, 5696-5705.

Snell, K. D., Peoples, O. P., 2002. Polyhydroxyalkanoate Polymers and Their Production in Transgenic Plants. *Metabolic Engineering*. 4, 29-40.

Song, C., Wang, S., Ono, S., Zhang, B., Shimasaki, C., Inoue, M., 2003. The Biodegradation of Poly(3-hydroxybutyrate-*co*-3-hydroxyvalerate) (PHB/V) and PHB/V-degrading Microorganisms in Soil. *Polym. Adv. Technol.* 14, 184-188.

Song, J. J., Yoon, S. C., Yu, S. M., Lenz, R. W., 1998. Differential Scanning Calorimetric Study of Poly(3-hydroxyoctanoate) Inclusions in Bacterial Cells. *Internat. J. Biol. Macromol.* 23, 165-173.

Spyros, A., Kimmich, R., Briese, B. H., Jendrossek, D., 1997. ^{1}H NMR Imaging Study of Enzymatic Degradation in Poly(3-hydroxybutyrate) and Poly(3-hydroxybutyrate-*co*-3-hydroxyvalerate). Evidence for Preferential Degradation of the Amorphous Phase by PHB Depolymerase B from *Pseudomonas lemoignei*. *Macromolecules.* 30, 8218-8225.

Steinbüchel, A., Hein, S., 2001. Biochemical and Molecular Basis of Microbial Synthesis of Polyhydroxyalkanoates in Microorganisms. *Adv. Biochem. Eng./Biotechnol.* 71, 81-123.

Steinbüchel, A., Valentin, H. A., 1995. Diversity of Bacterial Polyhydroxyalkanoic Acids. *FEMS Microbiol. Lett.* 128, 219-228.

Tercjak, A., Haponiuk, J. T., Masiulanis, B., 2003. Study of Thermal Property Changes of Biopol/Polyamide 11 Blends during Biodegradation in Compost. *J. Therm. Anal. Calorim.* 74, 605-608.

Tullo, A. 2005. Renewable Materials: Two Pacts May Help Spur Biomass Plastics. *Chemical and Engineering News*. 83:9.

USEPA, 2005. U. S. Environmental Protection Agency. Municipal Solid Waste in the United States: 2003 Data Tables. http://www.epa.gov/epaoswer/non-hw/muncpl/pubs/03data.pdf.

Valentin, H. E., Broyles, D. L., Casagrande, L. A., Colburn, S. M., Creely, W. L., DeLaquil, P. A., Felton, H. M., Gonzalez, K. A., Houmiel, K. L., Lutke, K., Mahadeo, D. A., Mitsky, T. A., Padgette, S. R., Reiser, S. E., Slater, S., Stark, D. M., Stock, R. T., Stone, D. A., Taylor, N. B., Thorne, G. M., Tran, M., Gruys, K. J., 1999. PHA Production, from Bacteria to Plants. *Internat. J. Biol. Macromol.* 25, 303-306.

van der Walle, G. A. M., de Koning, G. J. M., Weusthuis, R. A., Eggink, G., 2001. Properties, Modifications and Applications of Biopolyesters. *Adv. Biochem. Eng.* 71, 263-291.

Verhoogt, H., Ramsay, B. A., Favis, B. D., Ramsay, J. A., 1996. The Influence of Thermal History on the Properties of Poly(3-hydroxybutyrate-co-12%-3-hydroxyvalerate). *J. Appl. Polym. Sci.* 61, 86-96.

Wallen, L. L., Rohwedder, W. K., 1974. Poly-β-hydroxyalkanoate from Activated Sludge. *Environ. Sci. Technol.* 8, 576-579.

Williams, S. F., Martin, D. P., Horowitz, D. M., Peoples, O. P., 1999. PHA Applications: Addressing the Price Performance Issue I. Tissue Engineering. *Internat. J. Biol. Macromol.* 25, 111-121.

Wong, H. H., Lee, S. Y., 1998. Poly-(3-hydroxybutyrate) Production from Whey by High-Density Cultivation of Recombinant *Escherichia coli*. *Appl. Microbiol. Biotechnol.* 50, 30-33.

Wróbel, M., Zebrowski, J., Szopa, J., 2004. Polyhdroxybutyrate Synthesis in Transgenic Flax. *J. Biotechnol.* 107, 41-54.

Yoshie, N., Nakasato, K., Fujiwara, M., Kasuya, K., Abe, H., Doi, Y., Inoue, Y., 2000. Effect of Low Molecular Weight Aditives on Enzymatic Degradation of Poly(3-hydroxybutyrate). *Polymer*. 41, 3227-3234.

Yue, C. L., Gross, R. A., McCarthy, S. P., 1996. Composting Studies of Poly(β-hydroxybutyrate-co-β-hydroxyvalerate). *Polym. Degrad. Stab.* 51, 205-210.

Appendix A – Raw Data, Calculations, and Statistics of Anaerobic Experiments

Experimental Setup for Biogas Production Experiments (Example given for EXP1)

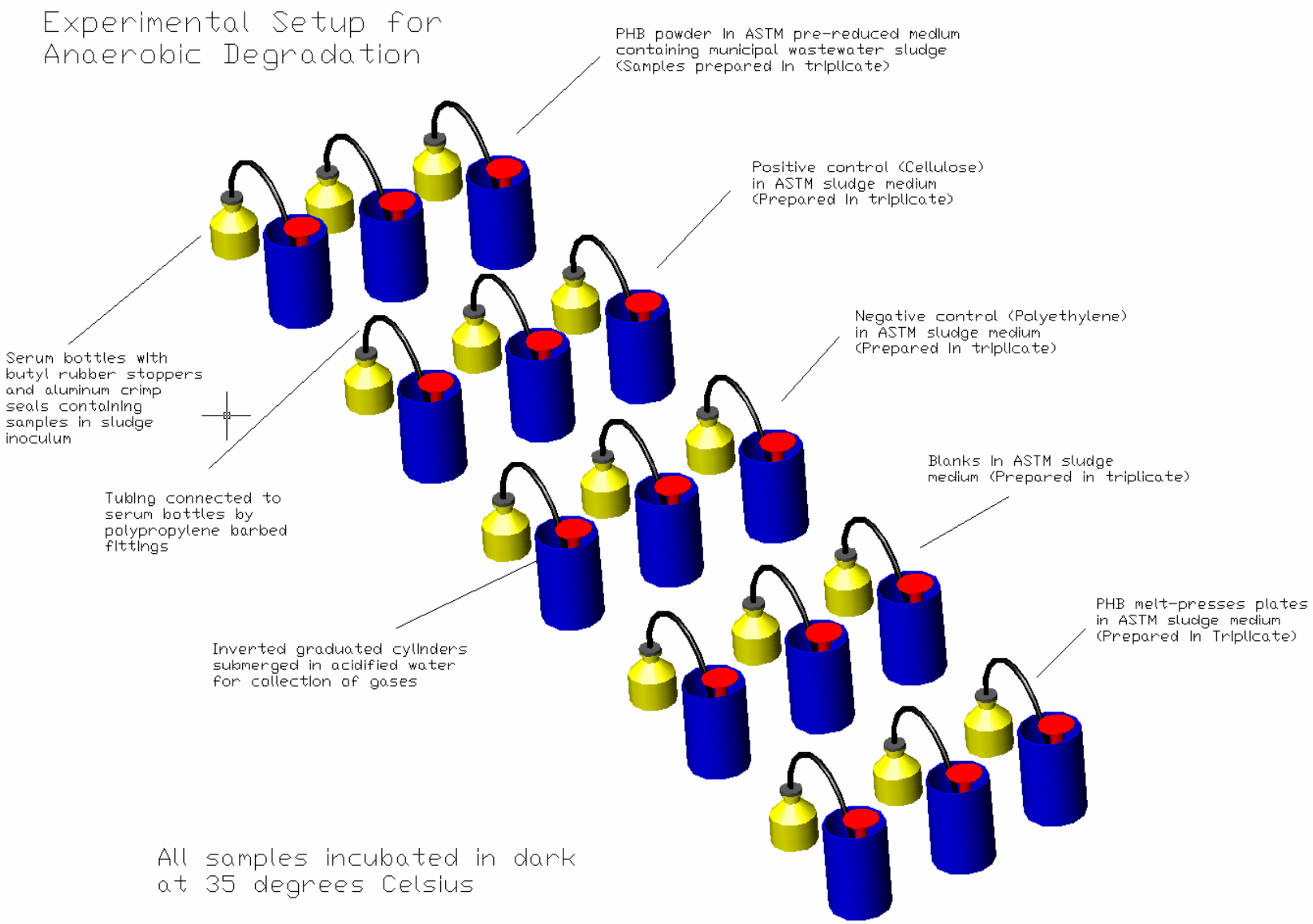

Calculations of Sewage Sludge Medium needed for EXP1 and First Mass Loss Experiment
In order to achieve equal ratios of initial surface area to medium volume for both experiments

STRIPS FOR SERUM VIALS

Strip Dimensions and properties

Length (cm)	3.5	Density (g/cm^3)	1.2089
Width (cm)	1.1		
Thickness (cm)	0.12	Surface area (cm^2)	35.216
Volume (cm^3)	0.462	per vial	
Mass (g)	0.559	Ratio (SA:mass)	63.053278

Carbon Content of Plastic	54.5%
Mass of Carbon in form of Plastic per vial (g)	1.217556
Carbon Content of Media in form of Plastic (mg/L)	8117.0
# Strips needed per vial	4
# Strips needed	12
Vol. of Media per vial (mL)	150
Total Vol. of media for strips (mL)	450

PLATES FOR FIRST MASS LOSS EXPERIMENT

0.5-mm plate Dimensions and properties

Length (cm)	2.5		
Width (cm)	2.5		
Thickness (cm)	0.05	Surface area (cm^2)	13
Volume (cm^3)	0.3125		
Mass (g)	0.38	Ratio (SA:mass)	34.411448

Mass of Carbon in form of Plastic per plate (g)	0.205891
Vol. of Medium needed per plate (mL)	55
# plates needed per flask	5
Vol. of Medium needed per flask (mL)	277
# DEA plates needed	35
Total Vol. of media for DEA plates (mL)	1938

1.2-mm plate Dimensions and properties

Length (cm)	7		
Width (cm)	1.5		
Thickness (cm)	0.12	Surface area (cm^2)	23.04
Volume (cm^3)	1.26		
Mass (g)	1.523	Ratio (SA:mass)	15.125911

Mass of Carbon in form of Plastic per plate (g)		0.830152		
Vol. of Medium needed per plate (mL)		98		
# plates needed per flask		2		
Vol. of Medium needed per flask (mL)		196		
# plates needed		14		
Total Vol. of media for plates (mL)		1374		
3.5-mm Plate Dimensions and properties				
Length (cm)	6.4			
Width (cm)	1.27			
Thickness (cm)	0.35		Surface area (cm^2)	21.625
Volume (cm^3)	2.8448			
Mass (g)	3.439		Ratio (SA:mass)	6.2880212
Mass of Carbon in form of Plastic per plate (g)		1.874298		
Vol. of Medium needed per plate (mL)		92		
# plates needed per flask		5		
Vol. of Medium needed per flask (mL)		461		
# plates needed		35		
Total Vol. of media for Izod plates (mL)		3224		
Total Volume of Media per flask for 1st mass loss experiment (mL)…….				934
ADDITIONAL NEEDS FOR MEDIA				
Additional serum vials (mL needed)		1800		
TOTAL MEDIA NEEDED FOR DEGRADATION EXPERIMENT (L) ……..				8.79
Number of batches of medium to prepare ……				3

First Mass Loss Experiment

0.5-mm PHA Plates

Time of Degradation	2 weeks		4 weeks		8 weeks		12 weeks	
	Before	After	Before	After	Before	After	Before	After
Observed Mass (g)	0.4128	0.3053	0.3960	0.2056	0.3940	-	0.3943	-
	0.4020	0.3394	0.4430	0.1914	0.4227	-	0.3968	-
	0.4449	0.3896	0.3952	0.2003	0.4214	-	0.3955	-
	0.4195	0.2837	0.4137	0.1560	0.4354	-	0.4004	-
	0.4105	0.3465	0.4238	0.3167	0.3912	-	0.4250	-
Total Weight (g)	2.0897	1.6645	2.0717	1.07	2.0647	0.056	2.012	0.0101
Mass Loss (g)	0.4252		1.0017		2.0087		2.0019	
Mass Loss/Surface Area (g/cm^2)	0.0065		0.0154		0.0309		0.0308	
Rate of Mass Loss (g/Day)	0.0304		0.0358		0.0359		0.0238	
Percentage of Mass Loss	20.35%		48.35%		97.29%		99.50%	

1.2-mm PHA Plates

Time of Degradation	2 weeks		4 weeks		8 weeks		12 weeks	
	Before	After	Before	After	Before	After	Before	After
Observed Mass (g)	1.521	1.349	1.635	0.8458	1.4485	-	1.4882	-
	1.4321	1.2411	1.5949	0.8851	1.5437	-	1.5119	-
Total Weight (g)	2.9531	2.5901	3.2299	1.7309	2.9922	0.0845	3.0001	0
Mass Loss (g)	0.363		1.499		2.9077		3.0001	
Mass Loss/Surface Area (g/cm^2)	0.0079		0.0325		0.0631		0.0651	
Rate of Mass Loss (g/Day)	0.0259		0.0535		0.0519		0.0357	
Percentage of Mass Loss	12.29%		46.41%		97.18%		100.00%	

3.5-mm PHA Plates

Time of Degradation	2 weeks		4 weeks		8 weeks		12 weeks		19 weeks	
	Before	After	Before	After	Before	After	Before	After	Before	After
Observed Mass (g)	3.328	3.1468	3.415	2.7964	3.2536	1.384	3.2016	-	3.3881	-
	3.1999	3.0531	3.1931	2.8131	3.2624	1.4955	3.2618	-	3.453	-
	3.2416	3.1131	3.2378	2.6432	3.3657	1.3247	3.358	-	3.2408	-
	3.4079	3.2776	3.2116	2.7171	3.2874	0.8272	3.2627	-	3.3774	-
	3.3183	3.1463	3.4094	2.7726	3.146	0.7872	3.3182	-	3.3369	-
Total Weight (g)	16.4957	15.7369	16.4669	13.7424	16.3151	5.8186	16.4023	1.2351	16.7962	0.0583
Mass Loss (g)	0.7588		2.7245		10.4965		15.1672		16.7379	
Mass Loss/Surface Area (g/cm^2)	0.0070		0.0252		0.0971		0.1403		0.1548	
Rate of Mass Loss (g/Day)	0.0542		0.0973		0.1874		0.1806		0.1258	
Percentage of Mass Loss	4.60%		16.55%		64.34%		92.47%		99.65%	

Curves for Calculation of Degradation Rate Coefficients

Remaining Mass/Surface Area vs. Time (0.5-mm Plates)

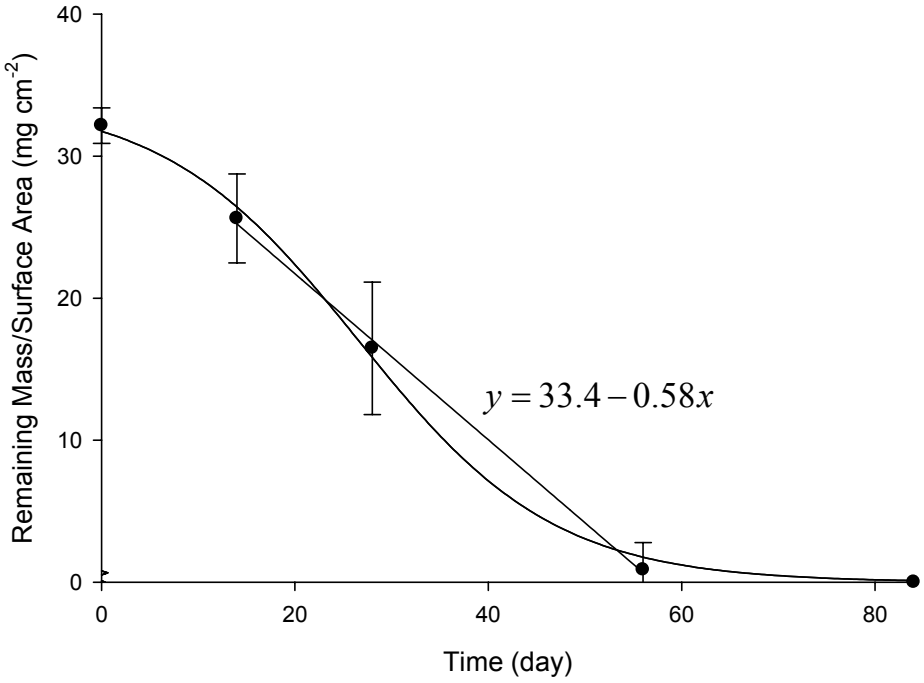

Remaining Mass/Surface Area vs. Time (1.2-mm Plates)

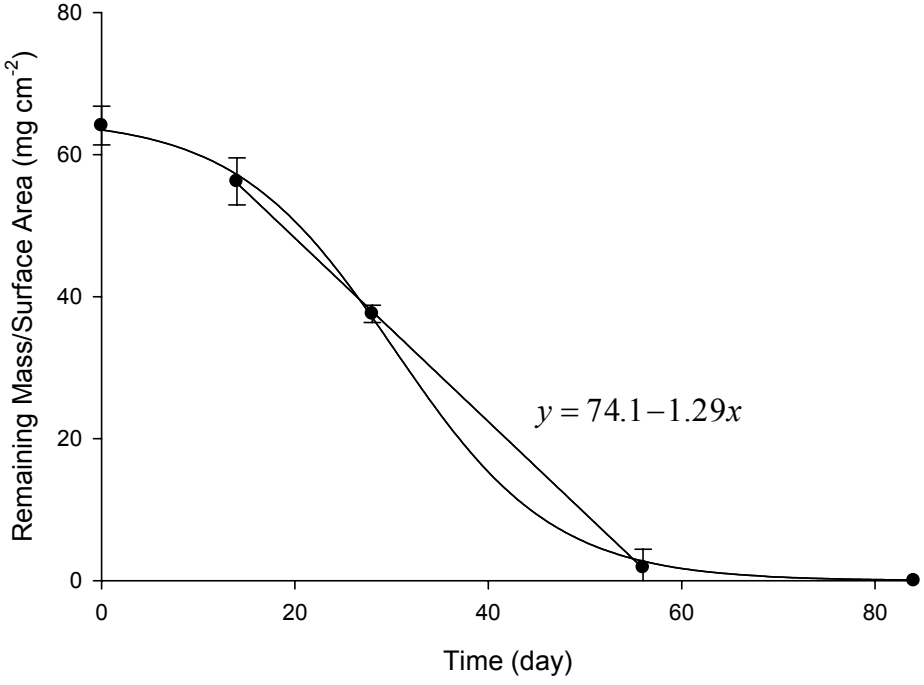

Remaining Mass/Surface Area vs. Time (3.5-mm Plates)

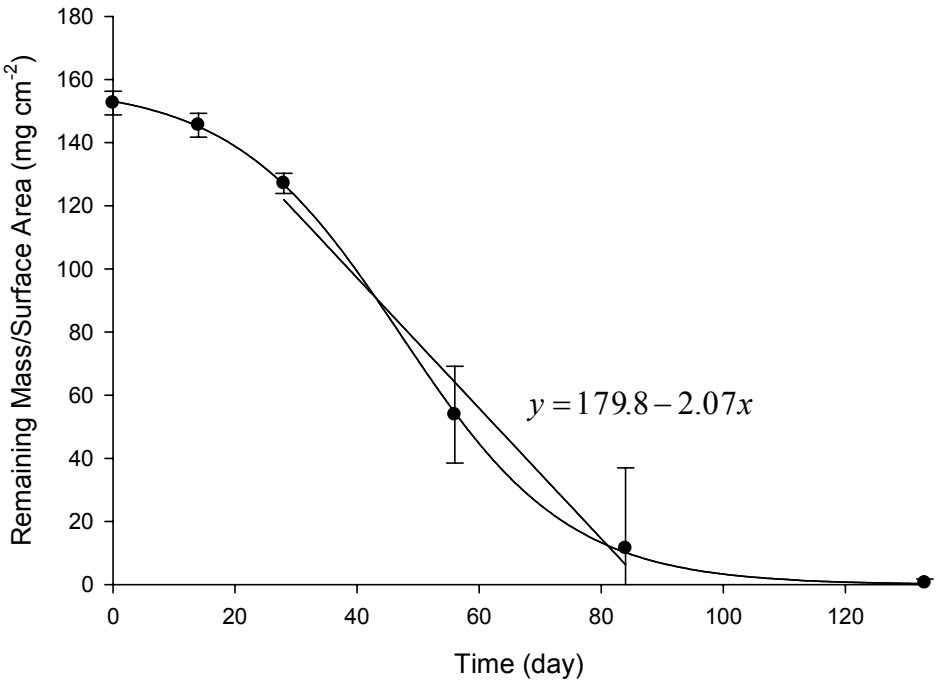

Analysis of Covariance for Degradation Rate Coefficients of PHA degraded in 1st Anaerobic Mass Loss Expt

Obs	Experiment	Thickness	Rep	Time	MperA
1	1st	0.5 mm	Rep1	14	23.485
2	1st	0.5 mm	Rep1	28	15.815
3	1st	0.5 mm	Rep1	56	4.308
4	1st	0.5 mm	Rep2	14	26.108
5	1st	0.5 mm	Rep2	28	14.723
6	1st	0.5 mm	Rep2	56	0.000
7	1st	0.5 mm	Rep3	14	29.969
8	1st	0.5 mm	Rep3	28	15.408
9	1st	0.5 mm	Rep3	56	0.000
10	1st	0.5 mm	Rep4	14	21.823
11	1st	0.5 mm	Rep4	28	12.000
12	1st	0.5 mm	Rep4	56	0.000
13	1st	0.5 mm	Rep5	14	26.654
14	1st	0.5 mm	Rep5	28	24.362
15	1st	0.5 mm	Rep5	56	0.000
16	1st	1.2 mm	Rep1	14	58.550
17	1st	1.2 mm	Rep1	28	36.710
18	1st	1.2 mm	Rep1	56	3.668
19	1st	1.2 mm	Rep2	14	53.867
20	1st	1.2 mm	Rep2	28	38.416
21	1st	1.2 mm	Rep2	56	0.000

Obs	Experiment	Thickness	Rep	Time	MperA
22	1st	3.5 mm	Rep1	28	129.313
23	1st	3.5 mm	Rep1	56	64.000
24	1st	3.5 mm	Rep1	84	57.114
25	1st	3.5 mm	Rep2	28	130.086
26	1st	3.5 mm	Rep2	56	69.156
27	1st	3.5 mm	Rep2	84	0.000
28	1st	3.5 mm	Rep3	28	122.229
29	1st	3.5 mm	Rep3	56	61.258
30	1st	3.5 mm	Rep3	84	0.000
31	1st	3.5 mm	Rep4	28	125.646
32	1st	3.5 mm	Rep4	56	38.252
33	1st	3.5 mm	Rep4	84	0.000
34	1st	3.5 mm	Rep5	28	128.213
35	1st	3.5 mm	Rep5	56	36.402
36	1st	3.5 mm	Rep5	84	0.000

Analysis of Covariance for Degradation Rate Coefficients of PHA degraded in 1st Anaerobic Mass Loss Expt

The Mixed Procedure

Model Information	
Data Set	WORK.ONE
Dependent Variable	MperA
Covariance Structure	Diagonal
Estimation Method	REML

Model Information	
Residual Variance Method	Profile
Fixed Effects SE Method	Model-Based
Degrees of Freedom Method	Residual

Class Level Information		
Class	Levels	Values
Thickness	3	0.5 mm 1.2 mm 3.5 mm

Dimensions	
Covariance Parameters	1
Columns in X	8
Columns in Z	0
Subjects	1
Max Obs Per Subject	36

Number of Observations	
Number of Observations Read	36
Number of Observations Used	36
Number of Observations Not Used	0

Covariance Parameter Estimates	
Cov Parm	Estimate
Residual	151.62

Fit Statistics

Fit Statistics	
-2 Res Log Likelihood	267.9
AIC (smaller is better)	269.9
AICC (smaller is better)	270.0
BIC (smaller is better)	271.3

Solution for Fixed Effects						
Effect	Thickness	Estimate	Standard Error	DF	t Value	Pr > |t|
Intercept		179.79	8.4118	30	21.37	<.0001
Time		-2.0656	0.1391	30	-14.85	<.0001
Thickness	0.5 mm	-146.38	10.7817	30	-13.58	<.0001
Thickness	1.2 mm	-105.71	13.5822	30	-7.78	<.0001
Thickness	3.5 mm	0	.	.	.	.
Time*Thickness	0.5 mm	1.4810	0.2291	30	6.46	<.0001
Time*Thickness	1.2 mm	0.7736	0.3197	30	2.42	0.0218
Time*Thickness	3.5 mm	0	.	.	.	.

Type 1 Tests of Fixed Effects				
Effect	Num DF	Den DF	F Value	Pr > F
Time	1	30	50.70	<.0001
Thickness	2	30	141.25	<.0001
Time*Thickness	2	30	21.16	<.0001

Type 3 Tests of Fixed Effects				
Effect	Num DF	Den DF	F Value	Pr > F

Type 3 Tests of Fixed Effects				
Effect	**Num DF**	**Den DF**	**F Value**	**Pr > F**
Time	1	30	114.80	<.0001
Thickness	2	30	93.14	<.0001
Time*Thickness	2	30	21.16	<.0001

Estimates					
Label	**Estimate**	**Standard Error**	**DF**	**t Value**	**Pr > |t|**
compare 0.5 mm vs 1.2 mm	0.7074	0.3406	30	2.08	0.0465
compare 0.5 mm vs 3.5 mm	1.4810	0.2291	30	6.46	<.0001
compare 1.2 mm vs 3.5 mm	0.7736	0.3197	30	2.42	0.0218

Calculations to determine PHA plate dimensions in 2nd Mass Loss Experiment needed for ratio of plastic mass to sludge volume to equal that of EXP3

Carbon Conc. of Media needed in form of plastic (mg/L)	3875.5

STRIPS FOR SERUM VIALS

Strip Dimensions and properties

Length (cm)	3.5	Density (g/cm^3)	1.154399
Width (cm)	1.1		
Thickness (cm)	0.12	Surface area (cm^2)	8.804
Volume (cm^3)	0.462	per strip	
Mass (g)	0.533	Ratio (mass:SA)	0.0605784

Carbon Content of Plastic	54.5%
Mass of Carbon needed in form of Plastic per vial (g)	0.581332
Carbon Content of Media in form of Plastic (mg/L)	3875.5
# Strips needed per vial	2
# Strips needed	6
Vol. of Media per vial (mL)	150
Total Vol. of media for strips (mL)	450

PLATES FOR ADDITIONAL ANALYSES

0.24-mm Plate Dimensions and properties

Length (cm)	2.533114		
Thickness (cm)	0.024	Surface area (cm^2)	13.076512
Volume (cm^3)	0.154		
Mass (g)	0.1778	Ratio (mass:SA)	0.0135952

Mass of Carbon needed in form of Plastic per plate (g)	0.096889
Vol. of Medium needed per flask (mL)	50
# plates needed per flask	2
# 0.24-mm plates needed	60
Total Vol. of media for 0.24-mm plates (mL)	1500

1.2-mm Strip Dimensions and properties

Length (cm)	1.602082		
Thickness (cm)	0.12	Surface area (cm^2)	5.9023327
Volume (cm^3)	0.308		

Mass (g)	0.36		Ratio (mass:SA)	0.0602397
Mass of Carbon needed in form of Plastic per plate (g)		0.193777		
Vol. of Medium needed per flask (mL)		50		
# plates needed per flask		1		
# 1.2-mm plates needed		18		
Total Vol. of media for 1.2-mm plates (mL)		900		

5-mm Plate Dimensions and properties

Length (cm)	1.109955			
Thickness (cm)	0.5		Surface area (cm^2)	4.6839099
Volume (cm^3)	0.616			
Mass (g)	0.7111		Ratio (mass:SA)	0.1518197
Mass of Carbon needed in form of Plastic per plate (g)		0.387555		
Vol. of Medium needed per flask (mL)		100		
# plates needed per flask		1		
# 5-mm plates needed		18		
Total Vol. of media for 5-mm plates (mL)		1800		

ADDITIONAL NEEDS FOR MEDIA

Additional serum vials (mL needed)	2250

Second Mass Loss Experiment

0.24-mm PHA Plates

Time of Degradation		5 days		10 days		15 days		3 weeks		4 weeks		6 weeks		8 weeks		10 weeks	
		Before	After	Before	After	Before	After	Before	After	Before	After	Before	After	Before	After	Before	After
Observed Mass (g)	Replicate 1	0.3263	0.3166	0.3040	0.2329	0.3203	0.0988	0.3204	0.2054	0.3511	0.2069	0.3373	0.1391	0.3550	0.0581	0.3333	0.0000
	Replicate 2	0.3221	0.2729	0.3116	0.2584	0.3574	0.3008	0.3295	0.1108	0.3268	0.0613	0.3170	0.0000	0.3214	0.0000	0.3158	0.0000
	Replicate 3	0.3022	0.2979	0.3054	0.2269	0.3170	0.0558	0.2984	0.1224	0.3307	0.0000	0.3240	0.0280	0.3145	0.0000	0.2939	0.0000
Total Weight (g)		0.9506	0.8874	0.9210	0.7182	0.9947	0.4554	0.9483	0.4386	1.0086	0.2682	0.9783	0.1671	0.9909	0.0581	0.9430	0.0000
Mass Loss (g)		0.0632		0.2028		0.5393		0.5097		0.7404		0.8112		0.9328		0.943	
Mass Loss/Surface Area (g/cm^2)		0.0008		0.0026		0.0069		0.0065		0.0094		0.0103		0.0119		0.0120	
Rate of Mass Loss (g/Day)		0.0126		0.0203		0.0360		0.0243		0.0264		0.0193		0.0167		0.0135	
Percentage of Mass Loss		6.65%		22.02%		54.22%		53.75%		73.41%		82.92%		94.14%		100.00%	

1.2-mm PHA Plates

Time of Degradation		2 weeks		4 weeks		8 weeks		12 weeks		16 weeks		20 weeks	
		Before	After	Before	After	Before	After	Before	After	Before	After	Before	After
Observed Mass (g)	Replicate 1	0.3963	0.3756	0.3890	0.3434	0.3570	0.0509	0.4053	0.2219	0.4037	0.0000	0.3969	0.0000
	Replicate 2	0.3625	0.3151	0.3691	0.3116	0.4192	0.3192	0.3700	0.0345	0.4573	0.3360	0.3957	0.0000
	Replicate 3	0.3700	0.3470	0.3896	0.3261	0.3880	0.0000	0.4509	0.0000	0.3904	0.0000	0.3744	0.0000
Total Weight (g)		1.1288	1.0377	1.1477	0.9811	1.1642	0.3701	1.2262	0.2564	1.2514	0.3360	1.1670	0.0000
Mass Loss (g)		0.0911		0.1666		0.7941		0.9698		0.9154		1.167	
Mass Loss/Surface Area (g/cm^2)		0.0051		0.0094		0.0448		0.0548		0.0517		0.0659	
Rate of Mass Loss (g/Day)		0.0065		0.0060		0.0142		0.0115		0.0082		0.0083	
Percentage of Mass Loss		8.07%		14.52%		68.21%		79.09%		73.15%		100.00%	

5-mm PHA Plates

Time of Degradation		2 weeks		4 weeks		8 weeks		12 weeks		16 weeks		20 weeks		32 weeks	
		Before	After	Before	After	Before	After	Before	After	Before	After	Before	After	Before	After
Observed Mass (g)	Replicate 1	0.8008	0.7902	0.9181	0.8529	0.8961	0.6418	0.9242	0.6925	0.7772	0.4040	0.8890	0.6963	0.8930	0.3995
	Replicate 2	0.8357	0.8207	0.8337	0.7653	0.8662	0.7184	0.8232	0.6201	0.8647	0.5744	0.7829	0.0712	0.9249	0.3649
	Replicate 3	0.8708	0.8410	0.8782	0.8189	0.8665	0.6776	0.8234	0.5684	0.8818	0.3131	0.8083	0.2405	0.9257	0.0886
Total Weight (g)		2.5073	2.4519	2.6300	2.4371	2.6288	2.0378	2.5708	1.8810	2.5237	1.2915	2.4802	1.0080	2.7436	0.8530
Mass Loss (g)		0.0554		0.1929		0.591		0.6898		1.2322		1.4722		1.8906	
Mass Loss/Surface Area (g/cm^2)		0.0040		0.0139		0.0426		0.0498		0.0889		0.1062		0.1364	
Rate of Mass Loss (g/Day)		0.0040		0.0069		0.0106		0.0082		0.0110		0.0105		0.0113	
Percentage of Mass Loss		2.21%		7.33%		22.48%		26.83%		48.83%		59.36%		68.91%	

1.2-mm PLA Plates

Time of Degradation		2 weeks		4 weeks		8 weeks		12 weeks		16 weeks		20 weeks	
		Before	After	Before	After	Before	After	Before	After	Before	After	Before	After
Observed Mass (g)	Replicate 1	0.4382	0.4390	0.4454	0.4461	0.4269	0.4280	0.3832	0.3828	0.3960	0.3960	0.4150	0.4160
	Replicate 2	0.4105	0.4110	0.4215	0.4230	0.4033	0.4045	0.4387	0.4382	0.3996	0.3994	0.4725	0.4732
	Replicate 3	0.4084	0.4097	0.4512	0.4525	0.2949	0.3960	0.4336	0.4333	0.4054	0.4053	0.4162	0.4173
Total Weight (g)		1.2571	1.2597	1.3181	1.3216	1.1251	1.2285	1.2555	1.2543	1.2010	1.2007	1.3037	1.3065
Mass Loss (g)		-0.0026		-0.0035		-0.1034		0.0012		0.0003		-0.0028	
Mass Loss/Surface Area (g/cm^2)		-0.0001		-0.0002		-0.0058		0.0001		0.0000		-0.0002	
Rate of Mass Loss (g/Day)		-0.0002		-0.0001		-0.0018		0.0000		0.0000		0.0000	
Percentage of Mass Loss		-0.21%		-0.27%		-9.19%		0.10%		0.02%		-0.21%	

1.2-mm PHA/15% TBC Blend Plates

Time of Degradation		2 weeks		4 weeks		8 weeks		12 weeks		16 weeks		20 weeks	
		Before	After	Before	After	Before	After	Before	After	Before	After	Before	After
Observed Mass (g)	Replicate 1	0.3522	0.3285	0.3844	0.3305	0.3394	0.2542	0.3569	0.0000	0.3385	0.0000	0.3567	0.0000
	Replicate 2	0.3797	0.3556	0.3591	0.3087	0.3536	0.2610	0.3827	0.2252	0.3487	0.1697	0.3494	0.1525
	Replicate 3	0.3760	0.3531	0.3841	0.3385	0.3561	0.1938	0.3782	0.2840	0.3825	0.2540	0.3435	0.0000
Total Weight (g)		1.1079	1.0372	1.1276	0.9777	1.0491	0.7090	1.1178	0.5092	1.0697	0.4237	1.0496	0.1525
Mass Loss (g)		0.0707		0.1499		0.3401		0.6086		0.646		0.8971	
Mass Loss/Surface Area (g/cm^2)		0.0040		0.0085		0.0192		0.0344		0.0365		0.0507	
Rate of Mass Loss (g/Day)		0.0050		0.0054		0.0061		0.0072		0.0058		0.0064	
Percentage of Mass Loss		6.38%		13.29%		32.42%		54.45%		60.39%		85.47%	

Curves for Calculation of Degradation Rate Coefficients

Remaining Mass/Surface Area vs. Time (0.24-mm Plates)

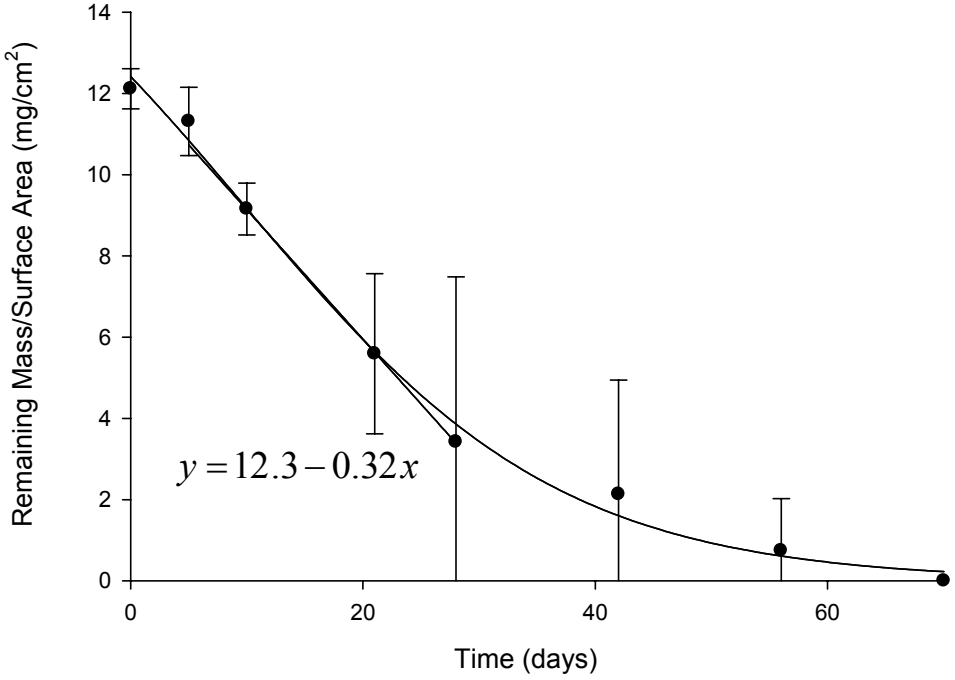

Remaining Mass/Surface Area vs. Time (1.2-mm Plates)

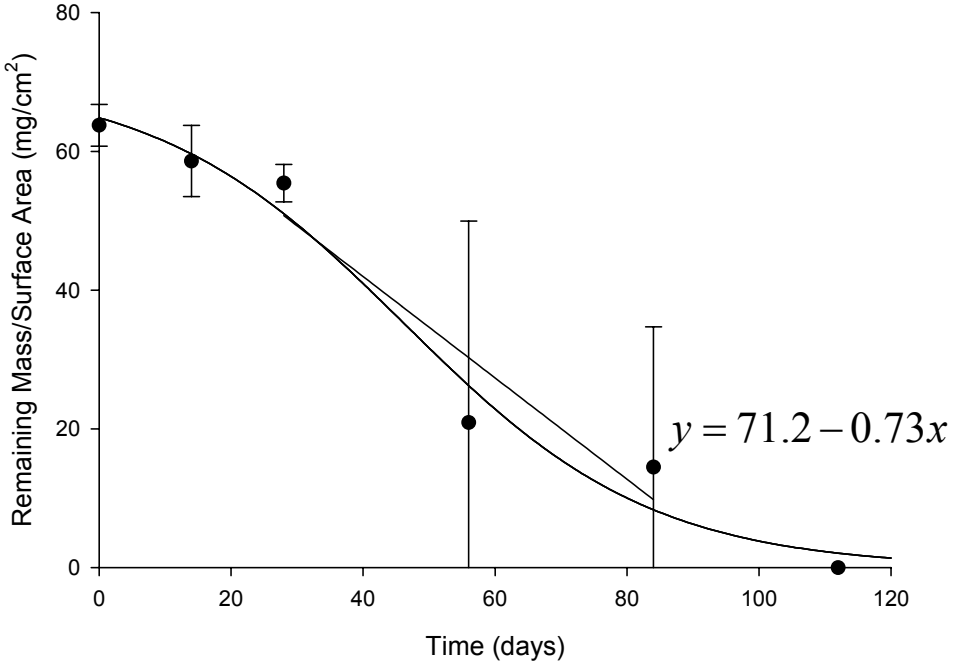

Remaining Mass/Surface Area vs. Time (5-mm Plates)

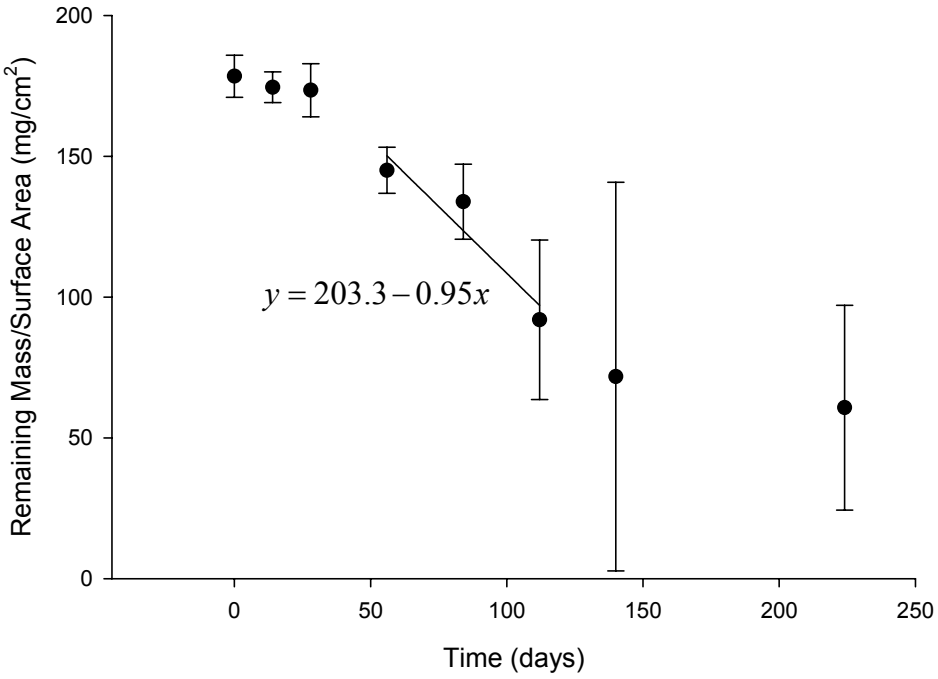

Remaining Mass/Surface Area vs. Time (1.2-mm PHA/15% TBC Plates)

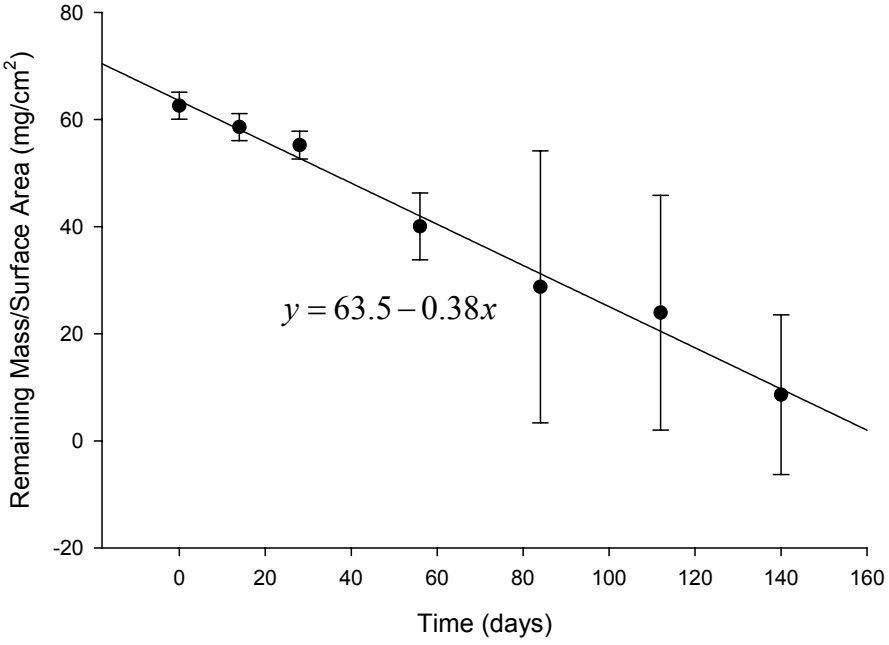

Analysis of Covariance for Degradation Rate Coefficients of PHA degraded in 2nd Anaerobic Mass Loss Expt

Obs	Experiment	Thickness	Rep	Time	MperA
1	2nd	0.24 mm	Rep1	10	8.905
2	2nd	0.24 mm	Rep1	21	7.854
3	2nd	0.24 mm	Rep1	28	7.911
4	2nd	0.24 mm	Rep2	10	9.880
5	2nd	0.24 mm	Rep2	21	4.237
6	2nd	0.24 mm	Rep2	28	2.344
7	2nd	0.24 mm	Rep3	10	8.676
8	2nd	0.24 mm	Rep3	21	4.680
9	2nd	0.24 mm	Rep3	28	0.000
10	2nd	1.2 TBC	Rep1	0	59.671
11	2nd	1.2 TBC	Rep1	14	55.656
12	2nd	1.2 TBC	Rep1	28	55.995
13	2nd	1.2 TBC	Rep1	56	43.068
14	2nd	1.2 TBC	Rep1	84	0.000
15	2nd	1.2 TBC	Rep1	112	0.000
16	2nd	1.2 TBC	Rep1	140	0.000
17	2nd	1.2 TBC	Rep2	0	64.330
18	2nd	1.2 TBC	Rep2	14	60.247
19	2nd	1.2 TBC	Rep2	28	52.301
20	2nd	1.2 TBC	Rep2	56	44.220
21	2nd	1.2 TBC	Rep2	84	38.154

Obs	Experiment	Thickness	Rep	Time	MperA
22	2nd	1.2 TBC	Rep2	112	28.751
23	2nd	1.2 TBC	Rep2	140	25.837
24	2nd	1.2 TBC	Rep3	0	63.704
25	2nd	1.2 TBC	Rep3	14	59.824
26	2nd	1.2 TBC	Rep3	28	57.350
27	2nd	1.2 TBC	Rep3	56	32.834
28	2nd	1.2 TBC	Rep3	84	48.117
29	2nd	1.2 TBC	Rep3	112	43.034
30	2nd	1.2 TBC	Rep3	140	0.000
31	2nd	1.2 mm	Rep1	28	58.180
32	2nd	1.2 mm	Rep1	56	8.624
33	2nd	1.2 mm	Rep1	84	37.595
34	2nd	1.2 mm	Rep2	28	52.793
35	2nd	1.2 mm	Rep2	56	54.080
36	2nd	1.2 mm	Rep2	84	5.845
37	2nd	1.2 mm	Rep3	28	55.249
38	2nd	1.2 mm	Rep3	56	0.000
39	2nd	1.2 mm	Rep3	84	0.000
40	2nd	5 mm	Rep1	56	137.022
41	2nd	5 mm	Rep1	84	147.847
42	2nd	5 mm	Rep1	112	86.253
43	2nd	5 mm	Rep2	56	153.376
44	2nd	5 mm	Rep2	84	132.389

Obs	Experiment	Thickness	Rep	Time	MperA
45	2nd	5 mm	Rep2	112	122.633
46	2nd	5 mm	Rep3	56	144.665
47	2nd	5 mm	Rep3	84	121.352
48	2nd	5 mm	Rep3	112	66.846

Analysis of Covariance for Degradation Rate Coefficients of PHA degraded in 2nd Anaerobic Mass Loss Expt

The Mixed Procedure

Model Information	
Data Set	WORK.ONE
Dependent Variable	MperA
Covariance Structure	Diagonal
Estimation Method	REML
Residual Variance Method	Profile
Fixed Effects SE Method	Model-Based
Degrees of Freedom Method	Residual

Class Level Information		
Class	**Levels**	**Values**
Thickness	4	0.24 mm 1.2 TBC 1.2 mm 5 mm

Dimensions	
Covariance Parameters	1
Columns in X	10
Columns in Z	0

Dimensions	
Subjects	1
Max Obs Per Subject	48

Number of Observations	
Number of Observations Read	48
Number of Observations Used	48
Number of Observations Not Used	0

Covariance Parameter Estimates	
Cov Parm	Estimate
Residual	210.71

Fit Statistics	
-2 Res Log Likelihood	371.1
AIC (smaller is better)	373.1
AICC (smaller is better)	373.2
BIC (smaller is better)	374.8

Solution for Fixed Effects						
Effect	Thickness	Estimate	Standard Error	DF	t Value	Pr > |t|
Intercept		203.26	18.4250	40	11.03	<.0001
Time		-0.9484	0.2116	40	-4.48	<.0001
Thickness	0.24 mm	-190.93	22.9754	40	-8.31	<.0001
Thickness	1.2 TBC	-139.76	19.1303	40	-7.31	<.0001
Thickness	1.2 mm	-132.07	22.4359	40	-5.89	<.0001

Solution for Fixed Effects						
Effect	**Thickness**	**Estimate**	**Standard Error**	**DF**	**t Value**	**Pr > |t|**
Thickness	**5 mm**	0	.	.	.	.
Time*Thickness	**0.24 mm**	0.6293	0.6865	40	0.92	0.3648
Time*Thickness	**1.2 TBC**	0.5640	0.2215	40	2.55	0.0149
Time*Thickness	**1.2 mm**	0.2176	0.2993	40	0.73	0.4715
Time*Thickness	**5 mm**	0	.	.	.	.

Type 1 Tests of Fixed Effects				
Effect	**Num DF**	**Den DF**	**F Value**	**Pr > F**
Time	1	40	1.37	0.2484
Thickness	3	40	132.19	<.0001
Time*Thickness	3	40	2.78	0.0534

Type 3 Tests of Fixed Effects				
Effect	**Num DF**	**Den DF**	**F Value**	**Pr > F**
Time	1	40	10.91	0.0020
Thickness	3	40	23.71	<.0001
Time*Thickness	3	40	2.78	0.0534

Estimates					
Label	**Estimate**	**Standard Error**	**DF**	**t Value**	**Pr > |t|**
compare 0.24 mm vs 1.2 mm	0.4117	0.6865	40	0.60	0.5521
compare 0.24 mm vs 5 mm	0.6293	0.6865	40	0.92	0.3648
compare 0.24 mm vs 1.2 TBC	0.06531	0.6564	40	0.10	0.9212

Estimates					
Label	**Estimate**	**Standard Error**	**DF**	**t Value**	**Pr > |t|**
compare 1.2 mm vs 5 mm	0.2176	0.2993	40	0.73	0.4715
compare 1.2 mm vs 1.2 TBC	-0.3464	0.2215	40	-1.56	0.1257
compare 5 mm vs 1.2 TBC	-0.5640	0.2215	40	-2.55	0.0149

Appendix B – DSC Data and Curves of Bioplastic Degraded in Anaerobic Mass Loss Experiments

First Anaerobic Mass Loss Experiment DSC Data

Time of Degradation	1st Heating				Cooling			2nd Heating			
	1st Peak (°C)	2nd Peak (°C)	T_m (°C)	ΔH_m (J g^{-1})	Peak (°C)	T_c (°C)	ΔH_c (J g^{-1})	1st Peak (°C)	2nd Peak (°C)	T_m (°C)	ΔH_m (J g^{-1})
1.2-mm PHB											
Undegraded	-	176.4	165.6	91.9	96.4	103.3	82.7	168.4	175.6	163.5	98.2
2 weeks	167.5	175.8	167.3	105.4	94.4	101.3	87.6	166.2	175.2	161.5	111.3
4 weeks	167.5	175.9	167.5	102.2	93.4	101.2	83.9	166.3	175.1	161.5	111.5
8 weeks	166.4	174.6	167.4	90.5	83.8	92.0	72.9	163.5	173.1	166.6	113.4
3.5-mm PHB											
Undegraded	-	174.0	168.4	99.2	97.4	103.6	82.4	167.9	175.5	163.6	98.7
2 weeks	-	174.6	168.3	109.1	94.1	101.1	83.5	167.9	175.8	163.1	106.4
4 weeks	-	173.4	168.0	102.8	95.3	102.0	81.7	167.2	175.4	162.9	107.5
8 weeks	169.6	174.6	165.4	109.4	91.0	99.4	82.6	163.9	173.6	167.0	109.7
12 weeks	169.9	174.2	165.1	99.1	90.9	100.6	78.4	164.0	173.6	159.9	107.6
16 weeks	-	173.4	167.1	107.8	95.7	102.9	80.1	166.9	175.0	162.2	107.9
19 weeks	-	173.6	166.8	79.4	88.0	94.7	51.9	158.1	169.9	126.3	75.8

Second Anaerobic Mass Loss Experiment DSC Data

Time of Degradation	1st Heating				Cooling			2nd Heating			
	1st Peak (°C)	2nd Peak (°C)	T_m (°C)	ΔH_m (J g^{-1})	Peak (°C)	T_c (°C)	ΔH_c (J g^{-1})	1st Peak (°C)	2nd Peak (°C)	T_m (°C)	ΔH_m (J g^{-1})
0.24-mm PHB											
Undegraded	-	173.0	167.6	89.9	94.3	102.2	74.3	167.9	175.3	162.9	96.0
5 days	170.7	175.8	165.6	93.7	94.1	100.9	76.1	167.1	174.8	161.7	100.7
10 days	171.2	175.4	165.3	95.6	94.7	102.6	76.5	166.1	174.2	159.8	98.2
15 days	170.4	175.9	164.7	94.0	94.0	100.3	77.1	166.7	174.8	161.6	98.4
3 weeks	170.1	175.8	165.3	95.2	95.7	103.1	78.7	166.9	174.7	161.9	97.1
4 weeks	-	172.9	167.9	95.4	95.1	102.9	76.7	168.0	175.4	163.4	98.0
6 weeks	-	172.7	167.9	100.6	94.5	101.8	79.2	167.3	175.0	162.9	103.2
8 weeks	-	172.7	167.6	80.7	92.9	100.5	63.1	167.7	175.4	163.1	83.7
1.2-mm PHB											
Undegraded	-	176.4	165.6	91.9	96.4	103.3	82.7	168.4	175.6	163.5	98.2
2 weeks	170.3	176.3	163.8	88.5	95.6	101.0	77.6	167.7	175.4	163.1	96.3
4 weeks	171.3	176.1	165.4	90.6	96.2	102.4	76.6	168.4	175.4	163.4	97.0
8 weeks	171.5	176.5	165.4	88.1	94.4	101.7	72.3	168.2	175.7	163.0	91.9
12 weeks	171.4	176.7	165.4	85.2	99.8	105.4	74.6	168.5	175.6	164.3	88.5
16 weeks	171.5	177.1	165.1	90.7	100.5	105.4	72.5	168.9	175.9	164.0	87.8
5-mm PHB											
Undegraded	172.1	180.4	163.5	104.1	95.3	103.3	73.3	166.2	174.8	160.9	92.3
2 weeks	171.6	179.7	163.5	108.5	96.0	103.2	75.0	165.3	174.3	161.0	94.9
4 weeks	171.8	179.9	162.1	117.9	95.3	103.4	79.6	165.7	174.2	160.2	101.2
8 weeks	-	178.9	173.1	115.4	95.7	102.6	77.0	166.2	174.6	161.4	94.7
12 weeks	-	179.9	173.7	110.4	101.1	105.9	74.8	166.4	174.7	160.9	90.5
16 weeks	171.8	181.6	175.6	114.1	100.8	105.4	75.2	166.8	174.9	162.3	90.4
20 weeks	171.8	181.2	174.2	111.7	100.1	107.0	75.0	165.7	174.2	160.4	90.6
32 weeks	168.0	181.0	175.2	115.3	100.6	105.3	76.7	166.5	174.4	161.5	92.7
1.2-mm PHB/ 15% TBC Blend											
Undegraded	161.4	170.4	153.4	81.9	83.9	101.7	59.2	154.1	167.4	144.5	82.2
2 weeks	161.6	171.0	153.7	88.8	78.1	89.6	60.3	154.2	168.2	146.1	87.3
4 weeks	162.7	171.2	155.3	87.1	77.6	87.7	60.9	154.3	168.7	147.8	86.3
8 weeks	162.5	171.6	155.0	90.3	80.1	91.5	58.7	155.4	169.4	149.8	84.7
12 weeks	161.3	170.8	161.9	88.3	87.3	93.2	66.2	154.9	168.6	152.3	88.3
16 weeks	162.5	172.1	163.3	91.8	89.8	96.0	67.8	162.5	172.1	153.5	91.8
20 weeks	162.4	171.7	163.4	91.2	88.0	98.1	63.3	162.4	171.7	153.0	91.2

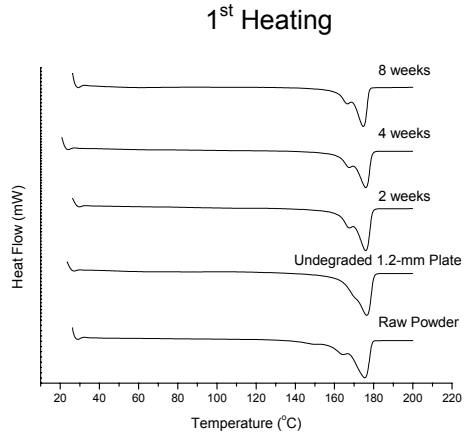

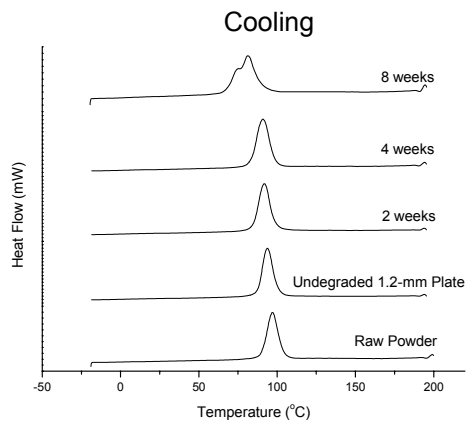

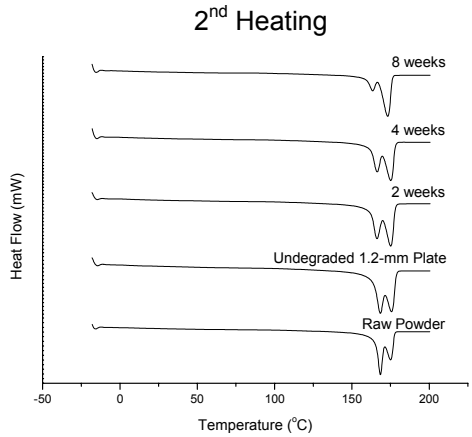

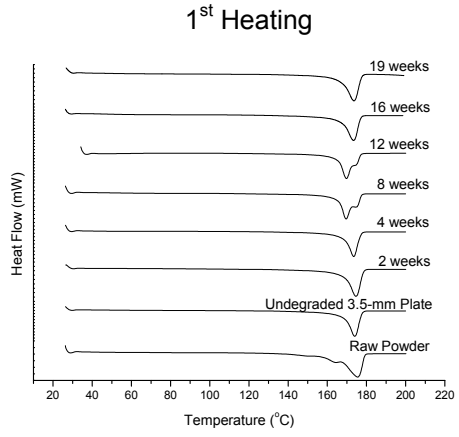

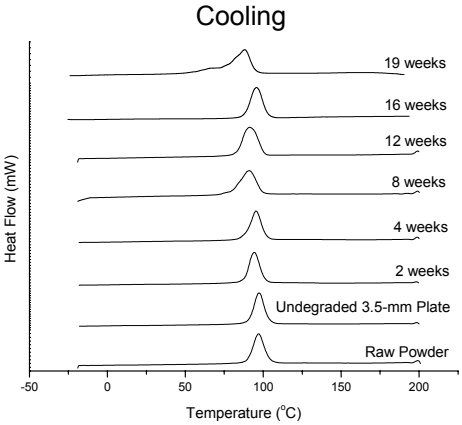

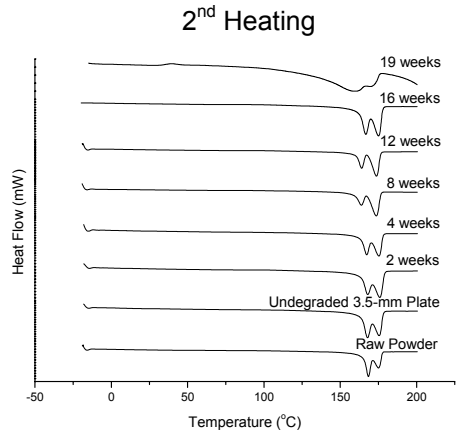

DSC curves for the 1.2-mm melt-pressed PHA plates before and after degradation in the first anaerobic mass loss experiment. Time of degradation is indicated next to the plot. Top graph represents first heating; middle graph is the cooling period; bottom graph illustrates the second heating. The curves for the raw PHA powder are also shown for comparison.

DSC curves for the 3.5-mm melt-pressed PHA plates before and after degradation in the first anaerobic mass loss experiment. Time of degradation is indicated next to the plot. Top graph represents first heating; middle graph is the cooling period; bottom graph illustrates the second heating. The curves for the raw PHA powder are also shown for comparison.

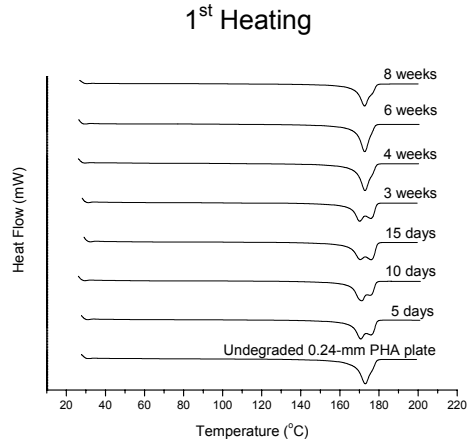

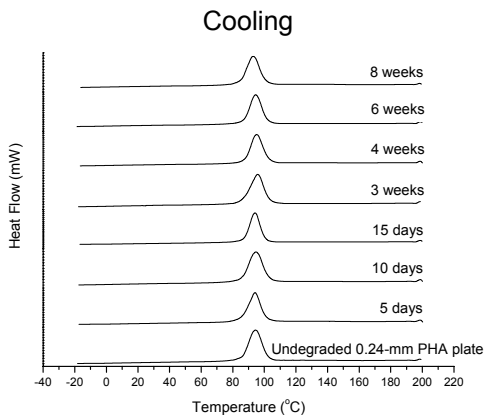

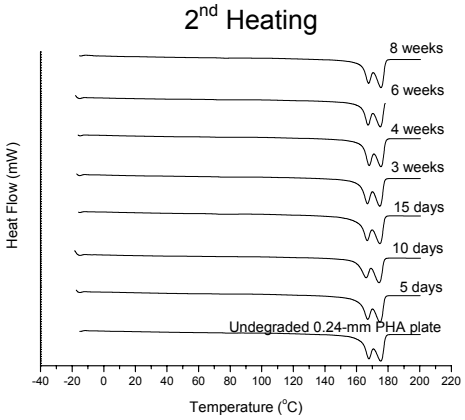

DSC curves for the 0.24-mm melt-pressed PHA plates before and after degradation in the second anaerobic mass loss experiment. Time of degradation is indicated next to the plot. Top graph represents first heating; middle graph is the cooling period; bottom graph illustrates the second heating.

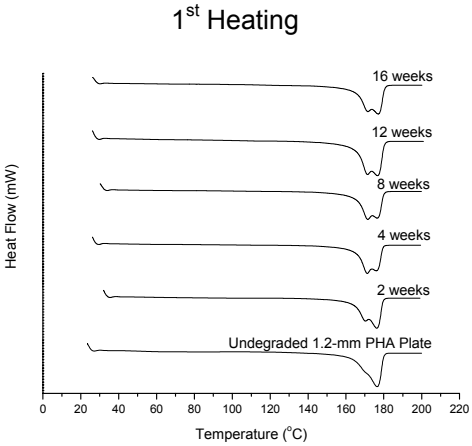

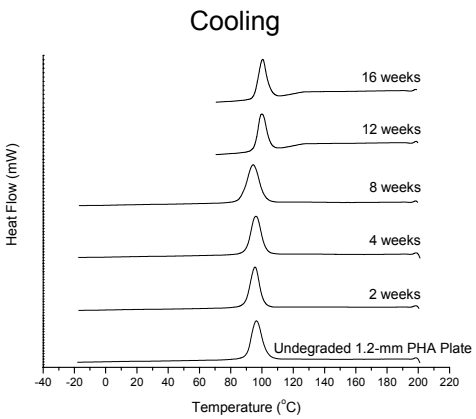

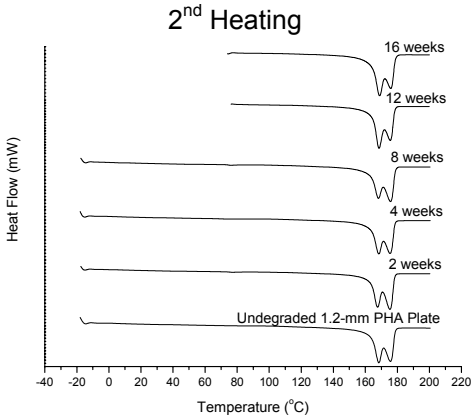

DSC curves for the 1.2-mm melt-pressed PHA plates before and after degradation in the second anaerobic mass loss experiment. Time of degradation is indicated next to the plot. Top graph represents first heating; middle graph is the cooling period; bottom graph illustrates the second heating.

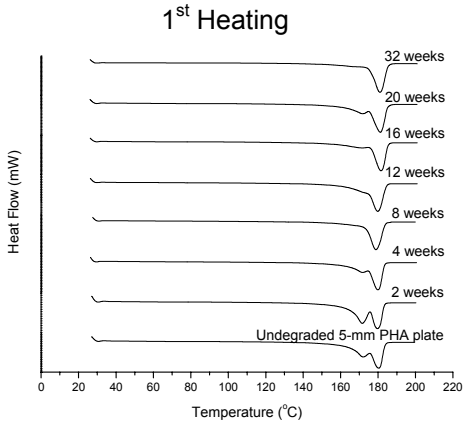

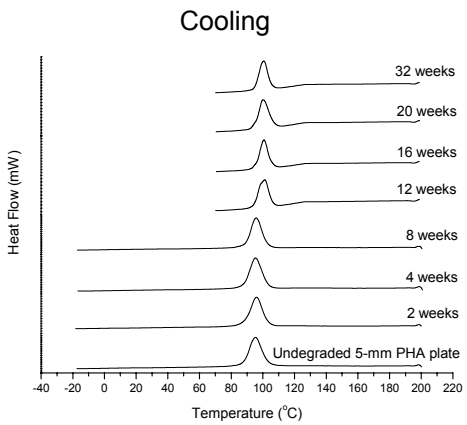

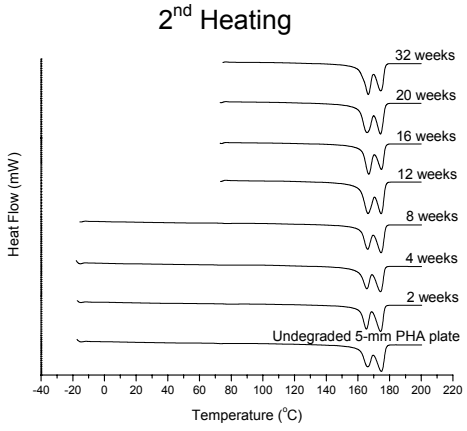

DSC curves for the 5-mm melt-pressed PHA plates before and after degradation in the second anaerobic mass loss experiment. Time of degradation is indicated next to the plot. Top graph represents first heating; middle graph is the cooling period; bottom graph illustrates the second heating.

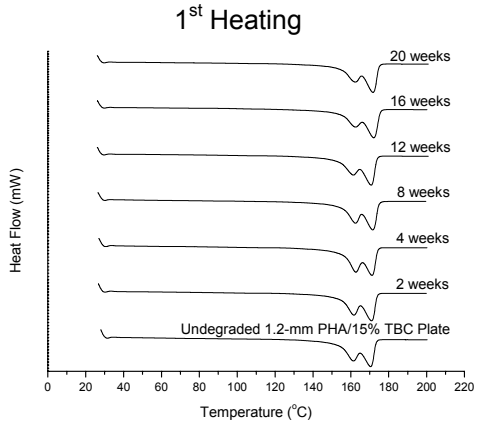

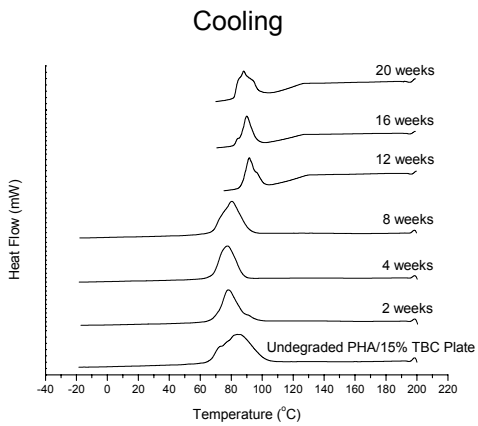

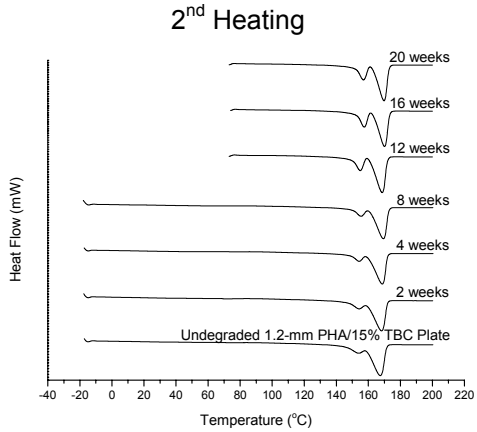

DSC curves for the melt-pressed plates of the PHA/15% TBC blend (1.2-mm plates) before and after degradation in the second anaerobic mass loss experiment. Time of degradation is indicated next to the plot. Top graph represents first heating; middle graph is the cooling period; bottom graph illustrates the second heating.

Appendix C – Raw Data, Calculations, and Statistics of Aerobic Experiments

Schematic of Respirometer Sample Flow during "Chamber Measurement" mode (from Columbus Instruments Micro-Oxymax Operation Manual)

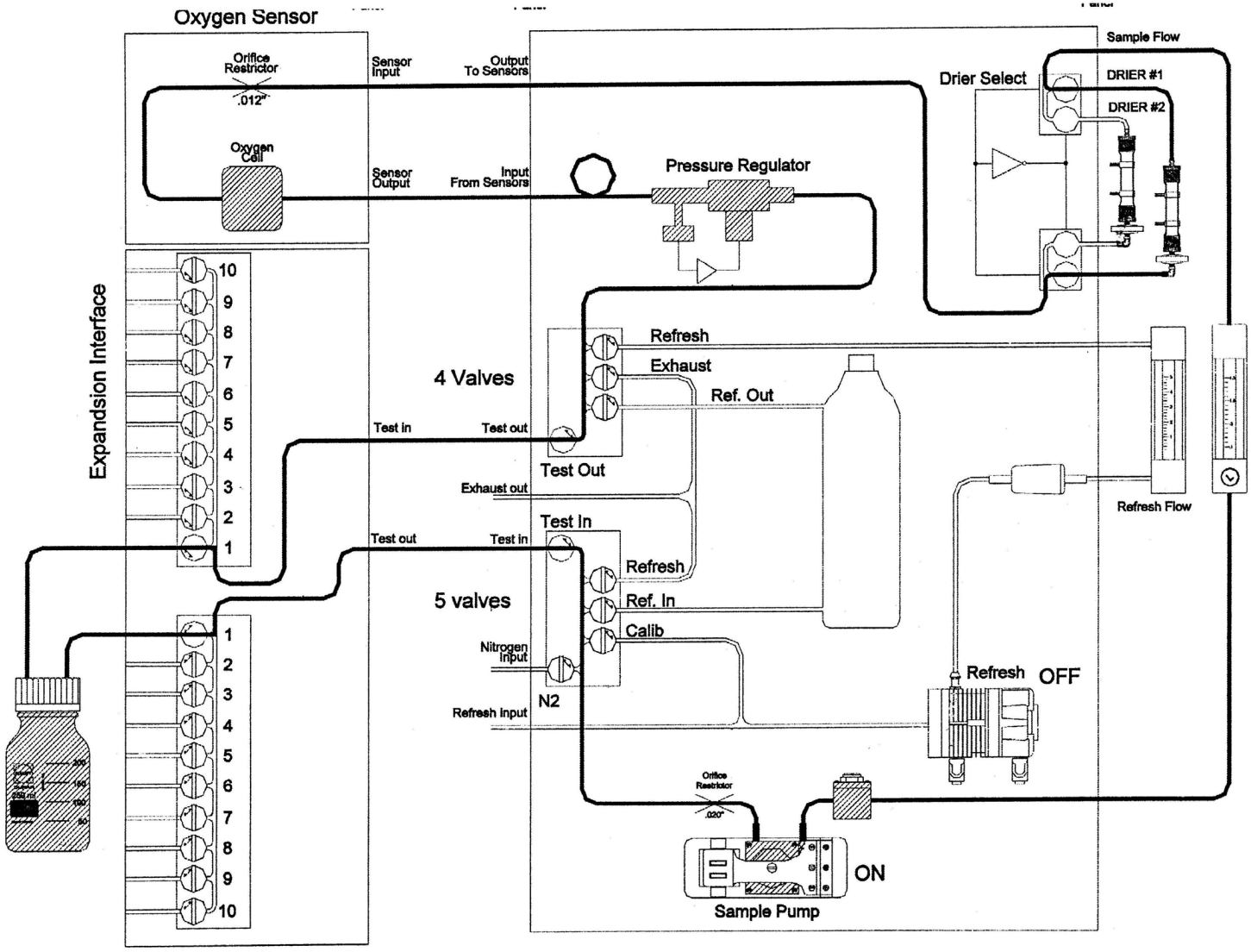

Calculations to determine amount of Compost and PHA plate dimensions needed for 2nd Mass Loss Experiment in order to achieve equal compost to plastic ratio as respirometric experiment

Moisture Content of Compost (Respirometer)	63.10%
Carbon Content of Compost	31.82%
Nitrogen Content of Compost	0.86%
Nitrogen Content of Plastic	0.13%
C:N Ratio of Compost	36.9
C:N Ratio of Compost + Plastic	46.3
Amount of NH4Cl needed for 30:1 ratio (g)	1.5668

STRIPS FOR Respirometer

Strip Dimensions and properties

Length (cm)	1.602081979	Density (g/cm^3)	1.2064365
Width (cm)	1.602081979		
Thickness (cm)	0.12	Surface area (cm^2)	5.9023327
Volume (cm^3)	0.308	per strip	
Mass (g)	0.372	Ratio (mass:SA)	0.0629552

Carbon Content of Plastic	54.5%
Mass of Carbon needed in form of Plastic per vial (g)	7.038675
Total Mass of Plastic per Chamber (g)	12.915
Carbon Content of Compost in form of Plastic (g/g)	0.03
# Strips needed per Chamber	34.76
# Strips needed	104.2703
Wet Mass of Compost per Chamber (g)	210
Total Wet Mass of Compost for Respirometer (g)	2100
Dry Mass of Compost per Chamber (g)	77.49
Total Dry Mass of Compost for Respirometer (g)	774.9

PLATES FOR ADDITIONAL ANALYSES

Moisture Content of Compost for Mass Loss Study 65.8%

0.24-mm Plate Dimensions and properties

Length (cm)	2.533114026		
Thickness (cm)	0.024	Surface area (cm^2)	13.076512
Volume (cm^3)	0.154		
Mass (g)	0.1858	Ratio (mass:SA)	0.014208

Mass of Dry Compost needed per flask (g)		3.34		
Mass of Wet Compost needed per flask (g)		9.78		
# plates per flask		3		
# 0.24-mm plates needed		81		
Total Dry mass of compost for 0.24-mm plates (g)		90		
Total Wet mass of compost for 0.24-mm plates (g)		245		
1.2-mm Strip Dimensions and properties				
Length (cm)	1.602081979			
Thickness (cm)	0.12		Surface area (cm^2)	5.9023327
Volume (cm^3)	0.308			
Mass (g)	0.37		Ratio (mass:SA)	0.0629552
Mass of Dry Compost needed per flask (mL)		4.46		
Mass of Wet Compost needed per flask (g)		13.04		
# plates per flask		2		
# 1.2-mm plates needed		54		
Total Dry Mass of compost for 1.2-mm plates (g)		120		
Total Wet mass of compost for 1.2-mm plates (g)		326		
5-mm Plate Dimensions and properties				
Length (cm)	1.109954954			
Thickness (cm)	0.5		Surface area (cm^2)	4.6839099
Volume (cm^3)	0.616			
Mass (g)	0.7432		Ratio (mass:SA)	0.1586634
Mass of Dry Compost needed per flask (mL)		8.92		
Mass of Wet Compost needed per flask (g)		26.08		
# plates needed per flask		2		
# 5-mm plates needed		54		
Total Mass of compost for 5-mm plates (g)		241		
Total Wet mass of compost for 5-mm plates (g)		653		
1.2-mm PHA + 15% TBC Strip Dimensions and properties				
Length (cm)	1.8			
Width (cm)	1.4			
Thickness (cm)	0.12		Surface area (cm^2)	5.808
Volume (cm^3)	0.3024			
Mass (g)	0.36		Ratio (mass:SA)	0.0628145
Mass of Dry Compost needed per flask (g)		4.38		
Mass of Wet Compost needed per flask (g)		12.80		
# plates per flask		2		

# 1.2-mm plates needed	54	
Total Mass of compost for 1.2-mm plates (g)	118	
Total Dry Mass of Compost needed per mass loss flask ……..		21.10
Total Wet Mass of Compost needed per mass loss flask ……..		61.69
Amount of NH4Cl to add to each mass loss flask		0.4266

First Mass Loss Experiment

0.5-mm PHA Plates

Time of Degradation	2 weeks		4 weeks		6 weeks		12 weeks		18 weeks		26 weeks	
	Before	After	Before	After	Before	After	Before	After	Before	After	Before	After
Observed Mass (g)	0.3785	0.3785	0.4204	0.4164	0.4346	0.4135	0.3902	0.3255	0.4142	0.2808	0.3857	0.0000
	0.4028	0.4026	0.4155	0.3995	0.3891	0.3620	0.3975	0.3488	0.4049	0.2513	0.3717	0.0000
	0.3826	0.3821	0.4098	0.3910	0.4017	0.4004	0.3761	0.2954	0.4037	0.1919	0.3848	0.0000
Total Weight (g)	1.1639	1.1632	1.2457	1.2069	1.2254	1.1759	1.16383	0.9697	1.2228	0.724	1.1422	0
Mass Loss (g)	0.0007		0.0388		0.0495		0.19413		0.4988		1.1422	
Mass Loss/Surface Area (g/cm^2)	0.0000		0.0010		0.0013		0.0050		0.0128		0.0293	
Rate of Mass Loss (g/Day)	0.0000		0.0014		0.0012		0.0023		0.0040		0.0063	
Percentage of Mass Loss	0.06%		3.11%		4.04%		16.68%		40.79%		100.00%	

1.2-mm PHA Plates

Time of Degradation	2 weeks		4 weeks		6 weeks		12 weeks		18 weeks		26 weeks	
	Before	After	Before	After	Before	After	Before	After	Before	After	Before	After
Observed Mass (g)	1.2276	1.2272	1.2730	1.2690	1.2247	1.1698	1.2089	1.1164	1.3028	0.8045	1.1874	0.0000
Mass Loss (g)	0.0004		0.004		0.0549		0.0925		0.4983		1.1874	
Mass Loss/Surface Area (g/cm^2)	0.0000		0.0002		0.0024		0.0040		0.0216		0.0515	
Rate of Mass Loss (g/Day)	0.0000		0.0001		0.0013		0.0011		0.0040		0.0065	
Percentage of Mass Loss	0.03%		0.31%		4.48%		7.65%		38.25%		100.00%	

3.5-mm PHA Plates

Time of Degradation	2 weeks		4 weeks		6 weeks		12 weeks		18 weeks		26 weeks		50 weeks	
	Before	After	Before	After	Before	After	Before	After	Before	After	Before	After	Before	After
	3.3875	3.3866	3.6016	3.5686	3.3339	3.2719	3.4002	3.3175	3.2612	2.8537	3.3352	1.5203	3.3904	0.9173
	3.4957	3.4959	3.2258	3.2155	3.3433	3.2995	3.4565	3.3704	3.2853	3.0427	3.2546	0.8922	3.2900	-
Observed Mass (g)	3.1110	3.1116	3.1236	3.0948	3.2845	3.2800	3.5170	3.4550	3.2730	3.0002	3.2727	1.3072	3.2806	-
	3.2203	3.2209	3.4478	3.4444	3.1959	3.1795	3.1543	3.1010	3.3685	3.0497	3.2371	0.8379	3.1160	-
	3.5257	3.5216	3.3313	3.3273	3.6314	3.6014	3.3586	3.2887	3.2674	2.9274	3.6377	0.8315	3.2538	-
Total Weight (g)	16.7402	16.7366	16.7301	16.6506	16.789	16.6323	16.8866	16.5326	16.4554	14.8737	16.7373	5.3891	16.3308	0.9173
Mass Loss (g)	0.0036		0.0795		0.1567		0.354		1.5817		11.3482		15.4135	
Mass Loss/Surface Area (g/cm^2)	0.0000		0.0007		0.0014		0.0033		0.0146		0.1050		0.1426	
Rate of Mass Loss (g/Day)	0.0003		0.0028		0.0037		0.0042		0.0126		0.0624		0.0440	
Percentage of Mass Loss	0.02%		0.48%		0.93%		2.10%		9.61%		67.80%		94.38%	

Curves for Calculation of Degradation Rate Coefficients

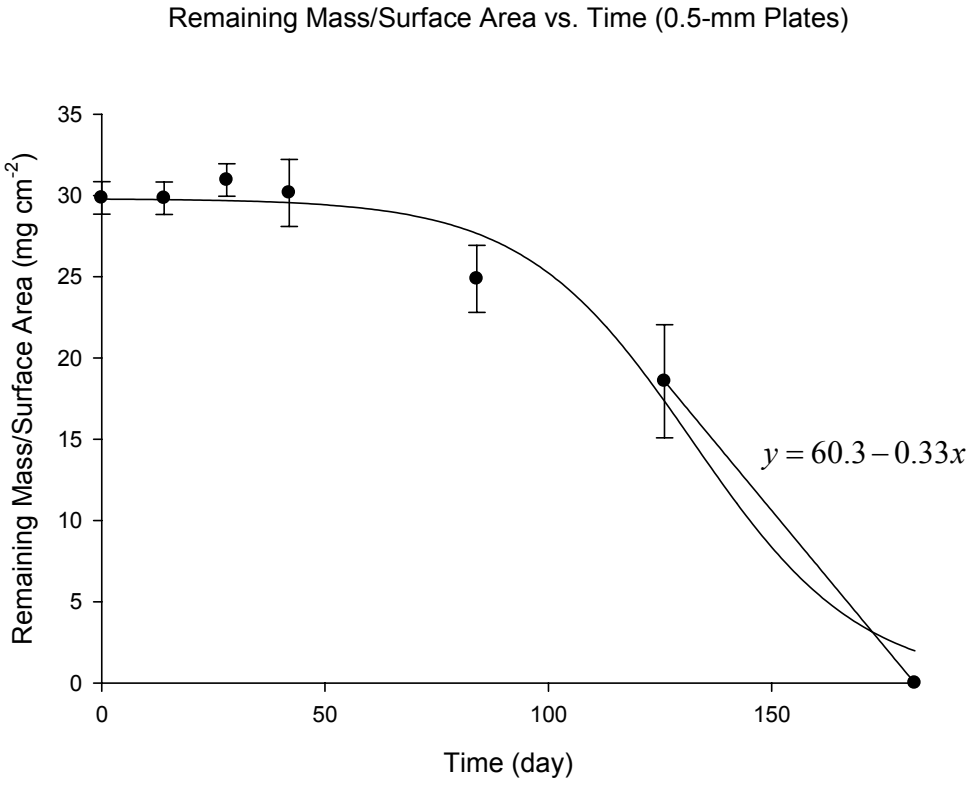

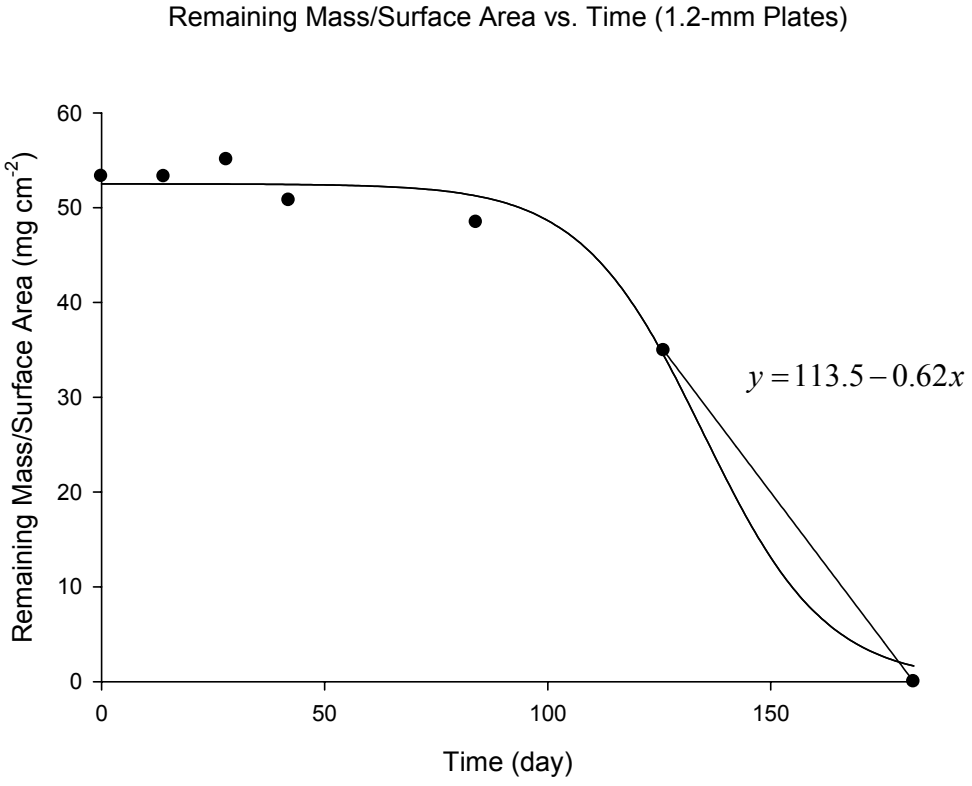

Remaining Mass/Surface Area vs. Time (3.5-mm Plates)

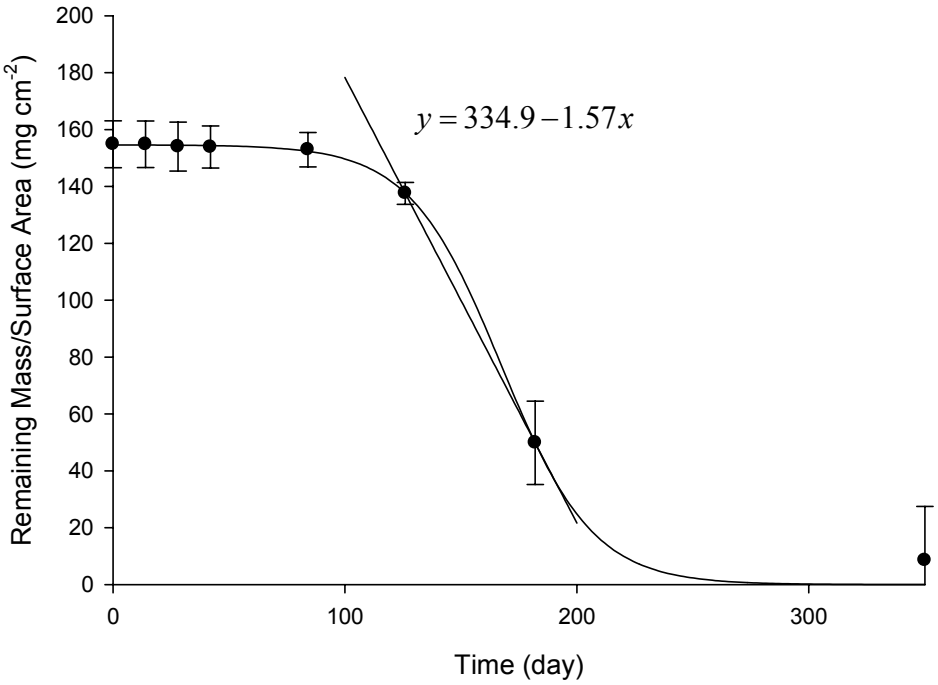

Analysis of Covariance for Degradation Rate Coefficients of PHA degraded in 1st Aerobic Mass Loss Expt

Obs	Experiment	Thickness	Rep	Time	MperA
1	1st	0.5 mm	Rep1	126	21.600
2	1st	0.5 mm	Rep1	182	0.000
3	1st	0.5 mm	Rep2	126	19.331
4	1st	0.5 mm	Rep2	182	0.000
5	1st	0.5 mm	Rep3	126	14.762
6	1st	0.5 mm	Rep3	182	0.000
7	1st	1.2 mm	Rep1	126	34.918
8	1st	1.2 mm	Rep2	182	0.000
9	1st	3.5 mm	Rep1	126	131.963

Obs	Experiment	Thickness	Rep	Time	MperA
10	1st	3.5 mm	Rep1	182	70.303
11	1st	3.5 mm	Rep2	126	140.703
12	1st	3.5 mm	Rep2	182	41.258
13	1st	3.5 mm	Rep3	126	138.738
14	1st	3.5 mm	Rep3	182	60.449
15	1st	3.5 mm	Rep4	126	141.027
16	1st	3.5 mm	Rep4	182	38.747
17	1st	3.5 mm	Rep5	126	135.371
18	1st	3.5 mm	Rep5	182	38.451

Analysis of Covariance for Degradation Rate Coefficients of PHA degraded in 1st Aerobic Mass Loss Expt

The Mixed Procedure

Model Information	
Data Set	WORK.ONE
Dependent Variable	MperA
Covariance Structure	Diagonal
Estimation Method	REML
Residual Variance Method	Profile
Fixed Effects SE Method	Model-Based
Degrees of Freedom Method	Residual

Class Level Information		
Class	**Levels**	**Values**

Class Level Information		
Class	Levels	Values
Thickness	3	0.5 mm 1.2 mm 3.5 mm

Dimensions	
Covariance Parameters	1
Columns in X	8
Columns in Z	0
Subjects	1
Max Obs Per Subject	18

Number of Observations	
Number of Observations Read	18
Number of Observations Used	18
Number of Observations Not Used	0

Covariance Parameter Estimates	
Cov Parm	Estimate
Residual	78.4466

Fit Statistics	
-2 Res Log Likelihood	116.0
AIC (smaller is better)	118.0
AICC (smaller is better)	118.4
BIC (smaller is better)	118.5

Solution for Fixed Effects						
Effect	**Thickness**	**Estimate**	**Standard Error**	**DF**	**t Value**	**Pr > |t|**
Intercept		334.93	15.6571	12	21.39	<.0001
Time		-1.5664	0.1000	12	-15.66	<.0001
Thickness	**0.5 mm**	-274.59	25.5680	12	-10.74	<.0001
Thickness	**1.2 mm**	-221.45	38.3520	12	-5.77	<.0001
Thickness	**3.5 mm**	0	.	.	.	.
Time*Thickness	**0.5 mm**	1.2349	0.1633	12	7.56	<.0001
Time*Thickness	**1.2 mm**	0.9429	0.2450	12	3.85	0.0023
Time*Thickness	**3.5 mm**	0	.	.	.	.

Type 1 Tests of Fixed Effects				
Effect	**Num DF**	**Den DF**	**F Value**	**Pr > F**
Time	1	12	198.34	<.0001
Thickness	2	12	192.86	<.0001
Time*Thickness	2	12	30.62	<.0001

Type 3 Tests of Fixed Effects				
Effect	**Num DF**	**Den DF**	**F Value**	**Pr > F**
Time	1	12	82.88	<.0001
Thickness	2	12	62.76	<.0001
Time*Thickness	2	12	30.62	<.0001

Estimates					
Label	**Estimate**	**Standard Error**	**DF**	**t Value**	**Pr > |t|**

Estimates					
Label	**Estimate**	**Standard Error**	**DF**	**t Value**	**Pr > |t|**
compare 0.5 mm vs 1.2 mm	0.2920	0.2583	12	1.13	0.2803
compare 0.5 mm vs 3.5 mm	1.2349	0.1633	12	7.56	<.0001
compare 1.2 mm vs 3.5 mm	0.9429	0.2450	12	3.85	0.0023

Second Mass Loss Experiment

0.24-mm PHA Plates

Time of Degradation		3 weeks		6 weeks		9 weeks		12 weeks		16 weeks		20 weeks		30 weeks	
		Before	After	Before	After	Before	After	Before	After	Before	After	Before	After	Before	After
Observed Mass (g)	Replicate 1	0.4979	0.4395	0.4640	0.1910	0.4716	0.2529	0.4987	0.0000	0.4910	0.0163	~~0.4859~~	~~0.1447~~	0.4966	0.0000
	Replicate 2	0.4907	0.2395	0.5060	0.4612	0.4643	0.0000	0.5050	0.0645	0.4954	0.0000	0.4891	0.0000	0.5201	0.0000
	Replicate 3	0.5032	0.2913	0.5078	0.4019	0.4589	0.0000	0.4849	0.0000	0.4923	0.0000	0.4865	0.0000	~~0.4665~~	~~0.1304~~
Total Weight (g)		1.4918	0.9703	1.4778	1.0541	1.3948	0.2529	1.4886	0.0645	1.4787	0.0163	0.9756	0.0000	1.0167	0.0000
Mass Loss (g)		0.5215		0.4237		1.1419		1.4241		1.4624		0.9756		1.0167	
Mass Loss/Surface Area (g/cm^2)		0.0044		0.0036		0.0097		0.0121		0.0124		0.0124		0.0130	
Rate of Mass Loss (g/Day)		0.0248		0.0101		0.0181		0.0170		0.0131		0.0070		0.0048	
Percentage of Mass Loss		34.96%		28.67%		81.87%		95.67%		98.90%		100.00%		100.00%	

1.2-mm PHA Plates

Time of Degradation		3 weeks		6 weeks		9 weeks		12 weeks		16 weeks		20 weeks		30 weeks	
		Before	After	Before	After	Before	After	Before	After	Before	After	Before	After	Before	After
Observed Mass (g)	Replicate 1	0.7452	0.6600	0.7753	0.4167	0.7494	0.4602	0.7195	0.0000	0.7434	0.0000	~~0.7684~~	~~0.0307~~	0.7629	0.0000
	Replicate 2	0.7323	0.5789	0.7781	0.6714	0.7380	0.1990	0.7465	0.0374	0.7330	0.0000	0.7406	0.0000	0.7621	0.0000
	Replicate 3	0.7380	0.6064	0.7853	0.5084	0.7145	0.0831	0.7320	0.0000	0.7511	0.0000	0.7691	0.0000	~~0.7157~~	~~0.0830~~
Total Weight (g)		2.2155	1.8453	2.3387	1.5965	2.2019	0.7423	2.1980	0.0374	2.2275	0.0000	1.5097	0.0000	1.5250	0.0000
Mass Loss (g)		0.3702		0.7422		1.4596		2.1606		2.2275		1.5097		1.525	
Mass Loss/Surface Area (g/cm^2)		0.0105		0.0210		0.0412		0.0610		0.0629		0.0639		0.0646	
Rate of Mass Loss (g/Day)		0.0176		0.0177		0.0232		0.0257		0.0199		0.0108		0.0073	
Percentage of Mass Loss		16.71%		31.74%		66.29%		98.30%		100.00%		100.00%		100.00%	

5-mm PHA Plates

Time of Degradation		3 weeks		6 weeks		9 weeks		12 weeks		16 weeks		20 weeks		30 weeks	
		Before	**After**	**Before**	**After**	**Before**	**After**	**Before**	**After**	**Before**	**After**	**Before**	**After**	**Before**	**After**
Observed Mass (g)	Replicate 1	1.8535	1.8018	1.6918	1.5795	1.6669	1.5504	1.7051	1.0853	1.6505	1.1578	~~1.7226~~	~~1.3085~~	1.6489	1.0588
	Replicate 2	1.7821	1.7028	1.6724	1.6500	1.7365	1.4212	1.6667	1.3814	1.7069	1.0624	1.7318	0.9871	1.6325	0.7404
	Replicate 3	1.6732	1.5936	1.7649	1.6849	1.6708	1.2688	1.7121	1.1400	1.6788	1.0516	1.6366	1.1382	~~1.6807~~	~~1.4810~~
Total Weight (g)		5.3088	5.0982	5.1291	4.9144	5.0742	4.2404	5.0839	3.6067	5.0362	3.2718	3.3684	2.1253	3.2814	1.7992
Mass Loss (g)		0.2106		0.2147		0.8338		1.4772		1.7644		1.2431		1.4822	
Mass Loss/Surface Area (g/cm^2)		0.0075		0.0076		0.0297		0.0526		0.0628		0.0663		0.0791	
Rate of Mass Loss (g/Day)		0.0100		0.0051		0.0132		0.0176		0.0158		0.0089		0.0071	
Percentage of Mass Loss		3.97%		4.19%		16.43%		29.06%		35.03%		36.90%		45.17%	

1.2-mm PHA/15% TBC Blend Plates

Time of Degradation		3 weeks		6 weeks		9 weeks		12 weeks		16 weeks		20 weeks		30 weeks	
		Before	**After**	**Before**	**After**	**Before**	**After**	**Before**	**After**	**Before**	**After**	**Before**	**After**	**Before**	**After**
Observed Mass (g)	Replicate 1	0.6696	0.6584	0.7032	0.6777	0.7247	0.6843	0.6838	0.6105	0.6953	0.6575	~~0.6558~~	~~0.6133~~	0.6958	0.5885
	Replicate 2	0.7217	0.6923	0.7100	0.6884	0.6788	0.6460	0.6760	0.6382	0.7030	0.4806	0.7264	0.6860	0.6883	0.6036
	Replicate 3	0.6963	0.6728	0.6818	0.6614	0.7195	0.6799	0.6779	0.6278	0.6731	0.6281	0.6862	0.6304	~~0.7255~~	~~N/A~~
Total Weight (g)		2.0876	2.0235	2.0950	2.0275	2.1230	2.0102	2.0377	1.8765	2.0714	1.7662	1.4126	1.3164	1.3841	1.1921
Mass Loss (g)		0.06407		0.0675		0.1128		0.1612		0.3052		0.0962		0.192	
Mass Loss/Surface Area (g/cm^2)		0.0018		0.0019		0.0032		0.0046		0.0088		0.0041		0.0083	
Rate of Mass Loss (g/Day)		0.0031		0.0016		0.0018		0.0019		0.0027		0.0007		0.0009	
Percentage of Mass Loss		3.07%		3.22%		5.31%		7.91%		~~14.73%~~		~~6.81%~~		13.87%	

Curves for Calculation of Degradation Rate Coefficients

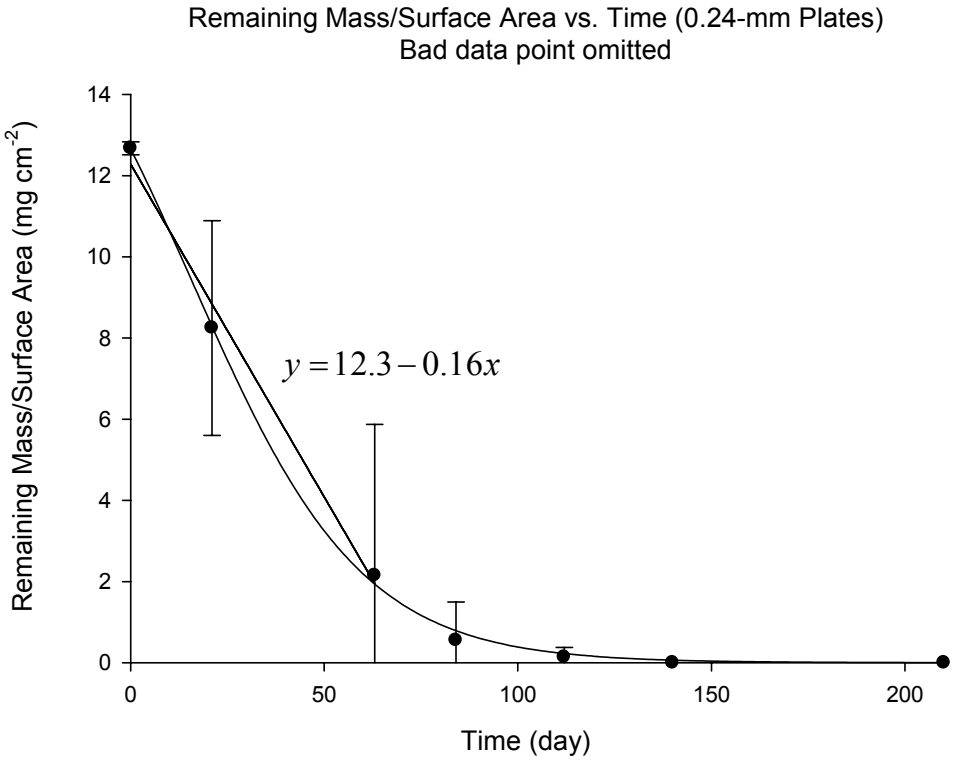

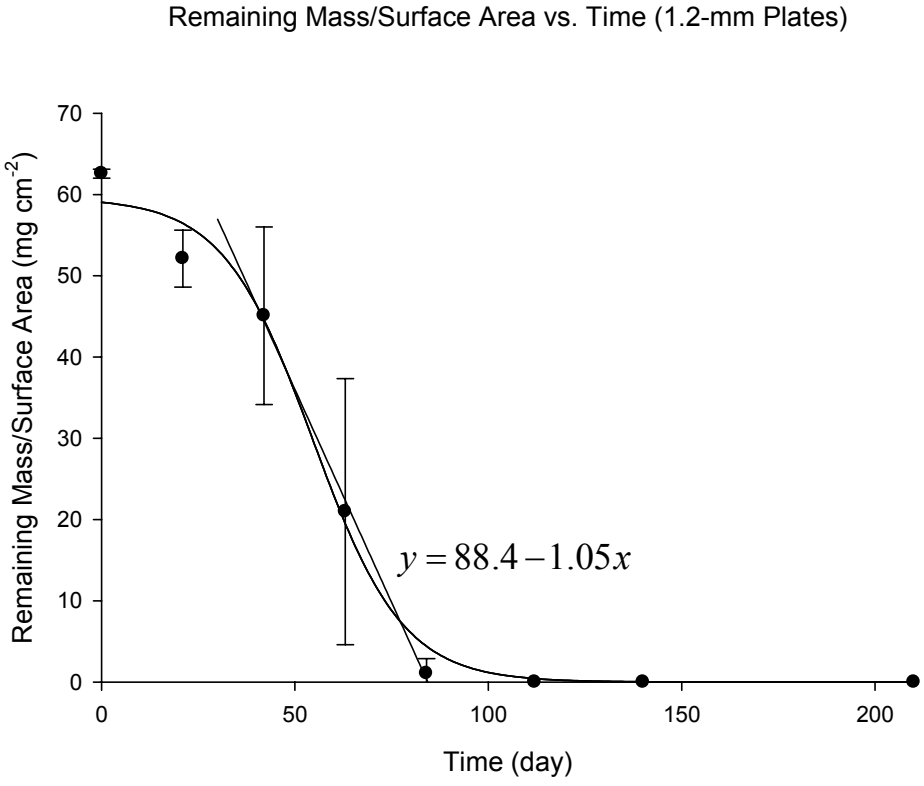

Remaining Mass/Surface Area vs. Time (5-mm Plates)

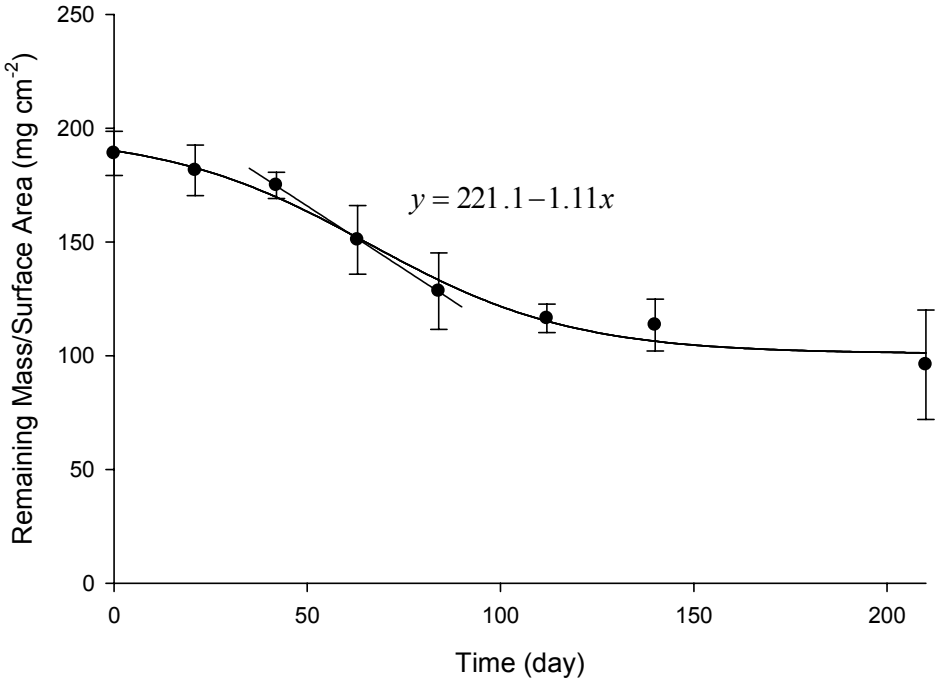

Remaining Mass/Surface Area vs. Time (1.2-mm TBC Blend Plates)
Bad points omitted

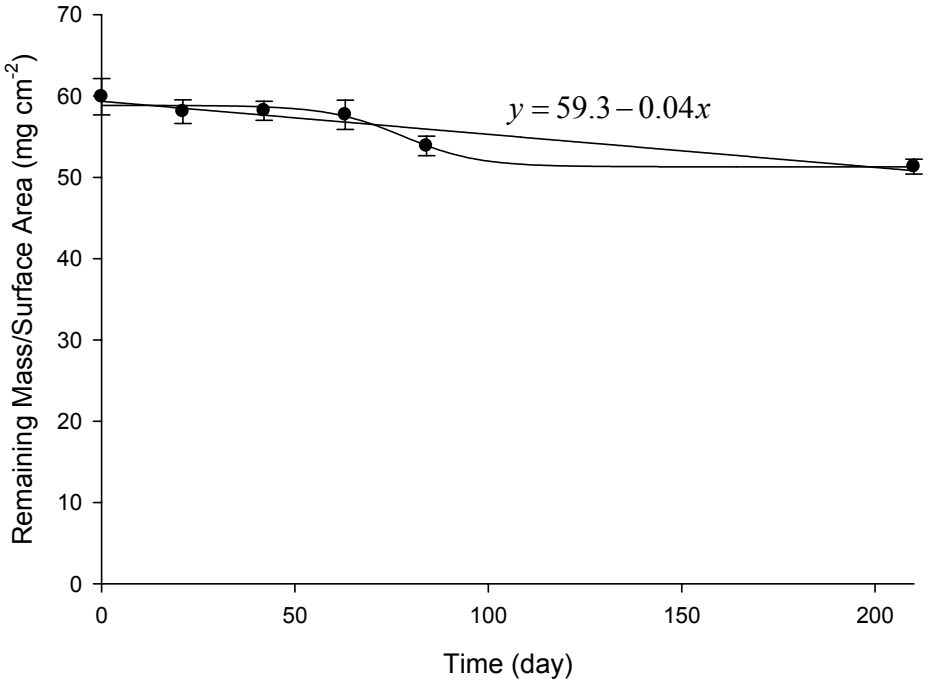

Analysis of Covariance for Degradation Rate Coefficients of PHA degraded in 2nd Aerobic Mass Loss Expt

Obs	Experiment	Thickness	Rep	Time	MperA
1	2nd	0.24 mm	Rep1	0	12.692
2	2nd	0.24 mm	Rep1	21	11.203
3	2nd	0.24 mm	Rep1	63	6.447
4	2nd	0.24 mm	Rep2	0	12.508
5	2nd	0.24 mm	Rep2	21	6.105
6	2nd	0.24 mm	Rep2	63	0.000
7	2nd	0.24 mm	Rep3	0	12.827
8	2nd	0.24 mm	Rep3	21	7.426
9	2nd	0.24 mm	Rep3	63	0.000
10	2nd	1.2 TBC	Rep1	0	57.645
11	2nd	1.2 TBC	Rep1	21	56.683
12	2nd	1.2 TBC	Rep1	42	58.342
13	2nd	1.2 TBC	Rep1	63	58.910
14	2nd	1.2 TBC	Rep1	84	52.557
15	2nd	1.2 TBC	Rep1	210	50.663
16	2nd	1.2 TBC	Rep2	0	62.130
17	2nd	1.2 TBC	Rep2	21	59.599
18	2nd	1.2 TBC	Rep2	42	59.263
19	2nd	1.2 TBC	Rep2	63	55.613
20	2nd	1.2 TBC	Rep2	84	54.941
21	2nd	1.2 TBC	Rep2	210	51.963

Obs	Experiment	Thickness	Rep	Time	MperA
22	2nd	1.2 TBC	Rep3	0	59.943
23	2nd	1.2 TBC	Rep3	21	57.920
24	2nd	1.2 TBC	Rep3	42	56.939
25	2nd	1.2 TBC	Rep3	63	58.531
26	2nd	1.2 TBC	Rep3	84	54.046
27	2nd	1.2 mm	Rep1	42	35.300
28	2nd	1.2 mm	Rep1	63	38.985
29	2nd	1.2 mm	Rep1	84	0.000
30	2nd	1.2 mm	Rep2	42	56.876
31	2nd	1.2 mm	Rep2	63	16.858
32	2nd	1.2 mm	Rep2	84	3.168
33	2nd	1.2 mm	Rep3	42	43.068
34	2nd	1.2 mm	Rep3	63	7.040
35	2nd	1.2 mm	Rep3	84	0.000
36	2nd	5 mm	Rep1	42	168.609
37	2nd	5 mm	Rep1	63	165.503
38	2nd	5 mm	Rep1	84	115.854
39	2nd	5 mm	Rep2	42	176.135
40	2nd	5 mm	Rep2	63	151.711
41	2nd	5 mm	Rep2	84	147.462
42	2nd	5 mm	Rep3	42	179.860
43	2nd	5 mm	Rep3	63	135.442
44	2nd	5 mm	Rep3	84	121.693

Analysis of Covariance for Degradation Rate Coefficients of PHA degraded in 2nd Aerobic Mass Loss Expt

The Mixed Procedure

Model Information	
Data Set	WORK.ONE
Dependent Variable	MperA
Covariance Structure	Diagonal
Estimation Method	REML
Residual Variance Method	Profile
Fixed Effects SE Method	Model-Based
Degrees of Freedom Method	Residual

Class Level Information		
Class	**Levels**	**Values**
Thickness	4	0.24 mm 1.2 TBC 1.2 mm 5 mm

Dimensions	
Covariance Parameters	1
Columns in X	10
Columns in Z	0
Subjects	1
Max Obs Per Subject	44

Number of Observations	
Number of Observations Read	44

Number of Observations	
Number of Observations Used	44
Number of Observations Not Used	0

Covariance Parameter Estimates	
Cov Parm	Estimate
Residual	54.5609

Fit Statistics	
-2 Res Log Likelihood	291.1
AIC (smaller is better)	293.1
AICC (smaller is better)	293.2
BIC (smaller is better)	294.7

Solution for Fixed Effects						
Effect	Thickness	Estimate	Standard Error	DF	t Value	Pr > |t|
Intercept		221.16	9.3757	36	23.59	<.0001
Time		-1.1079	0.1436	36	-7.72	<.0001
Thickness	0.24 mm	-208.88	10.0446	36	-20.80	<.0001
Thickness	1.2 TBC	-161.78	9.7167	36	-16.65	<.0001
Thickness	1.2 mm	-132.76	13.2592	36	-10.01	<.0001
Thickness	5 mm	0	.	.	.	.
Time*Thickness	0.24 mm	0.9439	0.1716	36	5.50	<.0001
Time*Thickness	1.2 TBC	1.0661	0.1466	36	7.27	<.0001
Time*Thickness	1.2 mm	0.05968	0.2031	36	0.29	0.7705

Solution for Fixed Effects						
Effect	Thickness	Estimate	Standard Error	DF	t Value	Pr > |t|
Time*Thickness	5 mm	0	.	.	.	.

Type 1 Tests of Fixed Effects				
Effect	Num DF	Den DF	F Value	Pr > F
Time	1	36	10.45	0.0026
Thickness	3	36	691.81	<.0001
Time*Thickness	3	36	32.12	<.0001

Type 3 Tests of Fixed Effects				
Effect	Num DF	Den DF	F Value	Pr > F
Time	1	36	109.50	<.0001
Thickness	3	36	156.58	<.0001
Time*Thickness	3	36	32.12	<.0001

Estimates					
Label	Estimate	Standard Error	DF	t Value	Pr > |t|
compare 0.24 mm vs 1.2 mm	0.8843	0.1716	36	5.15	<.0001
compare 0.24 mm vs 5 mm	0.9439	0.1716	36	5.50	<.0001
compare 0.24 mm vs 1.2 TBC	-0.1222	0.09850	36	-1.24	0.2228
compare 1.2 mm vs 5 mm	0.05968	0.2031	36	0.29	0.7705
compare 1.2 mm vs 1.2 TBC	-1.0064	0.1466	36	-6.87	<.0001
compare 5 mm vs 1.2 TBC	-1.0661	0.1466	36	-7.27	<.0001

Appendix D – DSC Data and Curves of Bioplastic Degraded in Aerobic Mass Loss Experiments

DSC Results for first aerobic mass loss experiment

Time of Degradation	1st Heating				Cooling			2nd Heating			
	1st Peak (°C)	2nd Peak (°C)	T_m (°C)	ΔH_m (J g^{-1})	Peak (°C)	T_c (°C)	ΔH_c (J g^{-1})	1st Peak (°C)	2nd Peak (°C)	T_m (°C)	ΔH_m (J g^{-1})
1.2-mm PHB											
Undegraded	-	176.4	165.6	91.9	96.4	103.3	82.7	168.4	175.6	163.5	98.2
2 weeks	168.5	176.1	167.3	93.8	95.5	102.1	79.5	166.5	175.0	162.3	96.1
4 weeks	168.0	175.5	167.6	91.4	94.8	103.1	75.1	166.0	174.6	161.9	93.0
6 weeks	167.8	175.5	167.3	92.0	94.7	102.1	73.7	165.6	174.6	161.6	93.8
12 weeks	167.7	175.4	167.3	90.8	94.9	101.4	76.6	166.7	174.7	161.7	93.9
18 weeks	-	175.7	166.4	91.7	94.1	101.2	76.5	166.1	174.9	162.0	94.6
3.5-mm PHB											
Undegraded	-	174.0	168.4	99.2	97.4	103.6	82.4	167.9	175.5	163.6	98.7
2 Weeks	-	173.1	167.4	87.6	95.0	102.5	69.1	167.5	175.5	162.3	86.5
4 Weeks	-	172.8	167.7	103.1	94.9	102.1	79.2	166.4	174.7	161.9	99.5
6 weeks	171.7	175.3	165.1	96.4	96.8	102.7	79.0	166.6	174.7	162.3	98.8
12 weeks	-	173.9	168.3	100.1	94.7	102.3	73.4	166.7	174.7	161.7	93.9
18 weeks	-	172.4	167.1	96.5	94.8	102.3	74.0	166.1	174.8	161.7	91.4
26 weeks	-	173.4	164.5	92.2	100.0	105.9	70.8	166.3	174.7	161.6	85.4
50 weeks	-	173.7	165.5	108.8	100.2	105.1	76.5	165.1	174.1	161.2	93.1

DSC Results for second aerobic mass loss experiment

Time of Degradation	1st Heating				Cooling			2nd Heating			
	1st Peak (°C)	2nd Peak (°C)	T_m (°C)	ΔH_m (J g^{-1})	Peak (°C)	T_c (°C)	ΔH_c (J g^{-1})	1st Peak (°C)	2nd Peak (°C)	T_m (°C)	ΔH_m (J g^{-1})
1.2-mm PHB											
Undegraded	-	176.4	165.6	91.9	96.4	103.3	82.7	168.4	175.6	163.5	98.2
3 weeks	-	173.1	166.2	94.5	101.3	106.4	74.5	167.9	175.3	163.8	88.4
6 weeks	171.0	174.6	164.9	103.6	102.0	108.0	78.5	166.4	174.5	162.4	97.8
9 weeks	166.7	174.3	161.5	100.8	102.0	108.0	78.3	165.7	174.0	161.7	96.9
12 weeks	165.6	172.8	160.0	103.1	104.3	113.9	75.7	164.2	172.5	159.0	97.7
5-mm PHB											
Undegraded	172.1	180.4	163.5	104.1	95.3	103.3	73.3	166.2	174.8	160.9	92.3
3 weeks	172.7	181.8	162.2	116.6	101.3	107.1	79.0	166.5	174.4	161.4	95.6
6 weeks	171.2	181.9	162.3	114.7	101.3	107.2	75.8	165.1	173.4	159.6	92.6
9 weeks	171.0	182.9	161.4	120.4	101.9	107.2	77.6	164.6	173.1	159.2	93.8
12 weeks	168.0	183.4	155.3	128.4	102.3	108.4	76.4	160.5	170.5	156.0	96.9
16 weeks	168.4	183.7	151.3	128.7	106.6	117.1	77.4	160.9	170.1	156.4	98.7
20 weeks	167.2	183.9	148.7	134.8	100.1	106.0	79.0	159.8	170.1	150.9	96.4
30 weeks	167.7	182.1	150.4	118.7	101.3	108.1	71.9	156.1	166.9	151.6	86.0
1.2-mm PHB/ 15% TBC											
Undegraded	161.4	170.4	153.4	81.9	83.9	101.7	59.2	154.1	167.4	144.5	82.2
3 weeks	165.0	171.2	157.4	92.3	101.4	112.3	63.7	159.8	170.5	152.8	84.8
6 weeks	164.2	170.5	156.1	95.2	94.4	104.0	65.6	157.2	169.6	151.6	85.3
9 weeks	164.4	168.8	154.7	100.9	93.1	99.8	68.1	156.3	168.6	149.6	84.5
12 weeks	162.5	168.1	153.1	105.4	91.9	99.9	68.6	153.7	166.9	148.5	88.7
16 weeks	162.5	-	153.3	109.7	94.5	103.5	70.7	151.0	164.8	145.2	91.0
20 weeks	162.3	-	152.4	107.8	92.0	96.9	71.2	149.8	164.1	144.2	87.5
30 weeks	161.9	-	152.4	111.9	93.7	99.2	67.7	147.2	160.9	140.9	87.0

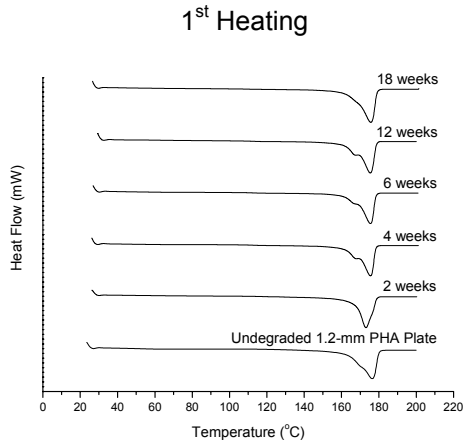

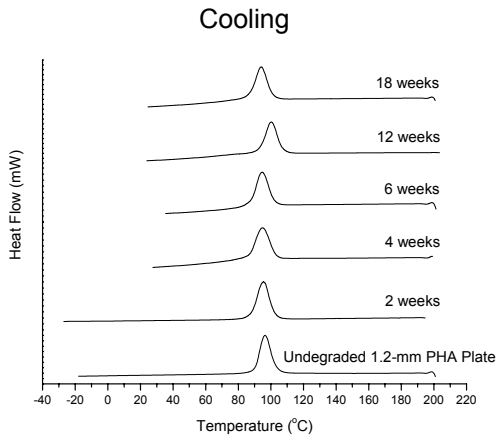

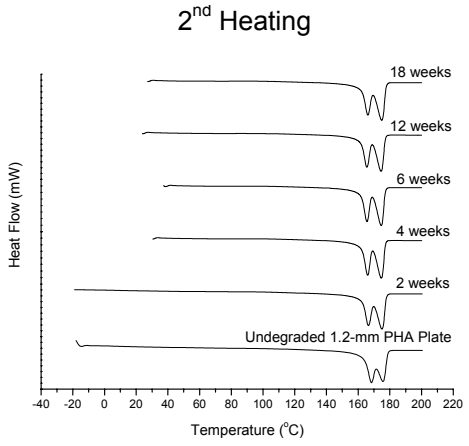

DSC curves for the 1.2-mm melt-pressed PHA plates before and after degradation in the first aerobic mass loss experiment. Time of degradation is indicated next to the plot. Top graph represents first heating; middle graph is the cooling period; bottom graph illustrates the second heating.

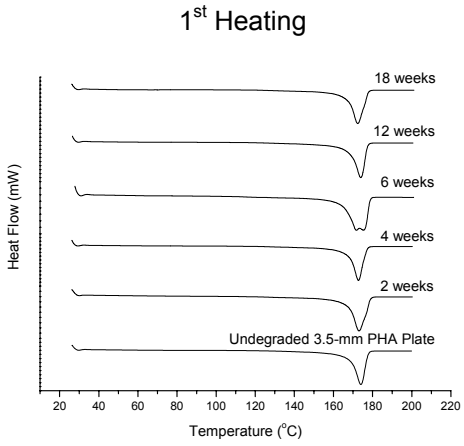

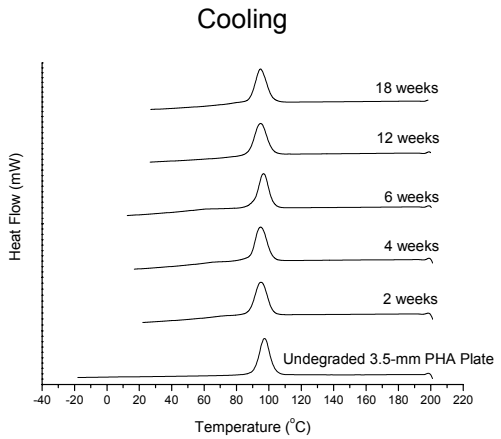

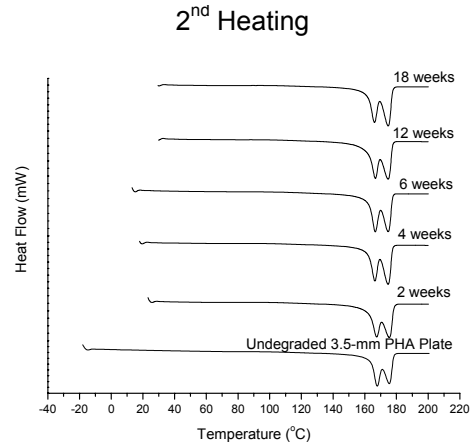

DSC curves for the 3.5-mm melt-pressed PHA plates before and after degradation in the first aerobic mass loss experiment. Time of degradation is indicated next to the plot. Top graph represents first heating; middle graph is the cooling period; bottom graph illustrates the second heating.

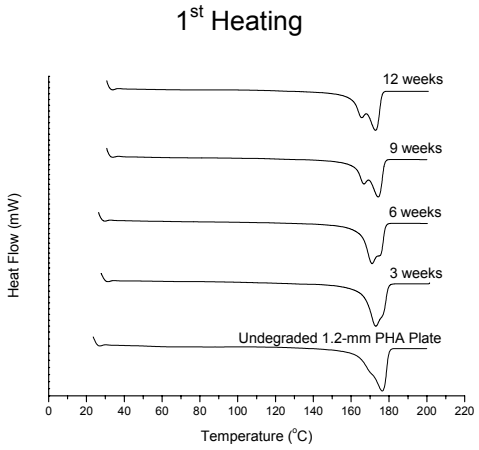

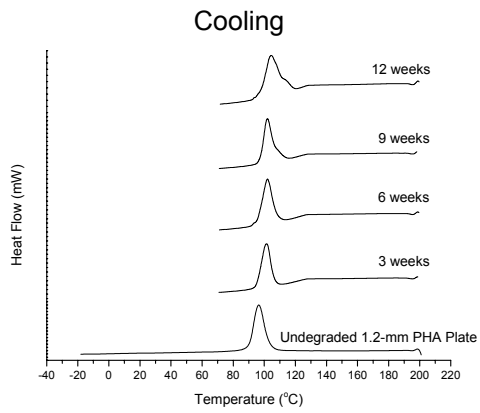

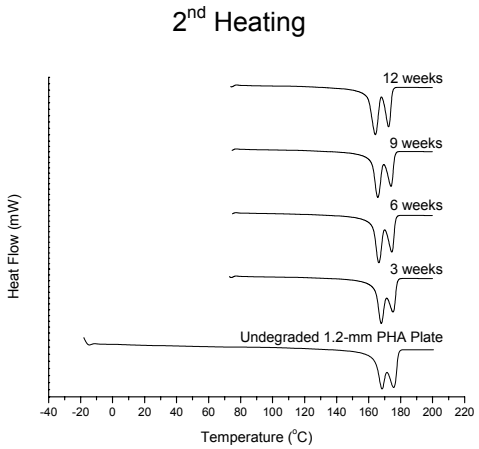

DSC curves for the 1.2-mm melt-pressed PHA plates before and after degradation in the second aerobic mass loss experiment. Time of degradation is indicated next to the plot. Top graph represents first heating; middle graph is the cooling period; bottom graph illustrates the second heating.

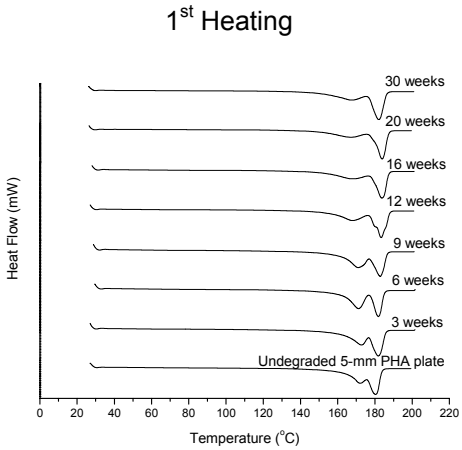

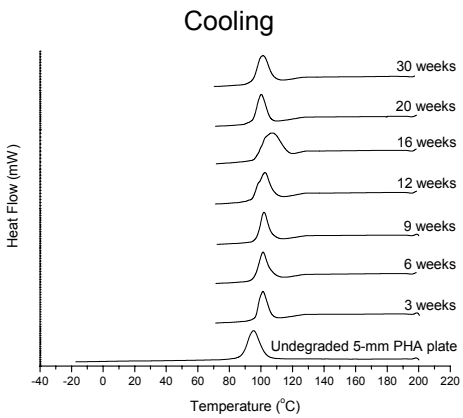

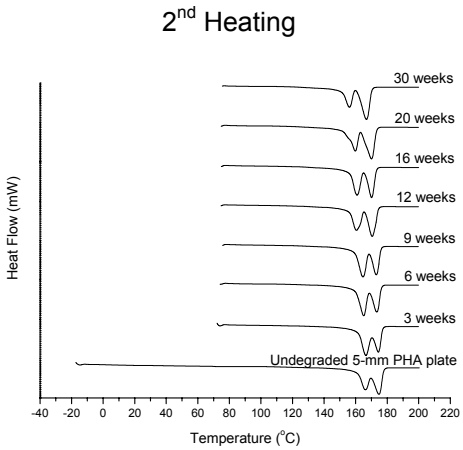

DSC curves for the 5-mm melt-pressed PHA plates before and after degradation in the second aerobic mass loss experiment. Time of degradation is indicated next to the plot. Top graph represents first heating; middle graph is the cooling period; bottom graph illustrates the second heating.

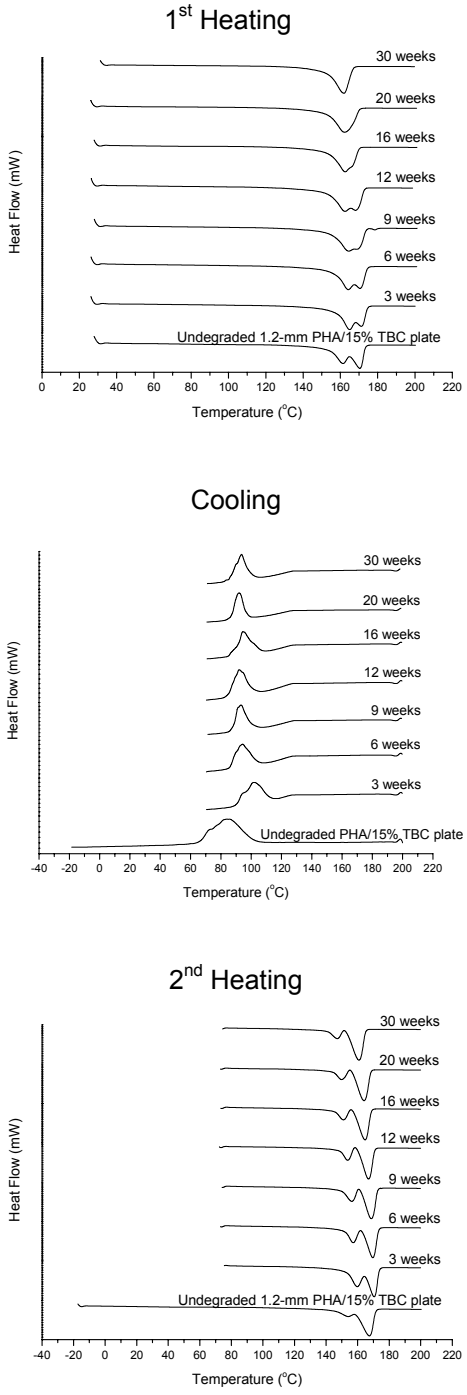

DSC curves for the 1.2-mm melt-pressed PHA/15% TBC plates before and after degradation in the second aerobic mass loss experiment. Time of degradation is indicated next to the plot. Top graph represents first heating; middle graph is the cooling period; bottom graph illustrates the second heating.

Vita

Benjamin Edward Stevens was born on December 4, 1983 in Baton Rouge, Louisiana. He attended college at Louisiana State University on a TOPS scholarship where he earned a Bachelor of Science in Biological Engineering in 2005. He chose to remain at Louisiana State University as a full-time graduate student. Presently, he is a candidate for the degree of Master of Science in Biological and Agricultural Engineering.